Seismic AVO Attributes and Rock Physics in Hydrocarbon Exploration

Vajiheh Jalali

Submitted to the
Institute of Graduate Studies and Research
in partial fulfillment of the requirements for the Degree of

Master of Science
in
Physics

Eastern Mediterranean University
January, 2014
Gazimağusa, North Cyprus

Approval of the Institute of Graduate Studies and Research.

Prof. Dr. Elvan Yılmaz
Director

I certify that this thesis satisfies the requirements as a thesis for the degree of Master of Science in Physics.

Prof. Dr. Mustafa Halilsoy
Chair, Department of Physics and Chemistry

We certify that we have read this thesis and that in our opinion it is fully adequate in scope and quality as a thesis for the degree of Master of Science in Physics.

Prof. Dr. Özay Gürtuğ
Supervisor

Examining Committee

1. Prof. Dr. Mustafa Halilsoy
2. Prof. Dr. Özay Gürtuğ
3. Assoc. Prof. Dr. Habib Mazharimousavi

ABSTRACT

During past two decades amplitude variation with offset (AVO) is a known technique that has been used in direct hydrocarbon exploration and exploitation, which uses the amplitudes of pre-stack seismic data to improve the reservoir forecasting in petroleum industry. There are significant number of studies in literature that incorporate with AVO analysis and inversion technique, especially in gas reservoirs to improve the risk assertion.

In this thesis, we apply AVO technique to map the attribute anomalies of the reservoir to survey the capability of AVO technique to indicate the exact location of the gas zones in approved hydrocarbon reservoir using the well log and seismic data with 2-D seismic interpretation method.

Keywords: AVO Technique, AVO Attribute, Hydrocarbon Exploration, Gas Reservoir, Pre-Stack Seismic Data, Rock Physics, Reflection Seismology.

ÖZ

Son yirmi yılda, genlik karşı offset (AVO) tekniği, hidrokarbon kaynaklarının keşif araştırmalarında ve kullanılmasında uygulanan bir teknik olarak bilinmektedir. Bu teknik, petrol endüstrisinde, rezerv kaynakların tesbit edilmesi aşamasında sismik veri yığınlarının iyileştirilmesi amacıyla geliştirilmiştir. Literatürde, AVO analizi ve ters tekniği ile ilgili önemli sayıda çalışma, doğal gaz yataklarının araştırılmasındaki risk faktörünün iyileştirilmesi amacıyla kullanılmıştır.

Bu tezde, AVO tekniği uygulanarak, bu tekniğin doğal gaz bölgelerinin tesbitindeki kullanılabilirliği, 2- boyutlu well log – sismik veri analiz yöntemiyle irdelenmiştir.

Anahtar Kelimeler: AVO tekniği, AVO vasfı, Hidrokarbon keşfi, Doğal gaz rezervi, ön-yığılmalı sismik veri, Kaya fiziği, Yansıma sizmolojisi.

This work is dedicated to my

Mother and Father for all their kinds,

continuous support and encouragement

in motivating me in all my life.

ACKNOWLEDGEMENT

First of all, I would like to express my sincere thanks to the scientific and executive directors of Eastern Mediterranean University, especially Prof. Dr. Mustafa Halilsoy, Chair of Department of Physics and Chemistry in believing me for giving a great opportunity to come and study in EMU. Then, I would like to express warm gratitude to Prof. Dr. Özay Gürtuğ, my supervisor, who has guided me along the path during the study at this university. Moreover, I would like to thank my other defense and assessment committee members especially Assoc. Prof. Dr. Habib Mazharimousavi and Assoc. Prof. Dr. Izzet Sakalli for their accuracy.

My thesis has been done under the supervision of Prof. Dr. Nasser Keshavarz Faraj Khah, as my cosupervisor. My deep appreciation goes to him for guiding me through every step of this project. My sincere thanks are to Prof. Dr. Behzad Tokhmechi initiating me at the start of this research. I am also thankful to Prof. Dr. Majid Bidhendi, and Prof. Dr. Amin Roshandel for all their help during this project.

I also would like to thank my friend Dr. Hoda Tahani and her housband, Eng. Saied Tarkhan for their guidance led me on this path. I wish to express my great gratitude to my friend,Mr. Morteza Kerachian and Mrs. Cilem Aydinlik, Secretary of Physics Department for their valuable assistance during college. I wish to express my fantastic thanks to my sister, Nasrin and her colleague in university of Shahrood, for their invaluable assistance throughout this research. Finally, special thanks to my lovely family, good brothers, kind sisters and all my dears for their devotions and understanding all time. This work could not be done without their help and support.

TABLE OF CONTENTS

LIST OF FIGURES

Chapter 1

INTRODUCTION

AVO which is the abbreviation of "Amplitude variation with offset" is a known technique that has been used in direct hydrocarbon exploration and exploitation using the amplitudes of pre-stack seismic data to improve the reservoir forecasting in petroleum industry. During past two decades, many success studies have been published, the usage of AVO analysis and inversion technique, especially in gas reservoirs to improve the risk assertion, moreover most companies use this method to estimate the composition of existing hydrocarbon reservoirs to reduce risks in this industry. As a result AVO method stands out as a quantitative indicator and cost effective technology to reduce the exploration risk factor in reservoir prediction and avoid pitfalls in drilling investments, especially in gas sands. There are several improved approaches in AVO inversion which proposed during recent years. Advances in inversion techniques and AVO analysis, would improve the quality of hydrocarbon exploration and exploitation. Looking some materials that I used in this study shows that most of reference materials are after 2000, which indicates that this subject is new subject and with further studies in this area, the other applications in hydrocarbon industry will be cleared more.

We applied this technique to map the attribute anomalies of the reservoir to survey the capability of AVO technique to indicate the exact location of gas zones in the

approved well, with Hampson Russel program by modeling of the empirical case study using well logs and seismic data using AVO attributes, especially the intercept and gradient, fluid factor and Poissin's ratio to optimize the area of gas zones. Two main necessary sciences in this technique are reflection seismology and rock physics which are the base knowledge for Geophysicists and those who interpret seismic data in hydrocarbon exploration.

The configuration of this study involves of five chapters; Chapter 2 is reflection seismology, which focuses on seismic method as a tool for the geophysicist in exploration of hydrocarbon industry in the field of Geophysics. Chapter 3 is involved of the rock physics. Rock physics is the other subject that is essential for AVO technique and is a science that has been considered as an effective technology in petroleum industry to connect the elastic properties of the reservoir and geophysical observable. There are several known theories and empirical relations which are available on handbooks and related materials, but we introduce some necessary materials to have a comprehensive view of this science which is used in this study. Chapter 4 is Amplitude variation with offset or AVO technique which deals with the basic concepts of AVO technique, AVO attribute, analyzing and interpretation. The core idea of AVO technique which is based on the propagation of energy from the boundary of two different media, is that the amplitude of recorded waves in each recorders are different and are related to the distances between shot and recorders or offsets. Chap 5 is AVO modeling and analyzing which is a practical case study is using the 2-D seismic data to clarify reservoirs properties with processing and analyzing of the well log data and seismic data which are available from well logging. And finally we conclude the thesis with a conclusion in chapter 6.

Chapter 2

REFLECTION SEISMOLOGY

2.1 Introduction

The basic of seismology established based on former studies on earthquakes. Nowadays seismic method is a tool for the geophysicist in exploration of hydrocarbon industry. Moreover seismic reflection method is widely used for exploration of oil and gas by detection and mapping of the subsurface boundaries using special recording systems based on advanced processing and interpretation techniques, which had been developed greatly in recent decades. Therefore, seismology is an important subject in the field of Geophysics that is taken into consideration in hydrocarbon industry.

This chapter, aims to outline the history of seismology, and the fundamental of physical principles of seismic waves, which seismic methods are based on. Subsequent section discusses the seismic phenomena of reflection, refraction and transmission. Besides, the essential knowledge of reflection seismology is discussed in detail. Another subject is about the recording of seismic reflection data and some approximation method to estimate velocity and other properties of subsurface named as normal move out (NMO) applied at common mid point (CMP). Information about 3-D and 4-D seismic reflection surveying will also be explained briefly in this introductory chapter.

2.2 Historical Background

Before getting through the main concepts of reflection seismology, a very brief historical development of seismology is presented. Seismoscope was the earliest instrument to record seismic waves, was built in China about A.D.100. In 1846 Robert Mallet, Irish scientist, assumed that the velocities of waves are different in various rocks, so he began studying the earth's crust using acoustic waves in 1848, moreover he performed field experiments to measure velocities in granite and loose sand in 1851. In 1876 U. S. General H. L. Abbot measured velocity of sound in rocks, and in 1889 Fouque and Levy used photography to record seismic data. The first geophone was built by Gray, Ewing and Milne in Tokyo in 1880. In 1912 Submarine Signal Corp. performed some experiments to send Morse code to the ships by sound waves. In 1914 in Germany, Mintrop devised the first seismograph during World War I to detect excavation activities. In 1917 in the United States, Fessenden designed a seismic method for locating ore bodies. The introduction of refraction methods for finding salt domes in the Gulf Coast region of the United States began in 1920, and in 1923, a German seismic service company used this method to locate oil traps. Later in 1930, after successful drilling of oil reserves based on seismic interpretations, the use of reflected and refracted waves became more applicable and popular.

The ability of recording and processing digitized seismic data in a computer led to great operation of reflection method after 1930. In the late 1970 there was a major development of the 3-D seismic survey to image entire volume of earth instead of a vertical cross-section of the earth. The technology improved during the 1980s, leading to more accurate and realistic imaging of the earth. A direct detection of

hydrocarbon based on the amplitude of a seismic section was first suggested by Ostrander (1982). During 30 years ago exploration seismology became an important tool for geophysics to estimate the presence of reservoirs and the location of places of mineral deposits.

2.3 Fundamental of Seismic Method

Fundamental of seismic science is based on the energy propagating of seismic waves. There are two main categories of seismic studies, earthquake seismology and controlled-source seismology. Earthquake seismology is the science of the structure and physical properties of the earth's interior in a passive energy source. Controlled-source seismology related to seismic waves are generated manually to obtain information about a particular area utilizing an active energy source.

The exploration seismic method includes two main areas, refraction seismic and reflection seismic. In refraction seismic method, the seismic signal returns to the surface by refraction at layer interfaces and records at distances much greater than depth of investigation. In reflection seismic, which is recorded at distances less than the depth of investigation, the seismic signal is reflected back to the surface so the angle of reflection is equal to the angle of incidence. As a result, refraction seismic has developed for engineering studies, while reflection seismic is in use for deep underground layer studies.

Some physical principles help to understand the wave propagation such as Huygens principle, Fermat's principles, Ray Theory, Snell's Law and so on. These principles are fruitful to describe the behavior of the wavefront of seismic disturbances in the Earth. As an example Huygens principle states that every point on a wavefront can

be regarded as a new source of waves as a secondary wavefront, besides the cover of the secondary wave fronts shows the primary wavefront.

2.4 Controlled Seismic Energy Sources

A seismic source is a localized resource which releases the adequate energy to a surrounding medium (the earth). Seismic waves are packets of energy produced from seismic sources such as explosives, vibrators or air guns with a wide range of frequencies, from 1Hz to hundred hertz that is emitted outwards from the sound sources at a velocity related to the physical properties of the surrounding rocks. As it can be seen in Fig (2.1), if the pulse travels through a homogeneous rock, the original energy transmitted outwards over a spherical shell.

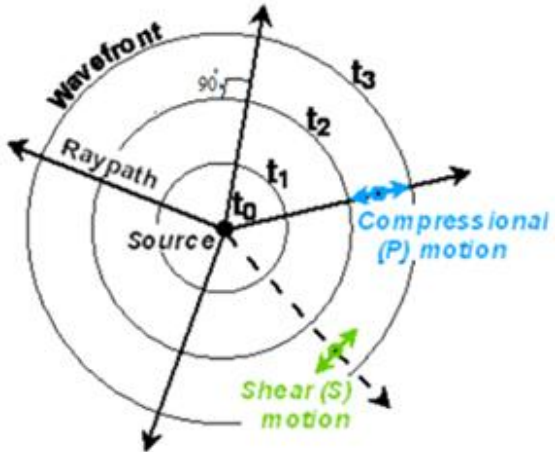

Figure 2.1: Wavefronts and raypaths in seismic wave propagation [6]

The operation of high-frequency seismic wave is in near-surface layers that is high resolution in use. Since the frequency is high so the energy is low and therefore, this wave does not reach to the further distances in deeper layers. On the other hand, low-frequency range of seismic waves has a lot of energy to reach the deeper layers and most distances which are beneficial to identify the subsurface layers of the earth in further distances. Sufficient energy, concentrated energy for a specific survey,

repeatable source waveform, safety, environmentally acceptable and reasonably cheap and highly efficient cost-effective as possible are some of the main requirements of the seismic sources. There are two main kinds of seismic sources, land and marine seismic sources.

Land seismic sources mainly include as dynamite and vibrator. Dynamite or explosive sources are exploded in shallow shot holes to minimize surface damage. Explosives normally require special permission to use, and have logistical difficulties for storage and transportation. Marine seismic sources are included as air Gun and water Gun. Each type of these sources have their own properties. As an example air guns are pneumatic sources which very high-pressure (typically 10–15MPa) compressed air is charged. The air is released into the water in the form of a high-pressure bubble. Water guns are an adaptation of air guns to avoid the bubble pulse problem. The compressed air, rather than being released into the water layer, is used to drive a piston that ejects a water jet into the water. Marine vibrators have been carried out using special base plates attached to a survey vessel and sparkers to converting electrical energy into acoustic energy. Hydrophones (the receivers) also tie to the survey vessels and move with its movement to detect the reflected waves.

2.5 Elastic Waves

There are two groups of seismic waves; body waves including, Primary and Secondary waves, and surface waves including, Rayleigh and Love waves.

2.5.1 Body Waves

There are two types of body waves; compression and transverse (shear) waves. These waves have a low frequency and high energy.

2.5.1.1 Compression Waves

In compression (longitude or primary) or P-waves the direction of vibration of specific point of medium is along in the direction of wave propagation. Compression waves can propagate in solid, liquid and gas, moreover P-wave velocity is a function of the rigidity and density of the medium. The speeds of P-wave is up to 6 km per second in surface rock of the earth and will be increased to about 10.4 km per second in 2,900 km below the surface, near the Earth's core. As the wave enters the core, its velocity drops to about 8 km per second. It increases to about 11 km per second near the center of the earth. Increasing of the speed with depth is resulting from hydrostatic pressure as well as from changes in rock composition. Moreover, in dense rock, P-wave velocity is from 2.5 to 7.0 km/s, while in spongy sand is from 0.3 to 0.5 km/s.

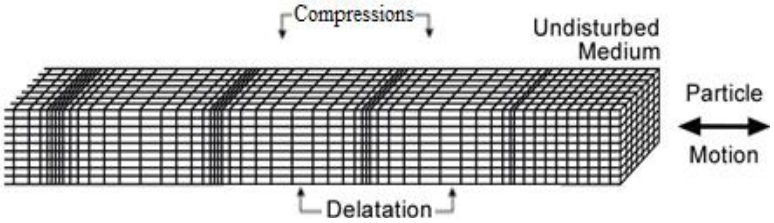

Figure 2.2: Elastic deformation and ground particle motion associated with the passage of P-wave propagation [16]

2.5.1.2 Transverse Waves

In transverse (shear or secondary) or S-waves, the direction of vibration and propagation are perpendicular to each other. If all the particles oscillate to a plane, the shear wave is a called plane-polarized. Transverse wave has two kinds of polarization, horizontal shear wave (SH) and vertical shear wave (SV). SH is the kind of S-wave that the vibration direction is horizontal, besides, SV is another kind of S-wave that the vibration direction is vertical. Shearwave or shake wave changes

as a result of the layering and cracking while compression wave are not so affected by cracks. Shearwave is rotational wave and cannot propagate in gas and liquids such as water, moreover the speed of S-wave is up to 3.4 km per second at the surface of the earth and will increase to 7.2 km per second near the boundary of the core. Since the core of the earth is liquid so S-wave cannot transmit to it and therefore its quantity will be zero. In marine also, only compression wave will be recorded by hydrophones, while in land, geophones often record a mixture of compression wave, shear wave and other types of wave, therefore, signal-to-noise ratio is higher in the land than in Marine.

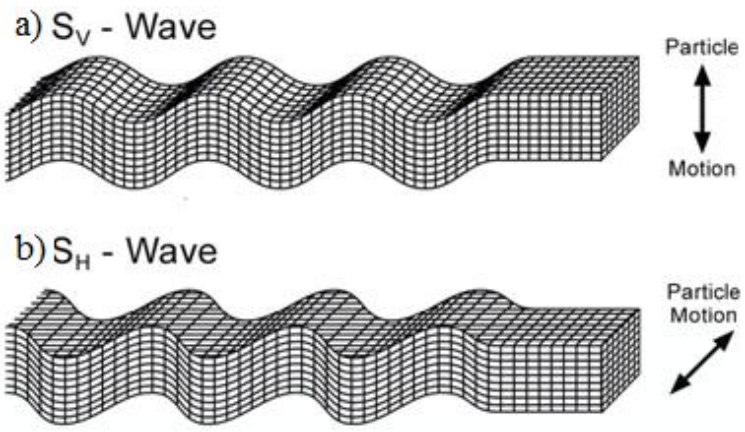

Figure 2.3: Elastic deformation and ground particle motion for vertical S-wave (a) and horizontal S-wave (b) propagation [16]

2.5.2 Surface waves

Surface wave can propagate along the boundary of the solid in a bounded elastic media. There are two types of surface seismic waves, Love wave and Rayleigh wave. Love wave, which is predicted by a British seismologist, A.E.H. Love (1911), firstly are appearing when two solid medium near the surface have varying vertical elastic properties and the direction of propagation wave is perpendicular to the displacement of the medium. Rayleigh wave also demonstrated mathematically by a British

physicist, Lord Rayleigh that propagates as an elliptical motion along the boundary between dissimilar solid media and the free surface of an elastic solid such as the earth. The amplitude of Rayleigh wave decreases exponentially with distances, below the surface. Having knowledge about the surface waves is beneficial for data analyzing, however they are not used for this study and they will not be focused in this thesis.

2.6 Reflection Seismology

Reflection seismic method is the most dominant geophysical method in hydrocarbon exploration (i.e., petroleum, natural gas). Seismic reflection surveying is the wide and the well-known geophysical technique. In reflection seismic surveys, seismic waves are reflected from the subsurface and the reflections will be detected by a series of geophones at the surface. The travel times are measured and can be estimate to reconstruct the paths and depths of the seismic waves to the interfaces. In such a situation, velocity varies as a function of depth, physical properties of the rocks and attitudes of the beds. Reflection seismic method is based on the equality of radiation and reflection angle ($i = i'$) as is shown in Fig (2.4) and Fig (2.5). As waves reflect from underlying layers, their amplitude change and we can get important information about the geological structures of the subsurface and physical properties of their material. Analyzing of the variation between amplitude and source-receiver distance (offset) on the recorded seismic signal can build an image of the subsurface layers accumulations to determine their depths, helping oil and gas companies to be aware of the presence of hydrocarbons and detect correct drilling locations, therefore hydrocarbon companies uses such information to reduce risk in exploration of hydrocarbon industry.

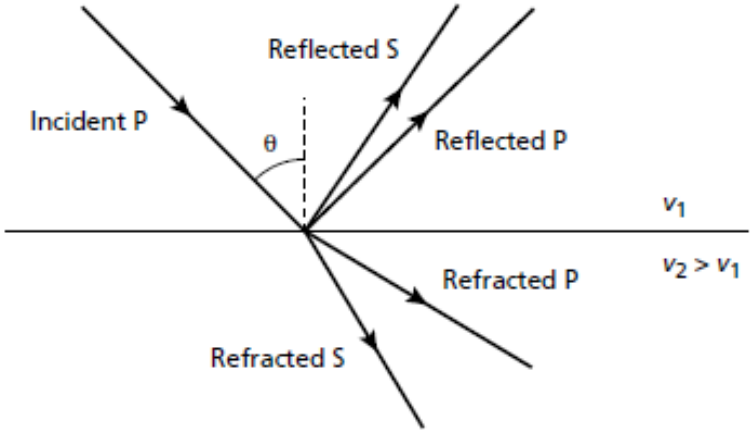

Figure 2.4: Schematic of a reflected and refracted ray [16]

For incident angles greater than the critical angle, incident seismic wave will refract to the second layer and will be received by the detector after several reflections. Therefore, if offsets are too large these refracted waves will detect and is not easy to distinguish between these refracted waves and reflected waves. In reflection seismology our job is to collect reflection waves, therefore the far offsets should be small enough so that the reflections waves be recorded rather than as refraction waves. Besides the near offset must be short enough to detect reflections rather refraction. Hence, it is important to determine both maximum and minimum near and far offsets for recording good-quality data. The near offset tends to be determined by the amount of noise that is generated by the source and the far-offset distance is determined by both the critical angle and the amount of NMO (normal move out speed) stretch allowed on the reflections expected in the far-offset traces.

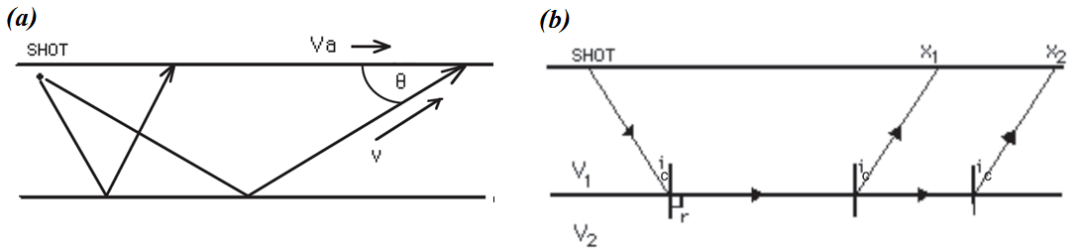

Figure 2.5: (a) Near offsets and far offset in reflected rays, (b) Refracted rays [10]

2.7 Seismic Waves Recording Systems

Modern seismic surveying systems distribute the task of amplification, digitization and recording of data from many detectors to individual computer units. The individual detectors are arranged along a multicore cable. These are connected together to make a field computer network using lightweight fibre-optic cables or telemetry links. The first recording system was designed by Frank Rieber in 1936, and then in 1952 was developed as magnetic recording, and therefore it was supplementing to moveable magnetic heads and dynamic corrections to seismic data in 1955. Seismic recording is a very difficult technical operation and must be performed as the international standard format approved by the Society of Exploration Geophysicists (SEG 1997). Each seismic trace has three primary geometrical factors which determine its nature. These are the shot position, the receiver position and the position of the subsurface reflection point as is shown in Fig (2.6). This position is unknown before seismic processing, but a good approximation can be made a correct view of the subsurface.

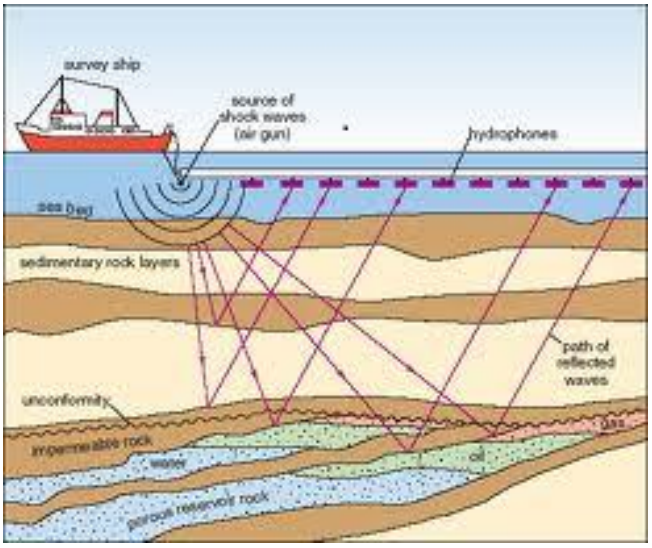

Figure 2.6: Seismic surveying system from http://geomaticsolutions.com/seismic-surveys

2.7.1 Spread Types of Field Layouts

There are several spread types of field layouts. The seismic detectors (e.g. geophones) may be distributed on either side of the shot, or only on one side as illustrated in Fig (2.7). The symmetrical split spread is split-dip recording that the source is at the center of a line on geophone or hydrophone groups, where half of the spread is moved forward to successive source locations, Fig (2.7.a). The symmetrical spread is another type of spread. A more common asymmetric spread is end-on or single-ended, where the source is at one end of in-line geophone groups as below.

The graphical plot of the output of seismic traces is due as the combination of the responses of the ground layers faced to a seismic pulse and the recording system. Any collection of one or more seismic traces is named as a seismogram. A collection of such traces from one shot is termed as the shot gathers. A collection of the traces at one surface mid point is termed as a common mid point gather (CMP gather). The collection of the seismic traces for each CMP presented as a seismic section is the main task of reflection seismic processing.

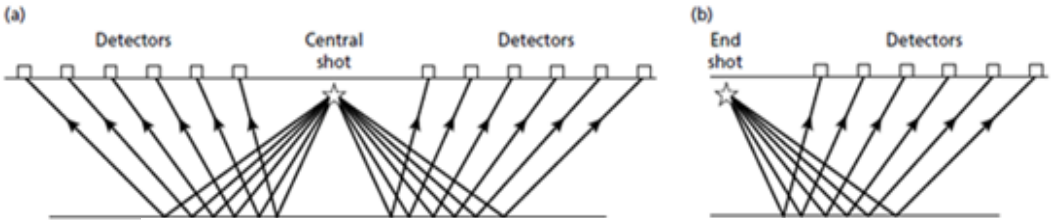

Figure 2.7: (a) Symmetric spread (b) Asymmetric spread [16]

2.7.2 The Common Mid Point(CMP) Method

The common mid point (CMP) profiling or “roll-along” recording common mid point method of seismic surveying is accepted as the standard approach to obtaining an image of earth layers universally. Collecting all the traces with a common mid

point forms a common mid point (CMP) gather. The flow of wave which is released from a shot has many rays that travel downward. When the incident wave is reflected from a horizontal boundary, the point of reflection is midway between the source position (shotpoint) and the receive position. This point is called mid point. The CMP gather is crucial in seismic processing for two main reasons:

1. The relation between travel time and offset is depending only on the velocity of the subsurface layers, and hence the subsurface velocity can be derived. Therefore such a set of traces can be applied with less error and simplest approximation.

2. The reflected seismic energy is usually very weak. It is possible to increase the signal-to-noise ratio of most data with some correction. Averaging all of the CMP gathers of a zero-offset traces named as NMO will reduce the noise, and increase the signal-to-noise ratio (SNR). These traces can be combined (stacked) together in the stacking process to have an accurate recording data in a subsequent data processing.

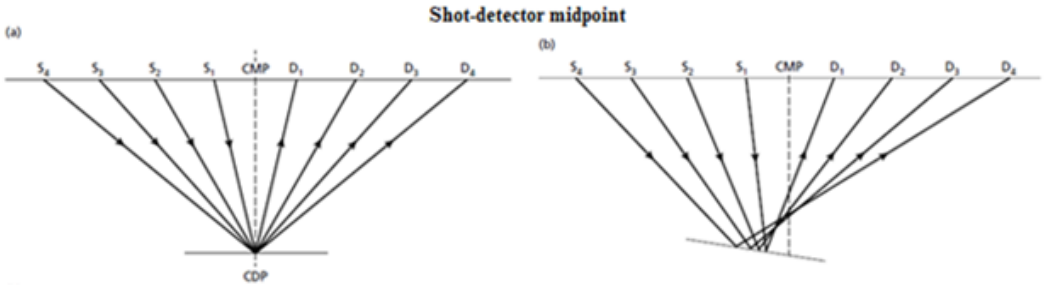

Figure 2.8: Common mid point
(a) horizontal reflector (b) dipping reflector [16]

As is shown in Fig (2.8.a), reflection point can be the mid point for a whole family of source-receiver offsets. For horizontal surface layers, the reflection point is in the middle between the source and receiver. If subsurface is sloped, the reflection points will be further from that and the distances between reflection point and the middle between the source and receiver depends on the slope.

2.8 Normal Move Out (NMO)

As discussed earlier, The two-way seismic travel time, through an isotropic, homogeneous and elastic layer from a horizontal reflector is hyperbolic. The time difference between travel time at a given offset and at zero offset is called normal move out (NMO). The normal move out depends on the velocity above the reflector and the distances between source and receiver (offset). Moreover it depends to the dip of the reflector, and the degree of complexity of the near-surface.

Fig (2.9) shows a schematic example of three primary and multiple events with horizontal reflectors and uniform speed of sound within the beds. At the small offsets, the travel time of M_2 is equal to that of P_2, but at far offsets, the travel time differs. In a simple case with homogeneous layers, since each of two events has different average velocities, so each of NMO's is different. As it is clear in Fig (2.9.a), M_2 travels through only the upper layer with velocity V_1 while P_2 travels through both the upper layer with velocity V_1 and the lower layer with velocity V_2. If $V_2$is greater thanV_1, then P_2 has a greater average velocity, Therefore P_2 will have less move out velocity than M_2, Fig(2.9.b).

Since the plot of time-offset is hyperbolic, it is necessary to apply NMO correction to have all traces as the zero-offset recorded traces for stacking. Normal move out velocity is the velocity required to correct for normal move out. Velocity estimating requires having the recorded data at nonzero offsets provided by a common mid point (CMP) recording.

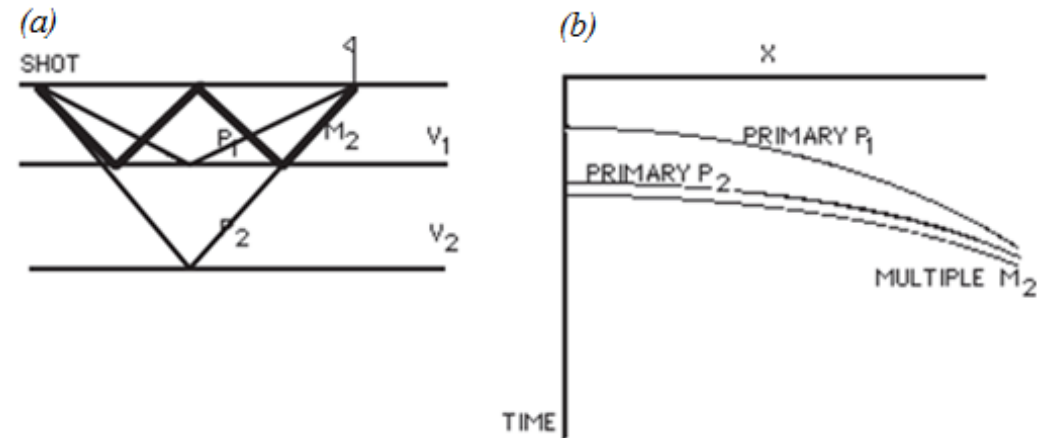

Figure 2.9: Multiple reflections and schematic of two primary event and one multiple event [10]

Estimating velocities, we can correct reflection travel times for nonzero offset and compress the recorded data volume to a stacked section for a single constant-velocity horizontal layer. The curve of reflection travel time is as a function of offset, and t. Fig (2.10.c) shows the stacked trace after NMO correction as below

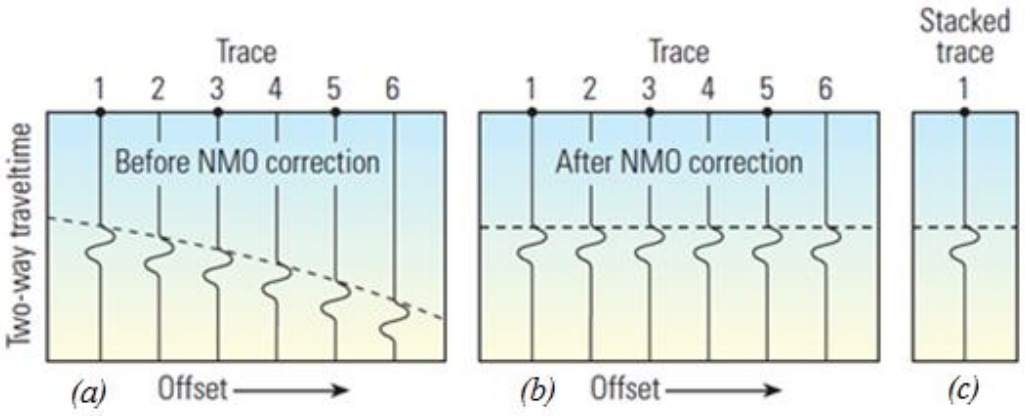

Figure 2.10: Curve of two-way travel time along offset. (a) Before NMO correction; (b) After NMO correction; (c) Stacked trace [5]

However, real geologic horizons rarely are flat with uniform sonic velocity. Therefore, the CMP method with simple NMO correction is not a more real process and it is necessary to correct by data-processing techniques such as dip move out

(DMO). By the way we have considered the ideal case in this study and would explain NMO corrections in some special cases further in this chapter.

2.8.1 Single Horizontal Reflector

The ideal geometry of the reflected ray path is shown in Fig (2.11.a). For the simple case of a single horizontal reflector at the depth z below a homogeneous top layer, the equation for the travel time t depending horizontal offset x , depth-layer z and the velocity v is below;

$$t = (x^2 + 4z^2)^{1/2}/v, \tag{2.1}$$

where:

t =*travel time for the reflected ray from shot to receiver*

x = *Shot-detector distinction*

v = *velocity of wave in homogeneous layer*

z = *the depth of layer*

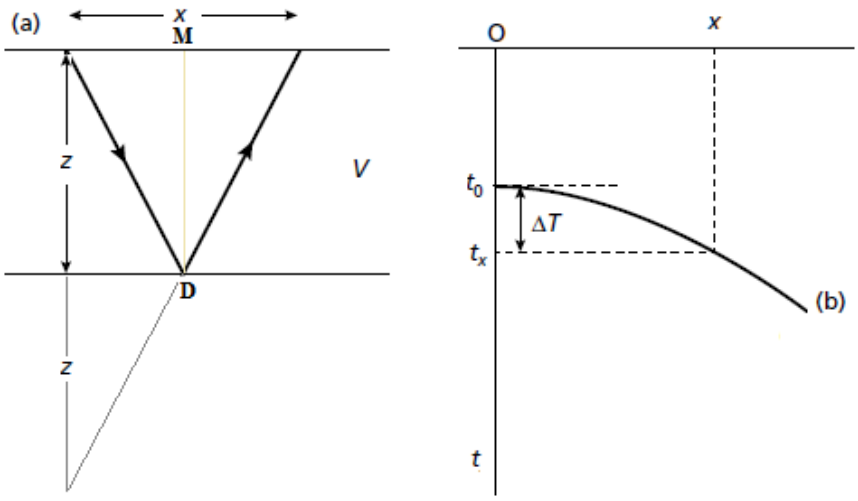

Figure 2.11: (a) The geometry of reflected ray paths (b) Time-distance curve for reflected rays from horizontal reflector [16]

From the equation (2.1), the reflection time *t* can be measured at an offset distance *x*, but still there are two unknown values related to the subsurface structure such as

depth, z and velocity, v. Some measured reflection times *t* at different offsets *x* will be enough information to solve equation (2.1) for these unknown values z and v. The graph of travel time of reflected rays and offset distance (the time–distance curve) is a hyperbola, Fig (2.11.b). Substituting *x* = 0 in equation (2.1) for vertically reflected ray, the travel time of zero offset t_0 will be obtained as:

$$t_0 = \frac{2z}{v}, \tag{2.2}$$

t_0 is twice the traveltime along the vertical path MD in Fig (2.11). t_0 is the intercept on the time axis of the time–distance curve Fig (2.11.b). Squaring equation (2.1) we will have:

$$t^2 = \frac{4z^2}{v^2} + \frac{x^2}{v^2}. \tag{2.3}$$

Considering (2.2) and (2.3) we will have:

$$t^2 = {t_0}^2 + \frac{x^2}{v^2}. \tag{2.4}$$

This equation describes a hyperbolic shape and it is called the normal move out hyperbola, or simply NMO as is shown in Fig (2.11). It describes the relation among the travel time along the vertical path t_0, offset *x*, and speed of sound in the earth layers v. Equation (2.4) is the simplest way to suggest for determination of the velocity v. If t^2 is plotted against x^2; the graph will be a straight line with slope $1/v^2$ and the vertical two-way time t_0 will be as an intercept on the time axis. However, since the range of values of *x* is restricted and the slope of the best-fit straight line associate with uncertainty, this method is unsatisfactory in practice. Another better method of estimation of velocity is to have a relation between time t, and offset x, by changing some equations. Considering both equation (2.3) and (2.2) and by factorization term $\frac{2z}{v}$, equation (2.3) will be rearranged as below:

$$t = \frac{2z}{v}\left[1 + \left(\frac{x}{2z}\right)^2\right]^{1/2} = t_0\left[1 + \left(\frac{x}{vt_0}\right)^2\right]^{1/2}, \quad (2.5)$$

In this equation v and t_0 are constant so it is useful to indicate clearly that the travel time at any offset x is the vertical travel time plus an additional amount related to offset x. Using the standard binomial expansion, equation (2.5) will reduce to an even simpler form as:

$$t = t_0\left[1 + \frac{1}{2}\left(\frac{x}{vt_0}\right)^2 - \frac{1}{8}\left(\frac{x}{vt_0}\right)^4 + \cdots\right]. \quad (2.6)$$

Since $t_0 = 2z/v$ from equation (2.2), then the term x/vt_0 can be written as $x/2z$. For small offset/depth ratios (i.e. *x/z* << 1), that is routine case in reflection surveying, equation (2.6) may be shortened to obtain the approximation as:

$$t \approx t_0\left[1 + \frac{1}{2}\left(\frac{x}{vt_0}\right)^2\right] \approx t_0 + \frac{x^2}{2v^2t_0}, \quad (2.7)$$

this equation is the most convenient form between time and distance and will be used more in the processing and interpretation of reflection data.

The Normal Move out (NMO) is the difference between the travel times t recorded at offset x, and the vertical two-way time, t_0 that we name here as Δt:

$\Delta t = t_x - t_0$; $t_x = t_0 + \frac{x^2}{2v^2t_0}$ from(2.7), therefore:

$$\Delta t = \frac{x^2}{2v^2t_0}. \quad (2.8)$$

As it is clear in equation (2.8), NMO is a function of offset x, velocity v and vertical two-way time t_0 , besides, since $t_0 = \frac{2z}{v}$ it can be a function of offset x, velocity v and depth *z*. The concept of normal move out is the fundamental concept to recognition, processing and interpretation of reflection events; moreover it is convenient to the calculation of velocities using reflection data.

Substituing $t_0 = \frac{2z}{v}$ from the equation (2.2) in equation (2.8) we will have:

$$\Delta t = \frac{x^2}{4vz}\,. \qquad (2.9.a)$$

Rearranging the equation (2.8) will yields:

$$v = \frac{x}{(2t_0\Delta t)^{1/2}}\,. \qquad (2.9.b)$$

Using these relations, the velocity v in any layer of the earth can be computed from knowledge of the zero-offset reflection time t_0 and Δt at a particular offset x.

In practice, such velocity values are obtained by computer analysis using large numbers of reflected ray paths. Once the velocity has been estimated, it can be used to compute the depth z by in conjunction with t_0 to compute the depth z from $t_0 = \frac{2z}{v}$ from the equation (2.2).

2.8.2 Sequence of Horizontal Reflectors

In exploration seismology in real cases we deal with several layers that reflect the seismic waves depending energy propagation in each layer, so reflected waves introduce a series of layers in subsurface to produce a complex travel path. Here we assume a simple physical ground model of horizontally-layered isolated interfaces to simplify as is shown in Fig (2.12). It is assumed that the uniform interval velocity v_i is constant within each homogeneous geological layer, moreover the average velocity over a depth interval contains some interval velocities. If z_i is the thickness of an interval and t_i is the one-way travel time of a ray through it, the interval velocity is given by:

$$v_i = \frac{z_i}{t_i} \qquad where\ i = [1, n] \qquad (2.10)$$

In a multilayered ground also the travel-time curve is still essentially hyperbolic at small offsets compared to reflector depths ($x << z$), except that average velocity or,

the root-mean square velocity of the layers must be replaced instead of the homogeneous top layer velocity v in equation (2.1) and (2.8).

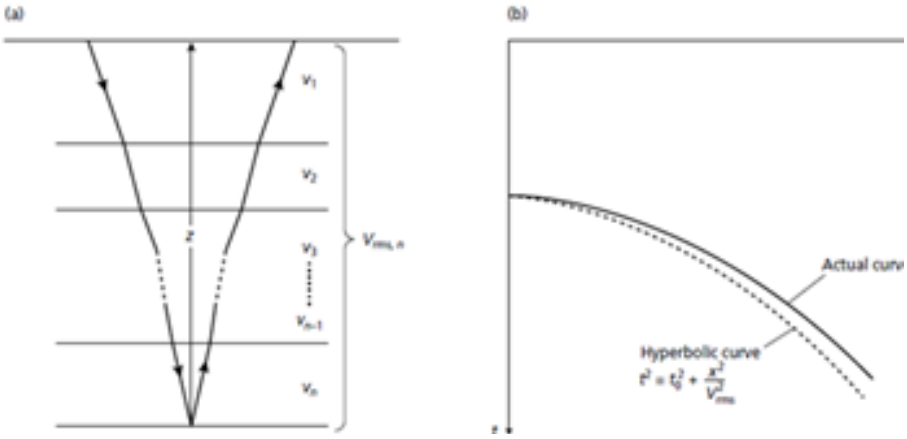

Figure 2.12: (a)Travel pass of reflected several horizontal layers
(b) Time-distance curve for reflected rays [16]

For average velocity or time average velocity $\bar{v}$, interval velocities should be averaged over several depth intervals. Thus the average velocity of the top n layers in Fig (1.12) is given by:

$$\bar{v} = \frac{\sum_{i=1}^{n} z_i}{\sum_{i=1}^{n} t_i} = \frac{\sum_{i=1}^{n} v_i t_i}{\sum_{i=1}^{n} t_i}. \tag{2.11}$$

The root-mean square velocity v_{rms} of a section of ground down to the nth interface is a closer approximation (Dix 1955) than the average velocity as below.

$$v_{rms,n} = [\sum_{i=1}^{n} v_i^2 t_i / \sum_{i=1}^{n} t_i]^{1/2}. \tag{2.12}$$

As we know from equation (2.4), $t = (x^2 + 4z^2)^{1/2}/v$ at small offsets x the total travel time t_n of the ray reflected from the nth interface at depth z is given to a close approximation by

$$t_n = (x^2 + 4z^2)^{1/2}/v_{rms}. \tag{2.13}$$

Moreover, the NMO for the nth reflector is given by:

$$\Delta t_n = \frac{x^2}{2v_{rms,n}^2\, t_0}. \tag{2.14}$$

Therefore the individual NMO value Δt_n associated with each reflection event may be used to derive a root-mean-square velocity value for the layers above the reflector. Values of v_{rms} down to each reflector can then be used to compute interval velocities using the Dix formula. To compute the interval velocity v_n for the nth interval;

$$v_n = \left[\frac{v_{rms,n}^2 t_n - v_{rms,n-1}^2 t_{n-1}}{t_n - t_{n-1}}\right]^{1/2}, \tag{2.15}$$

where $v_{rms,n-1}^2$ and $v_{rms,n}^2$ are the respectively root-mean-square velocity, moreover t_n and t_{n-1} are reflected ray travel times to the *(n -1)th* and nth reflectors (Dix 1955). To attain higher accuracy at far offsets it is necessary to give fourth and higher-order terms in equation (1.6), as given below,

$$t^2 = t_0^2 + \frac{x^2}{v_{rms}^2} + c_2 x^4 + \cdots, \tag{2.16}$$

where c_2 and other constants are related to mean-square velocities.

2.8.3 NMO for a Dipping Reflector

Fig (2.13) depicts a medium with a single dipping reflector. The aim is to compute the travel-time from source location *S* to receiver location *G* which is reflected at depth point D. For the dipping reflector, mid point *M* is no longer a vertical projection of the depth point to the surface. However, in horizontal stratified layers the terms CDP gather and CMP gather are equivalent. In dipping reflector or lateral velocity variation, these two terms are different.

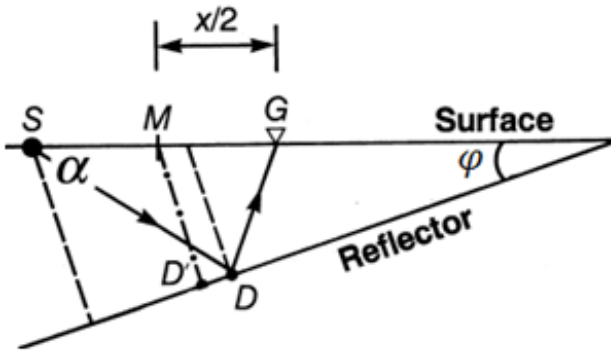

Figure 2.13: A single dipping reflector [26]

In a simple case that is shown in Fig (2.13), *S* is source point, *D* is reflection point and *G* is receiver point. Mid point *M* and the normal-incidence reflection point *D* remain common to all of the source-receiver pairs within the CMP gather that is not dependent to dips. Depth point *D*, however, is different for each source-receiver pair in a CMP gather recorded over a dipping reflector. Levin (1971) derived the two-dimensional travel time equation for a dipping reflector. Using the geometry of Fig (2.13).

$$t^2 = t_0^2 + \frac{x^2 \sin^2 \alpha}{v^2}, \tag{2.17}$$

where the two-way travel time *t* is associated with the nonzero-offset ray path *SDG* and the two-way zero-offset time t_0 is associated with the normal-incidence ray path *MD* at mid point *M*, and α is the angle between the normal to the dipping reflector and the direction of the line of recording from the Fig (2.13). The move out velocity is then given by;

$$v_{NMO} = \frac{v}{\sin \alpha}. \tag{2.18}$$

As is shown in 2-D geometry of the dipping reflector in Fig (2.13), $\sin \alpha = \cos \varphi$, where φ is the dip angle of the reflector. Hence, equations (2.17) and (2.18) are written in terms of the reflector dip φ. From the equation (2.17) we will have:

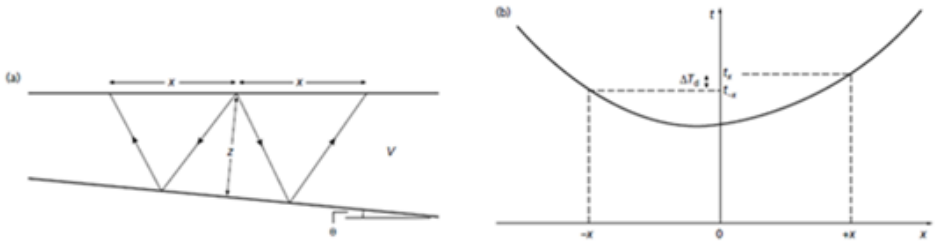

Figure 2.14: (a) Geometry of reflected ray path (b) Time-distance curve [16]

$$t^2 = t_0^2 + \frac{x^2 \cos^2 \varphi}{v^2}, \tag{2.19}$$

$$v_{NMO} = \frac{v}{\cos \varphi}. \tag{2.20}$$

The travel time of equation (2.19) represents that time-offset curve is a hyperbola for a dipping reflector as a flat reflector for small dip angle. Moreover as is shown in equation (2.20), NMO velocity for a dipping reflector is given by the velocity divided by the cosine of the dipping reflector, the greater the dip angle, the greater the NMO velocity.

2.8.4 NMO for Several Layers with Arbitrary Dips

Fig (1.15) shows a number of layers of two dimensional geometry with arbitrary dips. Here the travel time of ray path *SDG* will be considered so that the path of this ray is from source location, *S* to depth point, *D*, and receiver location, *G*, associated with mid point, *M*.

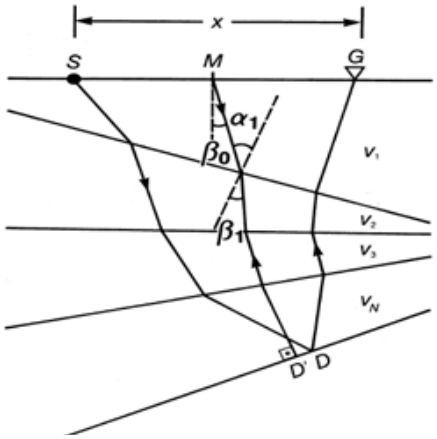

Figure 2.15: Geometry for ray path with arbitrary dips in each layer [26]

Note that the CMP ray from mid point M hits the dipping interface at normal incidence at D', which is not the same as D. The zero-offset time is the two-way time along the ray path from M to D'. Hubral and Krey (1980) derived the expression for travel time t along SDG as:

$$t^2 = t_0^2 + \frac{x^2}{v_{NMO}^2} + higher\ order\ term, \tag{2.21}$$

where the NMO velocity is given by:

$$v_{NMO}^2 = \frac{1}{t_0\ cos^2\beta_0} \sum_{i=1}^{N} v_i^2\ \Delta t_i \prod_{k=1}^{i-1} (\frac{cos^2\alpha_k}{cos^2\beta_k}), \tag{2.22}$$

the angles α and β are shown in Fig (2.15). For a single dipping layer, equation (2.22) reduces to equation (2.18).

In general the individual seismic traces obtained from seismology are rarely in use and a group of seismic traces are subject of the processing to increase signal to noise ratio (SNR) and improve the resolution of the seismic traces. Several data processing techniques are required to depict the seismic sections. Filtering and inverse filtering are of main data processing methods. The two main types of filtering method are frequency filtering and velocity filtering. Any coherent or incoherent noise event whose dominant frequency is different from that of reflected arrivals may be suppressed by frequency filtering. Frequency filtering can improve the SNR but mostly damages the vertical resolution, velocity filtering is also used to remove coherent noise events from seismic records could be carried out by computer in the time or frequency domain.

Inverse filtering or deconvolution is the analytical process of removing the effect of some previous filtering operation. Inverse filters discriminate against noise and improve resolution of signal characters. Deconvolution inverse filters are also designed to deconvolve propagated seismic pulses through a layered ground or through a recording systems and may be carried out on individual seismic traces before stacking.

2.9 3-D Seismic Reflection Surveying

The main goal of three-dimensional surveys is to gain a higher degree of resolution and accuracy. In a 3-D survey, the disposition of shots and receivers is not on a straight line while shots and detectors are distributed along orthogonal sets of lines to establish a grid of recording points. The analysis of 3-D data satisfies two major goals. One is the ability to identify both S-waves and P-waves in the same data, and another is the ability to remove unwanted wave energy by sophisticated filtering. This information is important to predict the presence of hydrocarbons with direct hydrocarbon indicators (DHIs) that are an important part of modern seismic interpretation. In fact, 3-D data is a routine method in the exploration for hydrocarbons now. Here is a schematic of 3-D common mid point reflected survey on Fig (2.16).

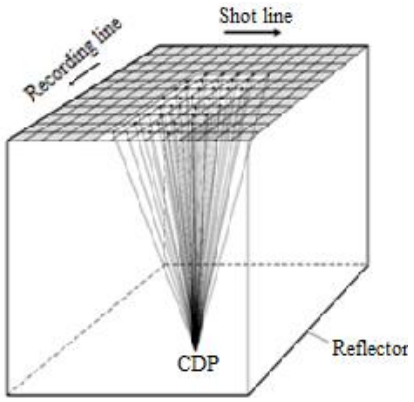

Figure 2.16: Reflected ray paths in three dimensional survey [16]

2.10 4-D Seismic Reflection Surveying

The time-lapse, or 4-D, seismic method as a mechanical modeling can explain the time shifts of movement of hydrocarbon fluids. Using 4-D survey rather than a 2-D or 3-D survey, the interpretation of production and development stages of a field can be more real and possible to monitor the flow of hydrocarbons within the reservoirs in time. Moreover understanding of the reservoir behavior and optimize its development will be greater. In addition 4-D survey method would improve the accuracy of the velocity model by a comprehensive set of techniques.

Since the pore fluids are changing in time, the seismic response of the formations would change resulting on extracting of oilfield regular intervals. Any factor which affects the location, amplitude or timing of seismic waves must be allowed for comparing two sets of data recorded in different surveys. Schematic of the 4-D reflected survey is shown below, Fig (2.17). Since the drilling boreholes in locating oil or gas reservoirs often are more expensive, the additional effort in three, four and further dimensions seismic data acquisition and processing to better estimation is more cost-effective.

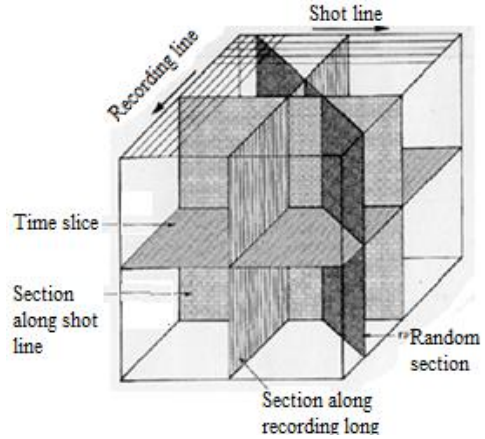

Figure 2.17: Reflection data volume in four dimensional seismic survey[16]

Chapter 3

ROCK PHYSICS

3.1 Introduction

Rock physics that has been considered as an effective technology in petroleum industry since 2000, is a science of Geophysics to connect seismic data and reservoir properties, which ultimately improve reservoir forecasting and reduce exploration risk in hydrocarbon industry. The main challenge of rock physics in seismic exploration is connections between geophysical observables and physical properties of rocks. To have a comprehensive view of these relations, it is crucial to understand the rocks and basic definition of their parameters. There are several known theories and empirical relations which are available on handbooks and related materials, but we will introduce some necessary materials to have a comprehensive view of this science in this study.

This chapter covers the basic concepts of rock physics and the theory of elasticity. Moreover some related material such as stress, strain and Hook's law and some known moduli will be discussed. In addition, some quantities such as Poisson's ratio, porosity, permeability, resistivity will be informed. More topics are about seismic wave velocities of rocks, and empirical relationships among the velocity with various parameters including density and porosity. This chapter will be finished with an explanation of the Biot's and Gassman's theories and Gregory's formulas.

3.2 Basic of Rock Physics

Rock physics contains the range of techniques that relate the geological reservoir properties (e.g. porosity, lithology, fractures, saturation and frequency influenced the rocks) of a rock at certain physical conditions (e.g. pressure, stress, temperature) with the corresponding elastic and seismic attributes (e.g. elastic modulus, velocity, Vs/Vp, impedance, reflectivity and refractivity attenuation). Rock physics is a combination of some other sciences such as Geophysics, Geomechanics and Petrophysics. Some concepts that are related to rock physics are included as the features of fluid distribution in the subsurface, energy partitioning, elasticity theory, seismic processing, signal analysis, seismic geomorphology, well log analysis and core measurements. In rock physics we will answer two main problems. One is how lithology and fluid content could be realized from physical parameters, and another is how rock physical parameters will be determined. This chapter is about first subject and in the third chapter, next subject would be discussed.

3.3 Theory of Elasticity

In physics, Elasticity is the tendency of materials to return to their initial condition after being deformed. The size and shape of the solid objects can be deformed by applying forces to the surface of the bodies. Similarly, a resistance fluid changes in size or volume due to the external forces. As a natural property, the body tends to return to its original condition, when the external forces are removed. The relations between the applied forces (stress) and the deformations (strain) are expressed in terms of elastic modulus.

In the last 50 years, it has been discussed that concerning hypothesis to describe the rock matrix and pore fluid properties in a given rock, more physical insight is

provided by the rigidity modulus. Homogeneous and isotropic materials with elastic properties have completely described by two elastic moduli, moreover having a pair of elastic moduli, other module can be measured by some known formula. To have a good understanding of elasticity of a material and elastic moduli which are described in terms of a stress-strain relation, we would bring the concepts of these issues here.

3.3.1 Stress, Strain and Hook's law

A rock may be deformed by compression, tension, and shear types as is shown in Fig (3.1). Compression is pushing from above, tension is pulling from above, and shear is pushing from the side. In compression and tension type, the volume will be changed but its shape will remain as before, but in the case of a shear, the volume does not change but the shape of the rock will be changes.

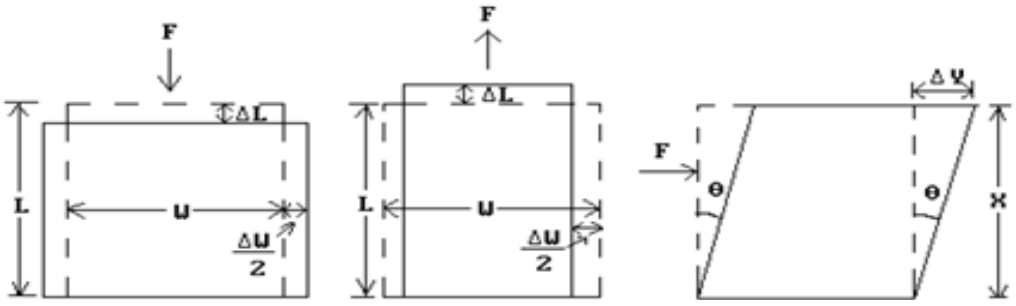

Figure 3.1: Deformation of rock by (a) compressional, (b) tension, (c) shear stress by force F [14]

When external forces are applied to a body, these forces are opposed by internal forces, therefore internal forces are going to be balanced within external forces. Stress is a measure of the intensity of these balanced forces and can be written as:

$$p = F/A\,, \tag{3.1}$$

where:

p = stress

F = force

A = area

Stress is given as a force per unit area and it measures in Pascal. When the force is perpendicular to the element of area, the stress is named as a normal stress or pressure. If the force is tangential to the area, the stress is a shearing stress. If the force is neither tangential nor perpendicular to the area, it can be divided into horizontal and vertical components as a normal and shearing stress. A fluid body has no shear strength, so there is not shear stress in a body under hydrostatic stress.

Strain is concerned to the proportional deformation of a material which is described by the ratio of the change caused by the stress. There are three types of strains in two-dimensional and one more in three-dimensional cross-section of a rock cube which are related to each of three types of the stress which are as below.

Longitudinal Strain: $e_l = \frac{\Delta L}{L}$. (3.2)

Transverse Strain: $e_w = \frac{\Delta W}{W}$. (3.3)

Shear Strain: $e_s = \frac{\Delta Y}{X} = tan\theta$. (3.4)

Volumetric strain or dilatation in three dimention: $\Theta = \frac{\Delta V}{V}$, (3.5)

where:

$\Theta = volumetric\ strain$

$\Delta V = change\ in\ volume$

$V = initial\ volume$

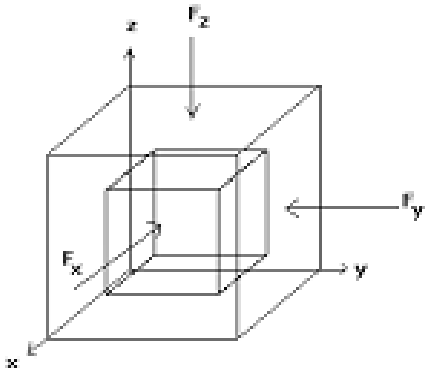

Figure 3.2: Volumetric stress [16]

The elasticity of materials is described by a stress-strain curve. In very early studies of mechanical deformation under applied stress Hooke, found that for most metals or crystal materials, the deformation was linearly proportional to the stress for small deformations, and so the relationship between stress and strain can be described by Hooke's law in small deformation and higher-order terms can be ignored. Linear elasticity as an elastic modulus describes the behavior of such materials. In a completely homogeneous and isotropic medium, stress and strain are related to each other by a linear relation known as Hooke's law as below:

$$Stress = Constant * Strain. \tag{3.6}$$

The constant is the elastic modulus and the dimension of the constant is same as stress which is [force ⁄ area] with unit dyne per square centimeter [dyn / cm^2]. A higher modulus indicates that the material is harder to deform. There are various elastic moduli, such as, the Young's modulus (E), Shear modulus (μ), Bulk modulus (K), Axial modulus (ψ), Lamé's first parameter, and P-wave modulus. Some of these moduli will be introduced as below.

3.3.2 Young's Modulus or Stretch Modulus (E)

Young's modulus named after Thomas Young, British scientist in the 19th century, is the most common elastic modulus describes the elastic properties in only one direction. Young's modulus, also known as the tensile modulus or tangent modulus is the slope of the stress-strain curve created during tensile tests conducted on a sample of the material to identify the quantity of isotropic materials. The Young's modulus is the proportional constant in Hooke's law that relates longitudinal stress and longitudinal strain together. This relation is only valid under the assumption of an elastic or linear response and is always zero in fluids.

Any real material will break or fail during very large stretched over a very large distance or with a very large force; hence, all materials have Hookean behavior in small enough strains or stresses. Similar to seismic Young's modulus study the situation of a sample that may extend under tension or will be shortened under compression. For a model of a rod with rectangular cross section of area dA and length l (Fig 2.3), the Young's modulus as a ratio of the stress to the strain will be as:

$$E = \frac{longitudinal\ stress}{longitudinal\ strain} = \frac{p_l}{e_l} = \frac{\frac{F}{dA}}{\frac{dl}{l}}, \qquad (3.7)$$

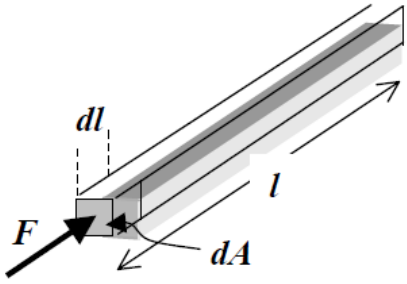

Figure 3.3: Young's Modulus (E) [16]

where:

$p_l = Compression\ stress$

$E = Young's\ modulus;\ (Pa) or\ (N/m^2)$

$e_l = Longitudinal\ strain$

3.3.3 Shear Modulus (μ)

Shear modulus or rigidity or second Lamé Elastic Constant for shear, describes the deformation of shape at constant volume when acted upon acting by opposing forces on the body. The shear modulus is the proportional constant in Hooke's law, that relates shear stress and shear strain together and is always positive for solids. Besides, since fluids cannot support shear stress, so the shear modulus is zero for fluids. The shear modulus shows the viscosity of medium, the bigger the shear modulus the more rigid the material; it means that for the same change in horizontal distance (strain), it requires bigger forces (stress) in rigid medium to deform the body geometry. This is the reason for calling modulus of rigidity rather than shear modulus optionally. Considering Fig (3.4), shear modulus will be defined as below:

$$\mu = \frac{p_s}{e_s} = \frac{\frac{F}{A}}{\frac{\Delta x}{l}} = \frac{F}{A\,tan\theta}, \qquad (3.8)$$

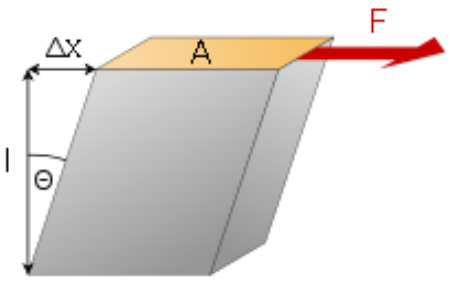

Figure 3.4. Shear Modulus (μ) [16]

where:

$\mu = shear\ modulus\ or\ rigidity\ (Pa),$

$p_s = shear\ stress$

$e_s = shear\ strain$

$A = the\ area\ on\ which\ the\ force\ acts$

$l = the\ initial\ length$

$\Delta x = the\ transverse\ displacement$

3.3.4 Bulk Modulus, or Incompressibility (K)

The bulk modulus of a medium measures the volumetric elasticity or substance's resistance in uniform compression which describes the tendency of an object to deform in all directions. The bulk modulus is defined as the ratio of the infinitesimal pressure increase to the resulting relative decrease of the volume in the case of a simple hydrostatic pressure P applied to a cubic element. The bulk modulus is an extension of Young's modulus to three dimensions. For a fluid, only the amount of bulk modulus is meaningful. The inverse of the bulk modulus gives a substance's compressibility which is another main quantity to identification of materials. Considering Fig (3.5), bulk modulus will be defined as below.

$$K = \frac{volume\ stress}{volume\ strain} = \frac{P}{\frac{\Delta v}{v}}, \qquad (3.9)$$

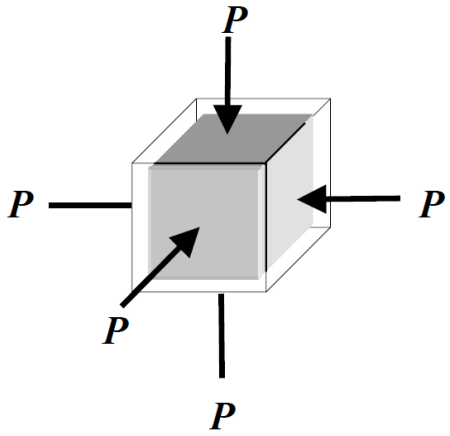

Figure 3.5: Bulk Modulus (K) [16]

where:

K = bulk modulus

P = hydrostatic stress

ΔV/V = volumetric strain or dilatation

3.3.5 Axial Modulus (y)

For an anisotropic solid, three moduli described above as Young's modulus, shear modulus (μ) and bulk modulus do not contain enough information to describe its behavior. The axial modulus is useful for the materials are constrained to deform uniaxially. Axial modulus is the proportional constant in Hooke's law that relates longitudinal stress or simple tension stress to longitudinal strain in the case when there is no lateral strain. Considering Fig (3.6), Axial modulus will be defined as below:

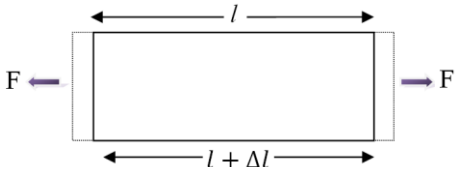

Figure 3.6: Axial Modulus (y) [16]

$$\psi = \frac{longitudinal\ stress(F/A)}{longitudinal\ strain\ or\ uniaxial(\Delta l/l)}. \quad (3.10)$$

3.3.6 Poisson's Ratio (σ)

Poisson's ratio, named after Siméon Poisson is an important physical property which is in use for direct hydrocarbon reservoir indication. Poisson's ratio is the negative ratio of the transverse strain to the axial strain. In certain cases, when an object is compressed, it tends to expand in the other direction perpendicular to this direction. Conversely, if the material is stretched in one direction, they become thicker and it usually tends to contract in the directions transverse to the direction of stretching. This phenomenon is called the Poisson effect.

As is shown in Fig (3.7) in two dimensions, the object will be compressed by force F, the compact size is dl along Z axis and extended size is dr along the perpendicular axis. The Poisson's ratio will be as below.

$$\sigma = -\frac{\text{transverse strain}}{\text{axial strain}} \qquad (3.11)$$

$$\sigma = \frac{\frac{dr}{r}}{\frac{dl}{l}} \qquad (3.12)$$

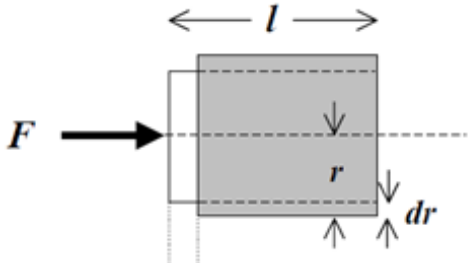

Figure 3.7: Poisson's Ratio (σ) [16]

3.4 Porosity($\emptyset$)

The fractional volume of non rock part of each rock sample to the total rock volume is the porosity of a rock. These non rock volume are include pores, vugs, cracks, inter and intra crystalline spaces and vice versa. Porosity is the primary parameter to estimate the amount of hydrocarbon in a reservoir. Porosity in sands and sandstones varies primarily with degree of connectivity of pores, the size and shape of the grains, distribution and arrangement of packing, cementation, and clay content. To calculate porosity, we have to simulate a sample of rock and calculate bulk volume and volume of matrix. There are four common methods of measuring the porosity of a rock core including buoyancy, helium porosimetry, fluid saturation and mercury porosimetry. In a simple case, porosity can be calculated with following relationship:

$$\emptyset = \frac{V_{pore}}{V_{bulk}} = \frac{V_{bulk} - V_{matrix}}{V_{bulk}} = \frac{V_{bulk} - \left(W_{dry}/\rho_{matrix}\right)}{V_{bulk}}, \qquad (3.13)$$

where:

V_{pore} = *pore volume;*

V_{bulk} = *bulk rock volume;*

V_{matrix} =*volume of solid particles composing the rock matrix*

W_{dry} = *total dry weight of the rock*

ρ_{matrix} = *mean density of the matrix minerals.*

There are several types of defined porosities in hydrocarbon industry including, total porosity, connected porosity, intercrystal porosity, primary porosity, secondary

porosity, micro porosity, intergranular porosity, fracture porosity, moldic porosity, effective porosity, fenestral porosity and Vug porosity. In addition to the initial porosity, secondary porosity is the quantity that has a great impact on the identification of the material. Secondary porosity is arises from mechanical processes and geochemical processes. Mechanical processes will be due to several factors such as stress compaction, plastic and brittle deformation and fracture evolution. Geochemical process also is due to some analysis and volume reductions upon mineralogical changes and vise versa. Four main types of porosity in sandstones are intergranular (primary), fracture porosity, dissolution and microscopy porosity.

The porosity of sands and sandstones is almost 10 - 40 percent. Porosity in carbonate rocks is much more variable than sands and sandstones. In deposited, unconsolidated sediments, porosity may be very high (up to 80%). Most common materials, such as loose sands, can have porosities as high as 45% that are either extremely unstable or stabilized by cements. Similarly, porosities can be very low in massive fractured carbonates as low as 1%.

However, knowing the porosity does not give any information about the distribution of pores, their sizes and their degree of connectivity, thus rocks with the same porosity sometimes show different behavior and physical properties. Therefore, knowing porosity is more useful actually if one knows other quantities too.

3.5 Permeability (μ)

Permeability is the essential quantity to estimate the reservoir characterization in hydrocarbon exploration and exploitation industry. The permeability of a rock is the ability of fluids that can flow easily and it depends on the amount and circumstances

of the connectivity of the pore spaces. In other word permeability depends on the presence of the fluid flow paths that it depends on rock properties such as shape and size of the grains, distributions of pores, frictions between the fluid and the rock, porosity and vice versa.

Further, in some situations pore space may be saturated with two or more fluids such as oil, water and etc. rather than just one fluid , therefore permeability of each fluid depends upon the saturation and properties of each fluid at different rates too. If the rock contains one fluid, its permeability is absolute permeability with maximum amount. If there are two or more fluids in pore spaces, the individual permeability related to each of fluid is called effective permeability. Clearly, theses permabilities will be different from each other and not the same as the permeability of the rock with a single fluid present. The amount of the effective permeabilities are always less than the absolute permeability of the rock of two or more fluids.

Permeability can only be measured on core samples in the laboratory by flowing a fluid of known viscosity in specific sample. Since the actual rock samples have a complex mixture of flows in their structures, we usually assume defined conditions to have a great simplification in the equations. This process can be done to measure pressure drop across the core sample by flowing a fluid of known viscosity through it; moreover the flow rate can be measured by setting the definite pressure on each side of the sample. In 1856 Darcy informed simple experiment to produce an empirical formula for main permeability that is used in the oil industry today yet. Moreover there are several relationships between permeability and different quantity such as porosity, which is available in related material. Here is a schematic of rock that is shown in Fig (3.8).

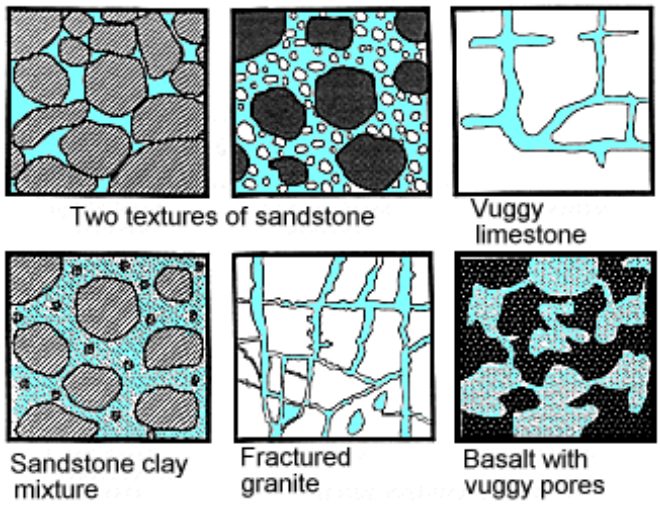

Figure 3.8: Cross-sectional view of several rocks [20]

3.6 Resistivity(ρ)

Resistivity is an electrical property of the subsurface that is more useful in geothermal exploration to distinguish characterize of reservoirs. This quantity is the most effective to identify the composition of the liquids in reservoirs. Resistivity is related to electrolytic, and conductivity property of material describing how well that material allows electric currents to flow through it. Conductivity (κ) is the inverse of resistivity (ρ) is given by ($\kappa=1/\rho$) in units of siemens per meter (S/m) that shows the ability of a material to conduct or transmit heat, electricity, or sound. The electrical resistivity of rocks is related to several properties including the amount of water saturation, salinity of the water, temperature and phase of pore fluid, porosity, permeability, modification of pressure, steam content in the water, and metallic content of the solid matrix.

Much of our understanding about resistivity of porous rocks comes from the oil/gas well-logging industry. Understanding how electrical resistivity (or conductivity) relates to the actual geologic properties of the earth is important. Archie's law is one of main relationship that relates the resistivity of a reservoir to the resistivity of its

fluid saturation. The other great empirical formula is Dakhnov (1962), which connecting temperature relativity with resistivity. The whole relations in this field are available in related material. The specific resistivity ρ is related to the amount of electrical field and the current density. This relation is based on Ohm's law, as is shown below.

$$\rho = \frac{E}{j}, \tag{3.14}$$

where:

ρ *is the specific resistivity* $[\Omega m]$

E is the electrical field, $[V/m]$

j is the current density, $[A/m^2]$

Another relation that relates resistivity, potential difference and current is as below:

$$\rho = \frac{\Delta V}{I}, \tag{3.15}$$

where:

ΔV *is the potential difference,*(v/m)

I is the current, [A]

3.7 Seismic Wave Velocities of Rocks

By virtue of their various compositions, textures (e.g.grain shape and degree of sorting), porosities and contained pore fluids, rocks differ in their elastic moduli and densities and, hence, in their seismic velocities. Information on the velocities of sound in rocks is useful to encounter travel time of rock layers in depths by seismic surveys, moreover it provides several knowledge of the lithology of the rock and the nature of the pore fluids. Rock velocities may be measured in the laboratory and in the field. Laboratory velocity measurement is prepared with a suitable rock sample which is determined by measuring the travel-time of high-frequency (about 1MHz)

acoustic pulses. Since the natural conditions such as temperature, pore fluid pressure, confining pressure or composition cannot be provided completely in laboratory, so the laboratory measurement is unrealistic. Field measurement also will be delineated by seismic surveys of sonic log or continuous velocity log (CVL) with reflecting or refracting interface method through the borehole.

Two types of waves, which are more interesting in analyzing seismic data are included as, primary wave or P-wave and secondary wave or S-wave. Primary wave can travel through any type of material, including solid and fluid. Secondary wave can only travel through solid by moving up and down or side-to-side of rock particles. Since S-wave will not travel through liquid and gas so it cannot travel through the pore spaces, so the derivation of bulk velocity is more complex. This is more interesting that the properties of matrix grain and their texture should be considered for S-wave estimation, while the P-wave velocity is influenced by the pore fluids as well.

In principle, it is beneficial to have both the P-wave and S-wave velocity to detect variations in pore fluid, but historically, most seismic surveying has used only primary waves to simplifying the survey techniques. Primary velocity is a function of some separate properties of the rock, so it is more ambiguous to indicate rock lithologies from the absolute primary wave. Therefore it is crucial to have some relations between velocities and lithology parameters. The equation for both of these two kinds of velocities of various propagation of seismic waves in homogeneous, isotropic, elastic material are described as below. Compression (P-wave) velocity relation will be as:

$$V_p = \left[\frac{appropriate\ elastic\ modulus\ of\ material}{density\ of\ material\ \rho}\right]^{1/2} = \left[\frac{\psi}{\rho}\right]^{1/2}. \quad (3.16)$$

$$\psi = K + \frac{4}{3}\mu, \quad (3.17)$$

$$V_p = \left[\frac{K + 4/3\,\mu}{\rho}\right]^{1/2}, \quad (3.18)$$

$$V_p = \left(\lambda + \frac{2\mu}{\rho}\right)^{1/2}, \quad (3.19)$$

$$\lambda = \rho V_p{}^2 - 2\rho V_s{}^2, \quad (3.20)$$

where:

$V_p = compression\ wave, or\ P\ wave$

$\lambda =$ *first Lamé Elastic Constant for volume.*

$\mu =$ *Shear modulus or Rigidity or second Lamé Elastic Constant for shear*

ρ = *density*

The velocity vs of a shear body wave, which involves a pure shear strain, is given by:

$$V_s = \left[\frac{\mu}{\rho}\right]^{1/2}, \quad (3.21)$$

where:

V_s = *transverse wave, or S-wave*

μ = *elastic modulus*

ρ = *density*

The ratio (Vp/Vs) is an important factor in seismic lithologic determination named as γ.

$$\gamma = \left(\frac{V_p}{V_s}\right)^2 = \frac{K}{\mu} + \frac{4}{3}. \quad (3.22)$$

In terms of Poisson's ratio one can also write:

$$\sigma = \frac{1}{2}\frac{\left(V_p^2 - 2V_s^2\right)}{\left(V_p^2 - V_s^2\right)}. \tag{3.23}$$

The ratio V_p/V_s in any material can be determined by Poisson's ratio as below:

$$V_p/V_s = \left[\frac{2(1-\sigma)}{(1-2\sigma)}\right]^{1/2}. \tag{3.24}$$

Moreover by rearranging there formula we will have:

$$\xrightarrow{\gamma = \left(\frac{V_p}{V_s}\right)^2} \sigma = \frac{\gamma - 2}{2(\gamma - 1)}, \tag{3.25}$$

$$\xrightarrow{\sigma = \frac{\gamma-2}{2(\gamma-1)}} \gamma = \frac{2\sigma - 2}{2\sigma - 1}. \tag{3.26}$$

Since Poisson's ratios for different rocks are definite, therefore using this relation, the ratio V_p/V_s will be defined, conversely the V_p/V_s ratio is independent of density and can be used to derive Poisson's ratio, which is a much more diagnostic lithology indicator, however this relation will be a useful quantity to reservoir identification

This equation also shows that V_p/V_s is greater than 1, so P-wave velocity is greater than S-wave velocity , which typically is around 60% of that of P-waves in any given material.

3.8 Empirical Relationships among the Various Parameters

There are several theoretical relations between velocities and some physical parameters including Poisson's ratio, density, porosity, the rock matrix, and fluid content which are available in reference material, but some of them are introduced in this chapter. To relate rock velocities to lithology, we have to consider rocks as isotropic and uniform medium with idealized pore geometries. Hence, it must consider two steps during the reservoir studies. One is establishing dry or water saturation using empirical relations among velocities, porosity and vice versa, the

other is using Gassmann's relations to map these empirical relations to other pore fluid states.

3.8.1 Relationship between P-wave Velocity and S-wave Velocity

Knowing the relationship between primary and secondary velocity will be used to predict each of velocities when only one of these quantities is defined. Empirical relationship Vp/Vs is useful to identify other quantities of seismic data such that a Vp-Vs relationship derived from modeling must be compared with empirical Vp-Vs from laboratory data as well as from well logging data. In order to have a broaden picture we will introduce some empirical relations presented between P-wave and S-wave velocities. Two maim experimental relations between P-wave and S- wave are Castagna and Krief Relationship that show a linear relationship between P-wave and S-wave velocity that derived from linear plotting to bore-hole measurements by Castagna et al. (1985) which is:

$$V_p = cV_s + d, \tag{3.27}$$

where the velocity is in km/s and this is the equation of straight line called as the mudrock. The values of c and d are different for different rocks that are presented by people based on their observations. In a much simpler empirical relationship between these two parameters Castagna suggested a relationship for small grained rocks such as mudstones as below:

$$V_p = 1.16V_s + 1.36; Castagna's\ relationship \tag{3.28}$$

Pickett,1963 and Milholland, 1980 offered those coefficients in the limestone at low speeds as:

$$V_p = 1.9V_s; Pickett\ and\ Milholland\ relationship \tag{3.29}$$

this equation is comfort for speeds less than 1.5 km/s, for speeds greater than 1.5 km/s , the least square method is presented by Castagna et al. is suited, which is:

$$V_s = -0.05509V_p^2 + 1.0168V_p - 1.030 \quad (3.30)$$

Castagna and Thomas gave the following equation for the sandstone and shale, that are Coincident of the Castagnas's laboratory measurements are:

$$V_s = 1.16V_p - 0.8559;\ for\ sandstone \quad (3.31)$$

$$V_s = 0.7700V_p - 0.8674;\ for\ shale \quad (3.32)$$

Han (1986), presented a similar relationship that was obtained from 75 rock samples,which was consistent with Castagna and Thomas relation as:

$$V_s = 0.7936V_p - 0.7868; for\ shale \quad (3.33)$$

Investigations on several other compounds such as dolomite in a certain area have shown a similar relationship too. There is the appropriate relation between P-wave reflectivity $\left(\frac{\Delta V_p}{V_p}\right)$ and S-wave reflectivity $\left(\frac{\Delta V_s}{V_s}\right)$ that is often reliable techniques to V_s prediction. Taking Castagna equation, we will obtain:

$$\left(\frac{\Delta V_p}{V_p}\right) = \gamma c \left(\frac{\Delta V_s}{V_s}\right);\ \gamma = \frac{V_s}{V_p} \quad (3.34)$$

As a result, V_p/V_s is a useful parameter in identifying of the reservoir. As a short instance, this parameter is more different in gas saturated reservoir and salt saturated reservoir rock in high speed, while, it is not more different in low speeds. Besides, based on laboratory observations presented in several papers, V_p/V_s is greater in feldspar sandstone than quartz sandstone, besides V_p/V_s is approximately 1.5 in gas sandstone and vise versa. There are some reference tables that collect the amount of V_p/V_s base on some observations.

Another relation is the Krief relationship. This relationship is proposed by Krief et al.(1990) that an excellent linear fit will be cross-plotted by squaring of two quantities, which be as below:

$$V_p^2 = aV_s^2 + b\ ;the\ unit\ of\ V_p and\ V_s\ are\ (km/s) \quad (3.35)$$

The coefficients that are determined in various lithologies by Krief et al is summarized here. For wet sandstone, a=2.213 and b=3.857; in gas sandstone, a= 2.282 and b=0.902, In shaly sandstone, a=2.033 and b=4.894, and finally in limestone a=2.872 and b=2.755.

3.8.2 Relationship between Velocity and Density

The prediction of density is an eminent goal of petroleum exploration, since it could be interpreted as a fluid detection parameter. Seismically speaking, we need to investigate a relationship between velocities and rock densities to have a better understanding of Petrophysics, inversion, and a lithology or porosity indicator. Density prediction using both *P*-wave and *S*-wave velocities might improve, if we have both relationship velocities are related to density. Since *Vp* and *Vs* show lithology discrimination, these can be useful for predicting density. Birch (1961) gave the fundamental empirical relation:

$$V_p = a + b\rho, \tag{3.36}$$

where a and b are experimental parameters and Vp is in km/s and ρ is in g/cm^3. Two well-known empirical relationships between primary and secondary velocities, and density are Gardner's equation and Lindseth's equation. Gardner's et al (1974) had been modeled from a series of controlled field and laboratory measurements of brine-saturated rocks such as shales, sandstones, sedimentary and carbonates, that has more been used in seismic analysis and is given by:

$$\rho = aV_p{}^b, \tag{3.37}$$

where a and b are experimental constants which are directly related to the type of rock. For sedimentary rocks, Gardner found that a = 0.23 and b = 0.25, for density in g/cm3 and P-wave velocity in m/s.

From this equation, we can derive the linear relationship between P-wave reflectivity $\left(\frac{\Delta V_p}{V_p}\right)$ and density reflectivity $\left(\frac{\Delta \rho}{\rho}\right)$ as:

$$\left(\frac{\Delta \rho}{\rho}\right) = b\left(\frac{\Delta V_p}{V_p}\right). \tag{3.38}$$

The other equation between P-wave velocity and density is suggested by Lindseth (1979). Lindseth's empirical is based on Gardner's empirical data to derive equation is a linear relation evaluated between impedance and velocity which is as:

$$V_p = a(\rho V_p) + b. \tag{3.39}$$

Considering velocity in m/s, this equation will be:

$$V = 0.308(\rho V) + 105. \tag{3.40}$$

Potter et al.(1998) was derived the S-wave velocity to predict density as a similar equation to the Gardener's equation.This equation is given by:

$$\rho = 0.37\, V_s^{0.22}. \tag{3.41}$$

From this equation, we can derive the linear relationship between S-wave reflectivity $\left(\frac{\Delta V_s}{V_s}\right)$ and density reflectivity $\left(\frac{\Delta \rho}{\rho}\right)$ as:

$$\left(\frac{\Delta \rho}{\rho}\right) = 0.22\left(\frac{\Delta V_s}{V_s}\right). \tag{3.42}$$

Moreover, some studies show that Lindseth's relationship that is discussed above is suitable for S-wave predicting; besides it is even more appropriate in some situations than P-wave velocities. The above empirical relationships may not be held for all positions, but there are common correlation between density and velocity.

Another important equation to relate density and velocity is derived by Wyllie to determine the density and velocity for single mineral type with two fluids, water and a hydrocarbon, filling the pores. Wyllie's equation for bulk density will be as:

$$\rho_b = \rho_m (1 - \emptyset) + \rho_w S_w \emptyset + \rho_{hc}(1 - S_w)\emptyset, \quad (3.43)$$

where:

S_w *is water saturation*

ρ_w *is water density*

ρ_{hc} *is hydrocarbon density*

ρ_b *is bulk density of the rock*

ρ_m *is rock matrix density*

ρ_f *is fluid density*

$\emptyset$ *is porosity of the rock*

Fig (3.9) shows a graph of density versus water saturation in a gas and oil reservoirs with porosity of 25%, gas density of 0.001 g/cc and oil density 0.8 g/cc. As is shown in this figure, density drops much more faster in the gas reservoir than the oil reservoir.

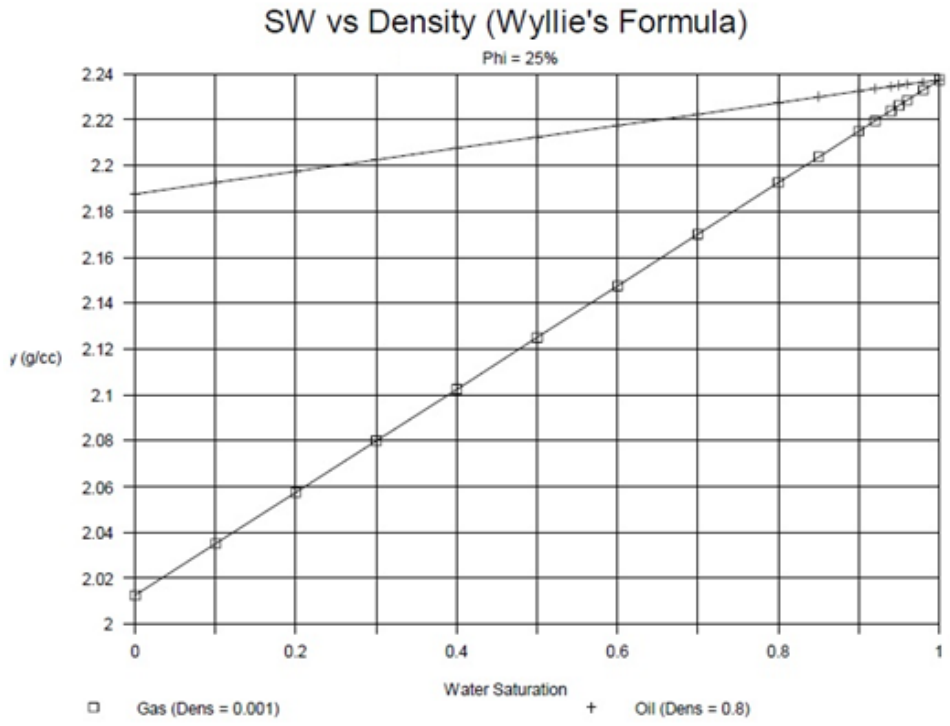

Figure 3.9: Wyllie's equation applied to an oil and gas reservoir [20]

3.8.3 Relationship between Velocity and Porosity

Numerous studies have been shown a relationship between primary velocity and porosity for a variety of sediment and rock types. One of the earliest and most widely used for relationship between porosity and velocity is the Wyllie time-average equation (Wyllie et al., 1958). This equation was proposed by Wyllie, Gregory and Gardner in 1956. The equation for single mineral type is as follows:

$$\frac{1}{V_{p_{rock}}} = \frac{\emptyset}{V_{p_{fluid}}} + \frac{1-\emptyset}{V_{p_{matrix}}}. \tag{3.44}$$

For overall rock matrix with several fluids filling the pores, this equation will be:

$$\frac{1}{V_{p_{rock}}} = \sum_{i=1}^{N} \frac{X_i}{V_{p_{matrix_i}}} + \frac{\emptyset}{V_{p_{fluid}}}, \tag{3.45}$$

where:

$\emptyset$ = *bulk porosity;*

$V_{p_{rock}} = bulk\ rock\ velocity;$

$V_{p_{fluid}}$ = *fluid velocity;*

$V_{p_{matrix}} = matrix\ or\ solid\ grain\ velocity;$

$X = the\ fractional\ volume\ of\ a\ mineralogical\ component\ in\ the\ rock$

Rearranging this equation as a term of interval travel-times, one can rewrite this equation as:

$$\Delta t = \emptyset\Delta t_{fluid} + (1-\emptyset)\Delta t_{matrix}, \tag{3.46}$$

where:

Φ= is the total porosity

Δt= the measured interval travel-time

Δt_{matrix} *= the interval travel-time of the rock matrix*

Δt_{fluid} *= the interval travel-time of the saturating fluid.*

As an instance for two fluids filling the pores such as water and hydrocarbon, willie's equation will be:

$$1/V_b = (1\text{-}\emptyset)/V_m + S_w\emptyset/V_w + (1\text{-}S_w)\emptyset/V_{hc}, \quad (3.47)$$

where:

V_b = *bulk velocity,*

V_{hc} = *hydrocarbon velocity,*

V_m = *matrix velocity*

V_w = *water velocity*

A plot of P-wave velocity versus water saturation of Wyllie's equation for the porous gas and oil sands of differing water saturation is given in Fig (3.10).

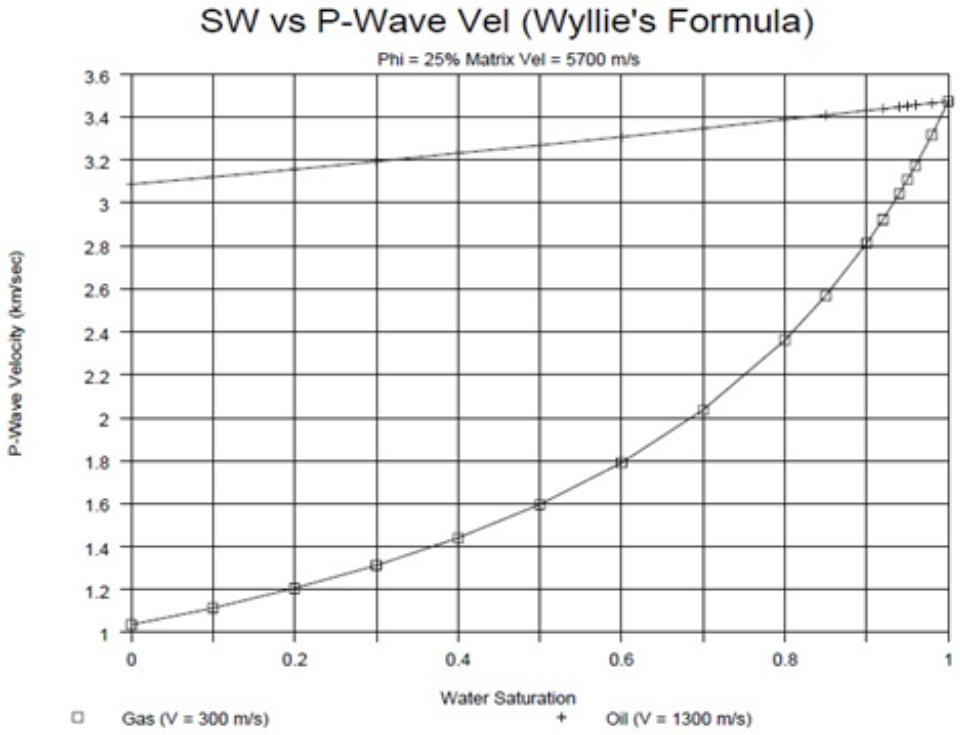

Figure 3.10: P-wave velocity - water saturation graph of gas and oil sands [20]

3.9 Fluid Replacement Theories

Fluid and Lithology substitution could be considered as the heart of rock physics. To find fluid substitution in sands, it is essential to predict how the seismic velocity depends on the pore. Biot's and Gassmann's fluid substitution methods is greatly used for predicting the frequency-dependent velocities of saturated rocks based on the velocities from dry rock, and describe its fluid dispersion for saturated rock. The initial conditions in the formulation are such that we have a statistical isotropy of the pore space with homogeneous bulk and shear moduli in all minerals, but it is free of assumptions about the pore geometry.

3.9.1 Gassmann's Relations

Gassmann's relations (Gassmann, 1951) are simple, and widely used to estimate a rock modulus by a change of pore fluids. This relation is used at sufficiently low frequencies usually. The low-frequency Gassmann–Biot (Gassmann, 1951; Biot, 1956) theory predicts bulk modulus (K_{sat}), of the saturated rock using the following equation:

$$\frac{K_{sat}}{K_0 - K_{sat}} = \frac{K_{dry}}{K_0 - K_{dry}} + \frac{K_{fl}}{\emptyset\left(K_0 - K_{fl}\right)} \ , \ \mu_{sat} = \mu_{dry} \qquad (3.48)$$

where:

K_{sat} is the effective bulk modulus of the rock with pore fluid

K_{dry} is the effective bulk modulus of dry rock

K_0 is the bulk modulus of mineral material

Making up rock, $K_{fl}$is the effective bulk modulus of pore fluid, ∅is the porosity, μ_{dry} is the effective shear modulus of dry rock, and μ_{sat} is the effective shear modulus of rock with pore fluid. Although we often describe Gassmann's relations to predict saturated rock modulus from dry-rock modulus, the most common problem is to

predict saturated rock modulus of one fluid that is replaced with another. One procedure is simple to account the dry state moduli from the initial fluid saturation and then to count another fluid saturated with it. Equivalently, we can relate two saturated-rock modulus in terms of two fluid bulk modulus as follows:

$$\frac{K_{sat1}}{K_0 - K_{sat1}} - \frac{K_{fl1}}{\emptyset\left(K_0 - K_{fl1}\right)} = \frac{K_{sat2}}{K_0 - K_{sat2}} - \frac{K_{fl2}}{\emptyset\left(K_0 - K_{fl2}\right)}, \qquad (3.49)$$

where:

K_{sat1} and K_{sat2} are saturated-rock moduli

$K_{fl1}$and $K_{fl2}$are fluid bulk moduli of two fluids

$K_0$is dry rock modulus.

For two extensions**,** Gassmann's relations can be generalized for partially saturated rocks and mixed mineralogy of rocks that are explained here. For partially saturated rocks at sufficiently low frequencies, one can usually use an effective modulus for the pore fluid that is an isostress average of the moduli of the liquid and gaseous phases.

$$\frac{1}{K_{fl}} = \frac{S}{K_L} + \frac{1 - S}{K_G}, \qquad (3.50)$$

where:

S is the saturation of the liquid phase;

$K_L$and K_G are bulk moduli of the liquid and gas phase.

Brown and Korringa (1975) generalized Gassman's isotropic fluid substitution equations to the case where the solid phase of the rock has mixed mineralogy with equilibrated pore pressures throughout the pore space as:

$$\frac{K_{sat}}{K_s - K_{sat}} = \frac{K_{dry}}{K_s - K_{dry}} + \frac{K_{\emptyset s}}{K_s}\frac{K_{fl}}{\emptyset\left(K_{\emptyset s} - K_{fl}\right)}, \quad \mu_{sat} = \mu_{dry} \qquad (2.51)$$

There are other estimations on Gassman's isotropic fluid substitution for anisotropic rocks and multiple porous constituents and other conditions that are available on related material.

3.9.2 Biot's Characteristic Frequency

Biot (1956) provided theoretical formulas that can be used for estimating saturated-rock velocities from dry-rock velocities to estimate reservoir compaction. Frequency description of Biot's equation (Biot, 1956) is often used to describe the fluids in high frequency while Gassman's equation is used in low frequency. Biot's characteristic frequency (f_c) is the frequency that is defined to describe the transition between high and low frequency by Mavko et al. (2009) as below:

$$f_c = \frac{\emptyset\eta}{2\pi\rho_f k}, \tag{3.52}$$

where, η is fluid viscosity and ρ_f is fluid density, $\emptyset$ is porosity and k is permeability. Lowand middle-frequency (Geertsma and Smit, 1961) is one approximations of his relations is for more accuracy.

Chapter 4

AMPLITUDE VARIATION WITH OFFSET (AVO)

4.1 Introduction

Application of the AVO technique in as a useful exploration method started by Ostrander (1982) with the introduction of his article entitled as " Plane Wave Reflection Coefficients for Gas Sands at Nonnormal Angles of Incidence" at the 52nd annual meeting of the Society of Exploration Geophysicists (SEG). Ostrander (1982, 1984) indicated that the anomalies of seismic reflection amplitudes have specific behavior in gas, this opinion was later called AVO technique. Subsequent follow did with Rutherford and Williams (1989) and Burnett (1990). Moreover, Karl Zoeppritz (1919) had studied previously that the amplitudes of reflected waves from the interfaces of two different sub surfaces may change anomaly for each specific medium and is dependent on the angle of the incident waves. These observations led to the procedure to identification of ground layers named as amplitude variation with angle (AVA). However, in recording seismic data, the distances between shot point and receivers (offsets) are suitable parameter to measurement, so similar technique named as an amplitude variation with offset (AVO) was used as a new technology.

The goal of this method is understanding of the rock properties in reservoir, lithology identification, fluid parameter analysis , shape and structure of the underlying layers of the earth by this fact that the wave amplitude will change in the boundary of layers

by variation of physical properties. AVO is a regular and effective method for hydrocarbon exploration during the 20th century. Most companies use this method as a tool of “de-risk” exploitation targets to estimate the composition of existing hydrocarbon reservoirs to reduce risks in the hydrocarbon industry.

This chapter starts with the concepts of AVO basic. Further subject is on the concept of AVO attributes and introduction of Zoeppritz equation and its approximations, which is the main part of this study. This chapter will finish by a brief view of AVO analysis, and AVO inversion.

4.2 AVO Basics

Amplitude variation with offset is the geophysical method referred to the dependency of the variation of the amplitude to the distances between shot gather and receiver or offsets. AVO analysis is an increasingly attractive technique that geophysicists use to determine lithology and rock fluid contents using pre-stack seismic data for direct hydrocarbon indicator. AVO techniques can be subdivided into two categories as seismic reflectivity and impedance methods. The seismic reflectivity approach includes the study of near and far stacks, intercept vs Gradient and the fluid factor. Impedance approach also include as acoustic and shear impedance, and the elastic impedance. Acoustic and shear impedance include lambda-mu-rho and Poisson impedance.

This study is based on the seismic reflectivity method in AVO technique that is based on the propagation of the energy of the boundary of two different media. When the seismic wave travels into the earth with an arbitrary incident angle and encounters layer boundaries with own velocity and density in each layer, the energy

of the incident wave is partitioned as a P or S reflected and refracted wave in each boundary related to physical properties across the boundary. Using continuity of reflected and transmitted coefficients, some relations would be presented which are used to seismic data inversion and interpretation to have good information about subsurface of the earth. Another necessity is to make a model to process the raw seismic data and perform AVO inversion to actually estimate rock properties from the AVO character of the data. The relations between amplitude variations and reflection and transmission seismic waves will be introduced in following section, critically. One important thing to notice is that, there are several abnormal amplitude anomalies due to unknown factors, which may cause failures in results. Moreover some experiments show AVO method is not suitable in all situations; however this is an accepted approach in the hydrocarbon industry. In recent years, a growing number of theories, processing, and seismic data interpretation has been developed, updated, and employed to introduce credit of this method in the hydrocarbon industry.

4.2.1 Wave Reflection and Refraction Coefficients

As mentioned before, the main theory of AVO technique is based on reflection seismology which describes the separation of insight energy of waves at the boundary of two different layers. This technique will result various elastic properties of reservoirs such as the Poisson's ratio, besides knowing the ratio of P-wave to S-wave velocities implies the differentiation of fluid saturation within the reservoir rocks. Reflection and transmission coefficients of a beam are two useful and determinant factors to indicate characters of material properties. Considering a simple case as is shown in Fig (4.1) when a ray encounters the boundary between two media, part of its energy will reflect as a reflected ray and other part transmits in the medium named as transmitted rays. These coefficients can be defined by their

amplitudes. The reflection coefficient R is the ratio of the amplitude of reflected ray A_1, divided by the amplitude of the incident wave A_0 and the transmission

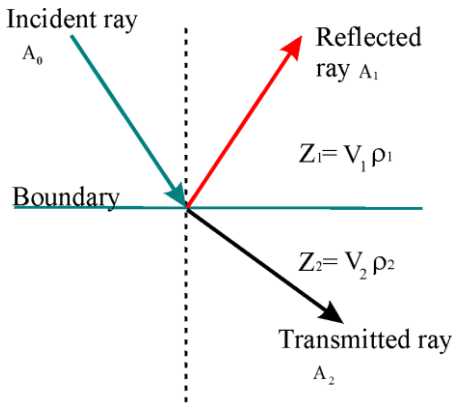

Figure 4.1: Scattered ray in simple case

coefficient T is also the ratio of the amplitude of the transmitted ray A_2 by the amplitude of the incident ray A_0 as below.

$$R = A_1/A_0, \tag{4.1}$$

$$T = A_2/A_0, \tag{4.2}$$

where $R + T = 1$

It should be noticed that some part of energy of incident wave can be transmitted or reflected by different mode, named as mode conversion, which is shown in Fig (4.2). This separation of the energy is a function of incident angle or similarly is a function of the distances between the source and receivers named as offset.

Considering an incident plane-wave at the interface between two semi-infinite isotropic homogeneous elastic media, as is shown in Fig (4.2). This plane-wave will separate into four parts, a reflected and transmitted P-wave and S-wave. These four kinds of velocities are related to angle of incidence by ray parameter (p) in Snell's law, as below:

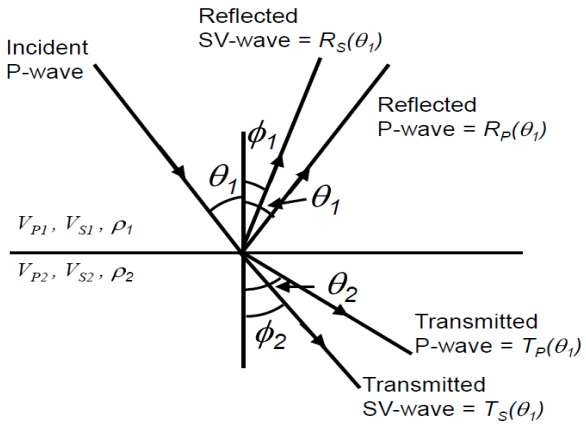

Figure 4.2: Wave reflection and refraction rays [16]

$$p = \frac{sin\theta_1}{V_{p_1}} = \frac{sin\theta_2}{V_{p_2}} = \frac{sin\emptyset_1}{V_{s_1}} = \frac{sin\emptyset_2}{V_{s_2}}, \tag{4.3}$$

where:

$V_{p_1} = P - wave\ velocity\ in\ medium\ 1;$

$V_{p_2} = p - wave\ velocity\ in\ medium\ 2;$

$V_{s_1} = S - wave\ velocity\ in\ medium\ 1;$

$V_{s_2} = S - wave\ velocity\ in\ medium\ 2;$

$\theta_1 = incident\ P - wave\ angle;$

$\theta_2 = transmitted\ P - wave\ angle;$

$\emptyset_1 = reflected\ S - wave\ angle$

$\emptyset_2 = transmitted\ S - wave\ angle.$

It seems that is difficult to have the reflected and transmitted coefficients as the physical properties of reservoirs, moreover is it more complicated to consider all situations of reflection and transmission coefficients by considering their mode conversion together. The formal solution of this physical problem was derived by Zoeppritz (1919) which is the subject of the next section of this study, and here only the basic of his idea will be discussed. The amount of transmitting or reflected coefficients of P or S-wave energies at each layer is also related to the quantity

named as acoustic impedance (Z) rather than wave amplitude, which is the product of density and velocity in each layer given the types of wave as below:

$$Z = \rho V, \tag{4.4}$$

where:

$Z\ is\ accoustic\ impedance,$

$\rho\ is\ density$

$V\ is\ the\ velocity$

Considering a simple case for a normally incident ray encounters the boundary of two homogeneous and isotropic media as is shown in Fig (4.3). The reflection and transmission coefficients related to acoustic impedance is defined as below.

For reflection coefficient, *R:*

$$R = \frac{\rho_2 V_2 - \rho_1 V_1}{\rho_2 V_2 + \rho_1 V_1} = \frac{Z_2 - Z_1}{Z_2 + Z_1}, \tag{4.5}$$

And for the transmission coefficient *T*:

$$T = \frac{2Z_1}{Z_2 + Z_1}, \tag{4.6}$$

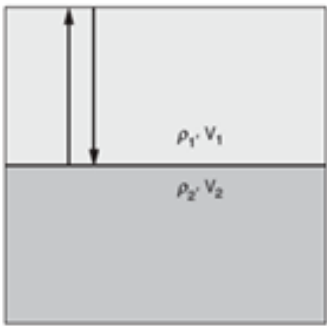

Figure 4.3: Normal incident ray [20]

where:

$\rho_1\ and\ \rho_2\ are\ the\ densities\ of\ the\ first\ and\ second\ mediums;$

$V_1 are\ V_2\ are\ the\ velocities\ of\ the\ first\ and\ second\ mediums;$

$and\ Z_1, Z_2\ are\ the\ accoutic\ impedances\ of\ the\ first\ and\ second\ mediums.$

The other expression of reflection and transmission coefficients is described in terms of energy intensity *I* rather than the acoustic impedance which defined as the amount of energy flowing into a unit normal area in a unit time. Reflection and transmission coefficients are defined as a function of the incident, reflected and transmitted rays intensities, I_0, I_1, I_2 which are as below.

$$R = \frac{I_1}{I_0} = \left[\frac{Z_2 - Z_1}{Z_2 + Z_1}\right]^2, \tag{4.7}$$

$$T = \frac{I_2}{I_1} = \frac{4Z_1Z_2}{(Z_2 + Z_1)^2}. \tag{4.8}$$

As a specific condition in a simple case with just one mode of wave include incident, reflection and transmitted ray, if $R = 0$, in each of the above formula, it means there is no reflection so all the incident energy is transmitted.

4.2.2 AVO Classification

AVO reflection coefficient curves (amplitude-offset or angle) were classified by Rutherford and Williams (1989) for gas sand into three classes. This classification was developed in gas saturated reservoirs. As is shown in Fig (4.4), the slope of the reflection coefficient is negative for all three classes and the amplitude of class 1 is decreased and the absolute values of amplitude are increased in class 2 and 3 toward far offsets. Over several years another researcher named as Castagna recorded new observation in gas saturated anomalies. Castagna et al (1998) claimed that some of amplitudes decrease slowly in gas saturated formation. This category called as class 4 and covers a large set of hydrocarbon amplitude anomalies.

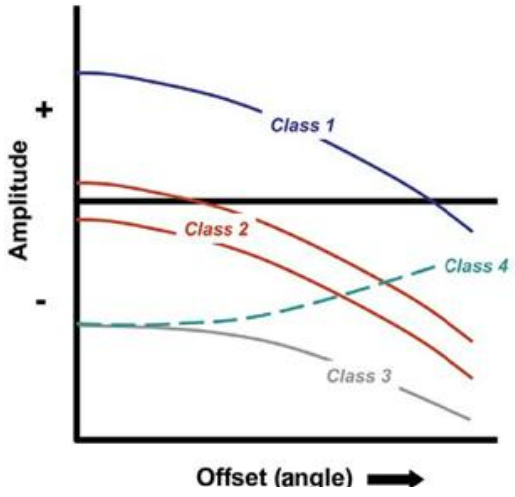

Figure 4.4: Classification of AVO.Rutherford and Williams (1989) and Castagna et al (1998).

AVO class 1 generally is found in hard sands and the value of $R_p(0)$ is positive with large amount and the polarization of waves will change in large offset. AVO class 2 generally is found in shales, which indicates too small impedance and the value of $R_p(0)$ are near zero. If the reservoir is saturated by water or oil, the impedance will be higher than shale. AVO class 3 generally found in gas or light oil and the value of $R_p(0)$ is negative with large amount. AVO class 4 generally found in the wet sands with low densities and its impedance is lower than the shale, moreover $R_p(0)$ decreases slowly or remains flat with increasing offset.

4.3 AVO Attributes

AVO attributes are the quantities derived to indicate the presence or absence of hydrocarbons from seismic data and reservoir rocks that can be analyzed in order to enhance information leading to a better interpretation of geological or geophysical properties of the earth. Some AVO attributes includes as AVO intercept, AVO gradient, intercept multiplied by gradient, far minus near amplitudes, fluid factor and etc. Another method of deriving AVO attributes had been suggested by Zoeppritz (1919), which is relation between the amplitudes of the incident and scattered rays of plain waves from the intersection of two different homogeneous and elastic substances.

4.3.1 Zoeppritz Equations

Knott–Zoeppritz equations (Knott, 1899; Zoeppritz, 1919) that more commonly is named as Zoeppritz equations are included as four formulas with six independent elastic parameters that relate the amplitude variation of incident P- wave or S-wave velocities and densities of the two different materials with the angle of reflection or refracted waves, and later on Koefoed (1955) described the Zoeppritz equations with Poisson's ratio. Due to the complexity of this equation related to the complexity of

the earth, Aki and Richards, 1980 and Castagna, 1993 indicated the matrix form of this equitation. Each of 16 coefficients can be obtained from the below relation.

$$\begin{pmatrix} R_{pp} & R_{sp} & T'_{pp} & T'_{sp} \\ R_{ps} & R_{ss} & T'_{ps} & T'_{ss} \\ T_{pp} & T_{sp} & R'_{pp} & R'_{sp} \\ T_{ps} & T_{ss} & R'_{ps} & R'_{ss} \end{pmatrix} = M^{-1}N, \qquad (4.9)$$

where, $R_{ij}\ and\ R'_{ij}$, are the reflection coefficients and $T_{ij}\ and\ T'_{ij}$ are translation coefficients, and the index 1 and 2 are related to the first and second layers. Moreover the first term *i* in the index indicates incident wave, and the second term *j* indicates output wave, which are shown in Fig (4.5) critically.

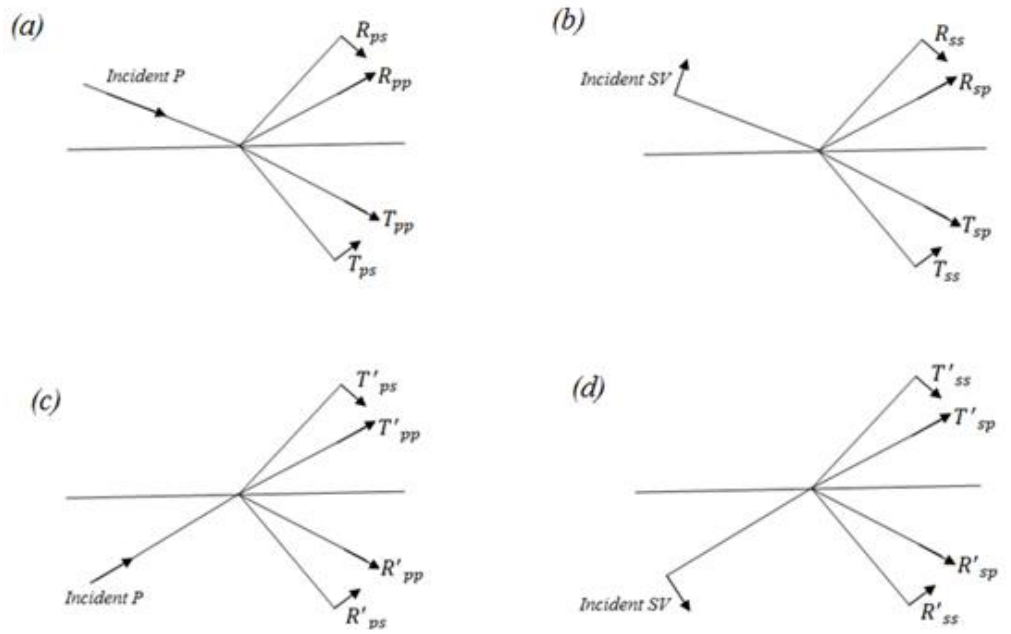

Figure 4.5: Four various types of wave propagation after Aki and Richards, 1980

where M and N will be as below.

$$\text{M}=\begin{pmatrix} -sin\theta_1 & -cos\theta_{s1} & sin\theta_2 & cos\theta_{s2} \\ cos\theta_1 & -sin\theta_{s1} & cos\theta_2 & -sin\theta_{s2} \\ 2\rho_1 V_{s1} sin\theta_{s1} cos\theta_1 & \rho_1 V_{s1}\left(1-2sin^2_{\theta_{s1}}\right) & 2\rho_2 V_{s2} sin\theta_{s2} cos\theta_2 & \rho_2 V_{s2}\left(1-2sin^2_{\theta_{s2}}\right) \\ -\rho_1 V_{p1}\left(1-2sin^2_{\theta_{s1}}\right) & \rho_1 V_{s1} sin2\theta_{s1} & \rho_2 V_{p2}\left(1-2sin^2_{\theta_{s2}}\right) & -\rho_2 V_{s2} sin2\theta_{s2} \end{pmatrix}$$

$$N=\begin{pmatrix} sin\theta_1 & cos\theta_{s1} & -sin\theta_2 & -cos\theta_{s2} \\ cos\theta_1 & -sin\theta_{s1} & cos\theta_2 & -sin\theta_{s2} \\ 2\rho_1 V_{s1} sin\theta_{s1} cos\theta_1 & \rho_1 V_{s1}(1-2sin^2_{\theta_{s1}}) & 2\rho_2 V_{s2} sin\theta_{s2} cos\theta_2 & \rho_2 V_{s2}(1-2sin^2_{\theta_{s2}}) \\ \rho_1 V_{p1}(1-2sin^2_{\theta_{s1}}) & -\rho_1 V_{s1} sin2\theta_{s1} & -\rho_2 V_{p2}(1-2sin^2_{\theta_{s2}}) & \rho_2 V_{s2} sin2\theta_{s2} \end{pmatrix}$$

As mentioned above, Zoeppritz Equation is too complex, which can be evaluated numerically, moreover this equation has not the ability to show the relation between the amplitudes of reflection waves and rock properties, so some approximations of this equation have been made by several researchers, but we will introduce just some outstanding approximations that are useful to the transparency of reservoir characterizations in this section.

4.3.2 Bortfeld Approximation

Bortfeld (1961) simplified Zoeppritz's equation, making it easier to understand how reflection amplitudes depend on the incident angle and physical parameters which emphasis on the fluid and rigidity terms. The first approximation of Zoeppritz equation has been made by Bortfeld (1961). His approximation shows the linear relation between variations of amplitude with the angle of the incident wave as a function of physical rock properties. Bortfeld had considered two terms in their results. The first term covers the variables of P-Wave reflection coefficients of the incident P-wave in fluid-fluid interconnection layers. Another term of Bortfeld approximation named as rigidity term, covers the dependency of S-Wave reflection coefficients of the incident P-wave. The first term of Bortfeld Approximation for $R_{pp}(\theta)$ will be as below.

$$R_{pp}(\theta) \approx \frac{1}{2} ln\left[\frac{V_{p2}\rho_2 cos\theta_1}{V_{p1}\rho_1 cos\theta_2}\right] + \left(\frac{sin\theta_1}{V_{p1}}\right)^2 \left({V_{s1}}^2 - {V_{s2}}^2\right) \times \left[2 + \frac{ln\left(\frac{\rho_2}{\rho_1}\right)}{ln\left(\frac{V_{s2}}{V_{s1}}\right)}\right], \qquad (4.10)$$

where:

V_{p1} *is p-wave velocity in layer1;*

V_{p2} *is p-wave velocity in layer 2;*

V_{s1} *is s-wave velocity in layer 1;*

V_{s2} *is s-wave velocity in layer 2;*

ρ_1 *is density of layer 1;*

ρ_2 *is density of layer 2;*

θ_1 *is insident angle;*

θ_2 *is the angle between transmitted p-wave and perpendicular line.*

This formula's implementation for AVO analysis has not been practical.

4.3.3 Aki, Richards and Frasier Approximation

The Aki, Richards and Frasier approximation is the other first order linear formula that is refined by Richards and Frasier (1976), and Aki and Richards (1980). Their formulas are weighted sum of three terms, P-wave reflectivity ($\frac{\Delta V_p}{V_{pa}}$), S-wave reflectivity $\left(\frac{\Delta V_s}{V_{sa}}\right)$ and density reflectivity ($\frac{\Delta \rho}{\rho_a}$). As an instance the incident P-wave and reflected P-wave, $R_{pp}(\theta)$ is as below.

$$R_{pp}(\theta) = a\frac{\Delta V_p}{V_{pa}} + b\frac{\Delta \rho}{\rho_a} + c\frac{\Delta V_s}{V_{sa}}, \qquad (4.11)$$

where:

a=$1/(2cos^2\theta) = (1 + tan^2\theta)/2$

b=$0.5 - \left[\left(2\,{V_s}^2/{V_p}^2\right)sin^2\theta\right]$

c=$-\left(4\,{V_s}^2/{V_p}^2\right)sin^2\theta$

$V_{pa} = \left(V_{p1} + V_{p2}\right)/2$; *Average of the two P-wave velocities on both sides of the reflector*

$V_{sa} = (V_{s1} + V_{s2})/2$; *Average of the two S-wave velocities on both sides of the reflector*

$\rho_a = (\rho_1 + \rho_2)/2$; *Average of the two densities on both sides of the reflector*

$\Delta V_p = V_{p2} - V_{p1}$ *; P-wave velocity contrast across interface*

$\Delta V_s = V_{s2} - V_{s1}$ *; S-wave velocity contrast across interface*

$\Delta\rho = \rho_2 - \rho_1$ *; Contrast across interface;*

$\theta = (\theta_i + \theta_t)/2$, *where* $\theta_t = arcsin\left[\left(V_{p2}/V_{p1}\right)sin\theta_i\right]$

4.3.4 Aki and Richards Approximation

Since the three separate differential effects in this equation do not seem very practical, so the above formula rearranged by Aki and Richards, to have a function of incident angle and the above reflectivity components. The usefulness of this equation goes to the dependency of this formula to the incident angle that can be calculated from offset, moreover each part of equations can be ignored due to initial conditions. This formula is as below.

$$R_{pp}(\theta) = R_p(0) + Gsin^2\theta + F(tan^2\theta - sin^2\theta), \qquad (4.12)$$

where:

$R_p(0) = \frac{I_{p2}-I_{p1}}{I_{p2}+I_{p1}} \approx \frac{\Delta I_p}{2I_p} \approx \frac{1}{2}\left[\frac{\Delta V_p}{V_{pa}} + \frac{\Delta\rho}{\rho_a}\right]$, $G = \frac{1}{2}\frac{\Delta V_p}{V_{pa}} - 2\left(\frac{V_{sa}}{V_{pa}}\right)^2\left[\frac{\Delta\rho}{\rho_a} + 2\frac{V_{sa}}{V_{pa}}\right]$,

$F = \frac{1}{2}\frac{\Delta V_p}{V_{pa}}$

R(0) is the reflection coefficient at normal incidence and is controlled by the contrast in acoustic impedances, G is named as the AVO gradient and describes the reflection amplitudes at intermediate offsets, and the third term, F, describes the behavior at large angles or far offsets that are close to the critical angle. Other rearranged formula had been by Gelfand and Larner (SEG Expanded Abstracts, 1986, p.335) to have an approximation of P-wave and S-wave reflectivity. For this reason Gelfand and Larner supposed $V_s/V_p = 0.5$, and ignored the third term, this approximation for $R_{pp}(\theta)\ is$ as below.

$$R_{pp}(\theta) = R_p(0) + Gsin^2\theta, \qquad (4.13)$$

where:

$R_p(0) = \frac{1}{2}\left[\frac{\Delta V_p}{V_{pa}} + \frac{\Delta \rho}{\rho_a}\right]$, $G = \left[\frac{1}{2}\frac{\Delta V_p}{V_{pa}} - \frac{\Delta V_s}{V_{sa}} - \frac{1}{2}\frac{\Delta \rho}{\rho_a}\right] = R_p(0) - 2R_s$; $R_{s=}\frac{1}{2}\left[\frac{\Delta V_s}{V_s} + \frac{\Delta \rho}{\rho}\right]$

$R_s = \left(R_p(0) - G\right)/2$

AVO intercept or true P-wave reflectivity, R_p, and gradient, G, are two attributes of AVO in this formula to derive the shear wave reflectivity R_s.

4.3.5 Shuey Approximation

Shuey's approximation (Geophysics 50, 609-614,1985) is an alternative form of Aki, Richards approximation in terms of elastic properties including Poisson's ratio (σ), P-wave velocity (V_p) and density (ρ) as a three-term Shuey equation. This equation for $R_{pp}(\theta)$ will be as:

$$R_{pp}(\theta) = R_p(0) + Gsin^2\theta + F(tan^2\theta - sin^2\theta), \qquad (4.14)$$

where:

$R_p(0) \approx \frac{1}{2}\left[\frac{\Delta V_p}{V_{pa}} + \frac{\Delta \rho}{\rho_a}\right]$, $G = A_0 R_p(0) + \frac{\Delta \sigma}{(1-\sigma)^2}$; $F = \frac{1}{2}\frac{\Delta V_p}{V_{pa}}$

$R_p(0)$ is the reflection coefficient at normal incident

ΔV_p *is* P-wave velocity contrast across interface;

$\sigma = (\sigma_1 + \sigma_2)/2$

$\Delta\sigma = \sigma_2 - \sigma_1$

$A_0 = B - 2(1+B)\frac{1-2\sigma}{1-\sigma}$; $B = \frac{\Delta V_p/V_p}{\Delta V_p/V_p + \Delta\rho/\rho}$

One of the Shuey's main attention is the dependence of the angle of incidence and formulas estimations. The second term indicates the reflection coefficient in middle angle, and the third term indicates the reflection coefficients in critical angle. If the incident angle is less than 30 degree (for small offsets), the third term can be ignored, this is the usual situation which can be considered in Shuey approximation as below:

$$R_{pp}(\theta) = R_p(0) + Gsin^2\theta, \tag{4.15}$$

where $R_p(0)$ is the intercept and G is the AVO gradient which is the slope of AVO model obtained as its the linear regression analysis.

Shuey's equation had been suggested by Hilterman (1989) as a following form.

$$R_{pp}(\theta) = R_p(0)cos^2\theta + B\ sin^2\theta, \tag{4.16}$$

where

$$B = \frac{\sigma_2 - \sigma_1}{(1-\tilde{\sigma})^2} \quad ;\ \Delta\sigma = \sigma_2 - \sigma_1$$

By setting $\tilde{\sigma} = 1/3$, so equation (3.16) will simplify as below:

$$R_{pp}(\theta) = R_p(0)[1 - sin^2\theta] + 9/4\ \Delta\sigma sin^2\theta, \tag{4.17}$$

$$\Rightarrow R(\theta) = R_p(0)\theta + 9/4\ \Delta\sigma sin^2\theta. \tag{4.18}$$

We can get either:

$$R_{pp}(\theta) = R_p + Gsin^2\theta\ ,\ G = 9/4\ \Delta\sigma - R_p. \tag{4.19}$$

By rearranging this equation, the Poisson's ratio changes can be estimated by:

$$\Delta\sigma = 4/9\big(R_p + G\big), \tag{4.20}$$

$R_p$and *G*, are two known attributes in this approximation. This equation also is linear for $R_p - G$ curve.

Other rearranged formula of Shuey's equation had done by Verm and Hilterman (1995) after Fatti approximation (1994), to show the depencency of the rock property and incident partial angle as below.

$$\xrightarrow{(3.12)} \quad R_{pp}(\theta) = R_p(0) + Gsin^2\theta + F(tan^2\theta - sin^2\theta)$$

$$R(\theta) = \frac{1}{2}\left(\frac{\Delta V_p}{V_p} + \frac{\Delta\rho}{\rho}\right)\left(1 - \frac{4V_s^2}{V_p^2}\ sin^2\theta\right) + \frac{\Delta\sigma}{(1-\sigma)^2}\ sin^2\theta$$

$$+ \frac{\Delta V_p}{2V_p}\left(tan^2\theta - \frac{4V_s^2}{V_p^2}\ sin^2\theta\right). \tag{3.21}$$

4.3.6 Smith and Gidlow Approximation

Another approximation of Zoeppritz equation based on Aki and Richard equation is the Smith and Gidlow approximation (1987) by considering Gardner's equation to remove density dependency. This approximation connects some parameters of reservoirs such as density to their weighted stacks $\frac{\Delta V_p}{V_p}$ and $\frac{\Delta V_s}{V_s}$, in correcting seismic gathers. Rearranging the equation (4.14) we will have:

$$R(\theta) = \frac{1}{2}\left[\frac{\Delta V_p}{V_p} + \frac{\Delta \rho}{\rho}\right] - 2\left(\frac{V_s}{V_p}\right)^2 \left[2\frac{\Delta V_s}{V_s} + \frac{\Delta \rho}{\rho}\right] sin^2\theta + \frac{1}{2}\frac{\Delta V_p}{V_p} tan^2\theta. \quad (4.22)$$

Using Gardner's equation ($\rho = aV_p{}^{1/4}$) we can remove density dependency in this equation as below.

Deviating of Gardner's equation we will have :

$$\Delta\rho = \frac{1}{4} aV_p{}^{-3/4}\Delta V_p \rightarrow \frac{\Delta\rho}{\rho} = \frac{1}{4}\frac{aV_p{}^{-3/4}}{\rho}\Delta V_p \xrightarrow{\rho = aV_p{}^{1/4}} \frac{\Delta\rho}{\rho} = \frac{1}{4}\frac{\Delta V_p}{V_p}. \quad (4.23)$$

Substituting equation (3.23) into equation (3.22) we will have:

$$R(\theta) = a\frac{\Delta V_p}{V_p} + b\frac{\Delta V_s}{V_s}, \quad (4.24)$$

Where a and b are derive weights of both $\frac{\Delta V_p}{V_p}$ and $\frac{\Delta V_s}{V_s}$.

$a = \frac{5}{8} - \frac{1}{2}\left(\frac{V_s}{V_p}\right)^2 sin^2\theta + tan^2\theta$ and $b = -4\left(\frac{V_s}{V_p}\right)^2 sin^2\theta$.

One more type of weighted stacks that are obtained from Smith and Gidlow's equation are Pseudo-Poisson's ratio reflectivity. Pseudo-Poisson's ratio reflectivity is a relation between P and S reflectivity as below.

$$\frac{\Delta\sigma}{\sigma} = \frac{\Delta V_p}{V_p} - \frac{\Delta V_s}{V_s}. \quad (4.25)$$

The fluid factor which is a relevant factor to distinct between wet sands and shales to indicate fluid anomalies defined by Smith and Gidlow (1987). This quantity is obtained by deviating of ARCO mudrock equation $\left(V_p = 1360 + 1.16V_s\right)$ as below:

$$\frac{\Delta V_p}{V_p} = 1.16\frac{\Delta V_s}{V_p} \rightarrow \frac{\Delta V_p}{V_p} = 1.16\frac{\Delta V_s}{V_p} * \frac{V_s}{V_s} \implies \frac{\Delta V_p}{V_p} = 1.16\frac{V_s}{V_p}\frac{\Delta V_s}{V_s}, \tag{4.26}$$

however, the fluid factor ΔF is defined as below:

$$\Delta F = \frac{\Delta V_p}{V_p} - 1.16\frac{V_s}{V_p}\frac{\Delta V_s}{V_s}. \tag{4.27}$$

4.3.7 Fatti Approximation

The Fatti et al. (1994) approximation is another approximation of Aki and Richards formula as a function of P-wave reflectivity impedance $\frac{\Delta I_p}{I_p}$ and S-wave reflectivity impedances $\frac{\Delta I_s}{I_s}$ as below.

$$R_{pp}(\theta) = a\,\frac{\Delta I_p}{I_p} + b\,\frac{\Delta I_s}{I_s} + c\,\frac{\Delta \rho}{\rho}, \tag{4.28}$$

where:

ρ *is density*

$I_p = \rho V_p$ *; P- wave acoustic impedance*

$I_s = \rho V_s$ *; S- wave shear impedance*

$a = \frac{1}{2}\left(1 + \tan^2\theta\right)$

$b = 4\frac{V_s^2}{V_p^2}\sin^2\theta$

$c = 2\frac{V_s^2}{V_p^2}\sin^2\theta - \frac{1}{2}\tan^2\theta$

Poisson's ratio reflectivity can be defined from this approximation same as the Smith and Gidlow approximation as below:

$$R_\sigma = \frac{\Delta\sigma}{2\overline{\sigma}} = I_p - I_s. \tag{4.29}$$

Fluid factor also is same as the Smith and Gidlow approximation as:

$$\Delta F = I_p - gI_s\,; g = 1.16\big(V_s/V_p\big). \tag{4.30}$$

Goodway et al.(1998) gave another estimation of Fatti approximation for small angles, so that the third term will be vanished, and thereby introduce two attributes such as below.

$$R_{pp}(\theta) = \frac{1}{2}(1 + \tan^2\theta)\,\frac{\Delta I_p}{I_p} - 4\frac{V_s^2}{V_p^2}\sin^2\theta\,\frac{\Delta I_s}{I_s}, \tag{4.31}$$

Goodway attributes are Lame's constant multiple by density $\lambda\rho$ and shear modulus multiple by density as below.

$$\mu\rho = I_s^2, \tag{4.32}$$

$$\lambda\rho = I_p^2 - 2\,I_s^2, \tag{4.33}$$

$$\mu\rho = I_s^2. \tag{4.34}$$

4.3.8 Gray Approximation

Gray et al. (1999) derived another equation based on Zoeppritz equation including reflectivity bulk modulus K, reflectivity shear modulus μ, and reflectivity bulk density ρ . For p- p reflectivity, $R_{pp}(\theta)$, will be as below.

$$R_{pp}(\theta) = \left(\frac{1}{4} - \frac{1}{3}\frac{\bar{V}_s^{\,2}}{\bar{V}_p^{\,2}}\right)(\sec^2\theta)\frac{\Delta K}{K} + \left(\frac{\bar{V}_s}{\bar{V}_p}\right)^2\left(\frac{1}{3}\sec^2\theta - 2\sin^2\theta\right)\frac{\Delta\mu}{\mu}$$
$$+ \left(\frac{1}{2} - \frac{1}{4}\sec^2\theta\right)\frac{\Delta\rho}{\rho}. \tag{4.35}$$

Rewriting this equation in term of reflectivity Lame's coefficient λ, rather than reflectivity bulk modulus K, Equation (4.35) Will be as below.

$$R_{pp}(\theta) = \left(\frac{1}{4} - \frac{1}{2}\frac{\bar{V}_s{}^2}{\bar{V}_p{}^2}\right)(\sec^2\theta)\frac{\Delta\lambda}{\lambda} + \left(\frac{\bar{V}_s}{\bar{V}_p}\right)^2\left(\frac{1}{2}\sec^2\theta - 2\sin^2\theta\right)\frac{\Delta\mu}{\mu} + \left(\frac{1}{2} - \frac{1}{4}\sec^2\theta\right)\frac{\Delta\rho}{\rho}. \quad (4.36)$$

The other kind of reflection and transmission coefficients by considering special conditions have been informed by Ruger (2001) and Aki and Richards (1980), and Gonzalez (2006) , Duffaut et al. (2000), Jilek (2002) and other researchers, which are available in related materials.

4.4 Seismic Analysis and Seismic Inversion

Seismic analysis is a process consists of special acquisition, processing and interpretation studies of a seismic dataset, which most of times are summarized in seismic inversion. Seismic analysis can be categorized in three groups; velocity analysis, amplitude analysis and impedance analysis that are used in relevant problems. Amplitude analysis is used to solve the relative impedance by considering the arrival time and the amplitude of reflected seismic waves at every reflection point. This analysis method that is named as seismic inversion is used to produce detailed models of rock properties and is consist of three kinds including model-based, space-adaptive and discrete spike inversion. Model-based seismic inversion that can be considered as the inverse of forward modeling which sometimes is named as modeling is included as the modeling of the earth properties that can be derived from well log data including velocity, density, thickness and depth in each layer; processing of the models by simulation of physical experiment and finally choosing the best modeled response is another requirement of seismic inversion. The accuracy of the modeled response is related to the initial model and verification of assumptions. One suitable of impedance method is elastic impedance (EI) in near and far angle which is based on the Aki and Richards equation. Seismic inversion is the

method to construct an image to evaluate the diversity of the physical parameters of the interface of subsurface materials including porosity, velocity of sound, fluid saturation, lithology, density and fluid content of the reservoirs with best quality. Several practical methods including fuzzy logic, genetic algorithms and neural networks are used to analysis of seismic data to increase the predictability of results. There are two kinds of problem in inversion, forward problem and inverse problem. Forward problem is direct modeling of a system that indicates the behavior of a system from known physical parameters. There are various adjusted diagrams by several researchers that show the relation between data and physical models which are used to estimate the output data and are available in reference materials. The inverse problem is used to estimate invisible properties from data measurement which is used in applied sciences such as geophysical exploration, usually. Several times forward modeling and inversion apply to have a model with less difference between synthetic trace and the data. There are several techniques in seismic inversion such as pre-stack or post-stack inversion.

4.5 Pre-stack and Post-stack Seismic Inversion

One of the accepted classifications of seismic inversion categories it into two groups as pre-stack or post-stack that are included as several techniques as the seismic colored inversion, post-stack inversion by simulated annealing (SA inversion), pre-stack joint inversion, simultaneous inversion. Each of these methods is valid to derive properties of the reservoir. In post-stack seismic inversion method, the reflection seismic data will transform to acoustic impedance as a property of the reservoirs to estimation of the detailed structural interpretation and earth stratigraphy including lithology, porosity and fluid saturation. On the other hand, in pre-stack seismic inversion three independent elastic properties of the rock including acoustic

impedance, shear impedance and density will be estimated. The combination of pre-stack seismic inversion, petrophysical modeling and seismic modeling is a useful method to address the non-uniqueness problem. Pre-stack method is used in cases that are not suitable with post-stack inversion.

4.5.1 Seismic Colored Inversion

This is the simplest method to have a quick view of the inverted comparable by "Sparse-Spike" method, which result the low frequency components of relative impedance.

4.5.2 Post-stack Inversion

Model-driven inversion and forward modeling are two kinds of SA inversion. Model-driven inversion is based on the comparison between pre-stack real seismic data and synthetic seismic data which are obtained from the initial model of the subsurface. In this type of inversion that is based on forward modeling, an objection function is constructed by comparison of the initial model and the synthetic data with the real data to modify the model to achieve a best fit with the real data. This updated model is the inversion result. A complex model is used to obtain synthetic seismic data in forward modeling by estimation the wavelet and iterative comparison of the log and related seismic segment to achieve the unique impedance solution.

4.5.3 Pre-stack Joint Inversion

Pre-stack inversion can generate both the Compression and shear information such as an acoustic (Ip) and shear (Is) impedances, acoustic and shear wave reflectivity, and Low frequency acoustic and shear impedance of a rock. Having two independent elastic parameters, the ambiguity of the results will be reduced by optimizing misfits and synthetic reflectivity reconstruction.

4.5.4 Simultaneous Inversion

This procedure can be used to gain three elastic parameters including acoustic impedance, shear impedance and density using the pre-stack inversion. Other elastic parameters including V_s/V_p, Poisson's ratio, Poisson reflectivity, $\lambda * \mu$, $\lambda * \rho$ and λ/μ can be attained from these parameters.

4.5.5 Simulated Annealing

In the realm of seismic inversion, the current usage of simulated annealing are in exploration geophysics in several fields including seismic, resistivity, gravity and AVO inversion, seismic modeling, deconvolution, fracture estimation, and vice versa. This method assumes stochastic distribution of elastic parameters and models in order to consider many pairs of them to achieve the best fit of synthetic and real seismic data.

4.6 AVO Inversion

AVO inversion, is the first step in analysis processing, which uses the pre-stack seismic data and well log data by a combination of visual, analytical and modeling processes to measure weighted stacking of each partial stack to estimate reservoir characterizations mostly in oil and gas industries. Since AVO method dealt with the information of each input partial stack with a unique wavelet separately, so stacking process in not suitable process in data analysis, and pre-stack seismic inversion is good choice. The ultimate goal of AVO inversion is to improve seismic data to have a better estimation and more detailed view of the subsurface structure and physical parameters, which is inevitable under certain conditions. Several oil and gas company use AVO inversion to have a better efficiency and quality estimation in rock properties such as porosity in their information to reduce risk in hydrocarbon exploration and exploitation now. AVO analysis and inversion techniques are based

on several algorithms. In AVO inversion one has to provide a model from pre-stack seismic data respect to time or depth by considering reflection amplitude data and well data information. This is one problem in AVO inversion that small change may occur big uncertainty results to estimate parameters, so it is crucial to have more accuracy in choice suitable data in AVO inversion. There are some methods to increase reliability of AVO inversion. Two of them are Cauchy probability distribution and Gaussian probability distribution that can increase the resolution of the estimated parameters using approximations of Zoeppritz equations. In one view the AVO inversion is categorized to four parametric models based on approximations of Zoeppritz equation that are most common to obtain several attributes in AVO inversion including Shuey's 2-term AVO inversion, Smith and Gidlow's 2-term AVO inversion, Fatti's 2-term AVO inversion, Fatti's 3-term AVO inversion. Choosing each of these categorizes or taking the combination of both of them is related to the desired objective and the characterization of subsurface. Each of these models explains specific attributes as below.

4.6.1 Shuey's 2-term AVO Inversion

As was discussed in 3.2.5, the relation between scattered coefficients with incident angle and rock properties to estimate elastic parameters can be inferred by Shuely approximation for intermediate angles ($0 < \theta < 30$ degrees) in terms of AVO Intercept $R_p(0)$ and AVO gradient G as below.

$$\xrightarrow{(3.15)} R_{pp}(\theta) = R_p(0) + G\sin^2\theta, \tag{4.37}$$

$$R_p(0) \approx \frac{1}{2}\left[\frac{\Delta V_p}{V_{pa}} + \frac{\Delta\rho}{\rho_a}\right],\ G = -\frac{2V_s^2}{V_p^2}\frac{\Delta\rho}{\rho} + \frac{\Delta V_p}{2V_p} - \frac{4V_s^2}{V_p^2}\frac{\Delta V_s}{V_s}$$

AVO Intercept $R_p(0)$ and AVO gradient G are two of attributes which can be obtained in CMP gathers from this equation by observed pre-stack seismic data P-

wave reflection coefficient and NMO corrected seismic gather. The other outputs from these attributes are included as Pseudo Poisson's ratio stack, potential hydrocarbon-indicator stack, fluid factor, restricted gradient stack and restricted P-wave stack.

4.6.2 Smith and Gidlow's 2-term AVO Inversion

As was discussed in part 4.3.6, the relation between scattered coefficients with incident angle and rock properties to estimate elastic parameters from the can be inferred by Smith and Gidlow approximation for intermediate angles ($0 < \theta < 30$ degrees) in terms of P-wave reflectivity and S- wave reflectivity , $\frac{\Delta V_p}{V_p}$ and $\frac{\Delta V_s}{V_s}$ as below.

$$\xrightarrow{(3.24)} R(\theta) = a\frac{\Delta V_p}{V_p} + b\frac{\Delta V_s}{V_s}, \tag{4.38}$$

$$\text{for } a = \frac{5}{8} - \frac{1}{2}\left(\frac{V_s}{V_p}\right)^2 sin^2\theta + tan^2\theta \text{ and } b = -4\left(\frac{V_s}{V_p}\right)^2 sin^2\theta$$

P-wave reflectivity and S- wave reflectivity, $\frac{\Delta V_p}{V_p}$ and $\frac{\Delta V_s}{V_s}$ are two of attributes which can be obtained in CMP gathers from this equation by observed pre-stack seismic data smoothed P- wave velocity and S-wave interval velocities or smoothed $\frac{V_s}{V_p}$ ration. Primary outputs from this equation are P-wave and S- wave velocities reflectivity, angle gather and synthetic gather. Secondary outputs are Pseudo-Poisson's ratio reflectivity and fluid factor.

4.6.3 Fatti's 2-term AVO Inversion

As was discussed in part 4.3.7, the relation between scattered coefficients with incident angle and rock properties to estimate elastic parameters from the can be inferred by Fatti et al (1994) approximation for small density contrasts and low

angles in terms of acoustic impedance reflectivity and shear impedance reflectivity, $\frac{\Delta I_p}{I_p}$ and $\frac{\Delta I_s}{I_s}$ from the equation (4.28) as below.

$$R_{pp}(\theta) = \frac{1}{2}(1 + \tan^2\theta)\,\frac{\Delta I_p}{I_p} - 4\frac{V_s^2}{V_p^2}\sin^2\theta\,\frac{\Delta I_s}{I_s}. \qquad (4.39)$$

Acoustic impedance reflectivity and shear impedance reflectivity are two attributes which can be obtained in CMP gathers from this equation by observed pre-stack seismic data.

4.6.4 Fatti's 3-term AVO Inversion

As was discussed in part 4.3.7, the relation between scattered coefficients with incident angle and rock properties to estimate elastic parameters can be inferred by Fatti et al (1994) approximation in terms of acoustic impedance reflectivity, shear impedance reflectivity and density reflectivity , $\frac{\Delta I_p}{I_p}$, $\frac{\Delta I_s}{I_s}$ and $\frac{\Delta \rho}{\rho}$ from the Equation (3.28) as below.

$$R_{pp}(\theta) = a\,\frac{\Delta I_p}{I_p} + b\,\frac{\Delta I_s}{I_s} + c\,\frac{\Delta \rho}{\rho}, \qquad (4.40)$$

$$for\ a = \frac{1}{2}(1 + \tan^2\theta), b = 4\frac{V_s^2}{V_p^2}\sin^2\theta, c = 2\frac{V_s^2}{V_p^2}\sin^2\theta - \frac{1}{2}\tan^2\theta$$

acoustic impedance reflectivity, shear impedance reflectivity and density reflectivity , $\frac{\Delta I_p}{I_p}$, $\frac{\Delta I_s}{I_s}$ and $\frac{\Delta \rho}{\rho}$ are three attributes which can be obtained in CMP gathers from this equation by observed pre-stack seismic data. Smoothed P-wave and S-wave interval velocities and NMO corrected seismic gather of long offsets are as the input data. Moreover, Zero-offset P-wave, S-wave and density reflection coefficients are as output data in this kind of inversion.

4.7 A Glimpse into the Future of the AVO Method

There are several improved approaches in AVO inversion studies which proposed during recent years. Advances in inversion techniques and AVO analysis, would improve the quality of interpretation. One of the best approaches is based on effective reflection coefficients (ERCs) which has more accurately near-critical and post-critical reflections. Another generation of AVO tools is as a multitude of sub-techniques such as WAVO utilizes as a wavelet-based rather than simply by simple, which is for harder rocks, deeper horizons, thinly-bedded or fractured reservoirs and tend to be a more effective technique to have a better accurate prediction of the presence of hydrocarbon.

Chapter 5

AVO MODELLING AND ANALYZING

5.1 Introduction

AVO modeling that is the combination of several sciences including Petrophysics, Rock Physics, Seismology, Geology and Petroleum Engineering, is based on the inversion method for processing and analyzing of the well log data and seismic data to identification of the rock and reservoir properties to predict the lithology and pore fluids using several applicable software, which is applied in the hydrocarbon industry, especially in gas sands. The usual parameters that are obtained from the well logging data including P-wave velocity, S-wave velocity, density and their compounds are combined by some geological factors including gamma ray and water saturation in AVO modeling. The main AVO inversion tutorial of the angle or offset method is the estimation of the synthetic log and its modification to have a best similarity with the measured seismic data logs in order to analyze the variation of the amplitude versus offset by estimate a separate wavelet for each partial stack.

Hampson-Russell is one safe and smart geophysical software that has been used in this study. This program is designed by Dan Hampson and Brian Russell (1987), that can be used in AVO modeling, inversion, processing and analyzing by considering the well log data and seismic data as an initial information. GEOVIEW is one platform that gathers all modules of geophysics Hampson-Russell program for easier

to use, which is included as Well Explorer, seisLoader, eLog, View 3-D, AVO, EMERGE, ISMap, proMC and STRATA.

This tutorial has been done to investigate the potential of amplitude versus offset anomalies technique for determining and estimating of gas zone via a case study on 2-D dimension. AVO Analysis on 3-D Data and further dimensions are other advanced techniques which are based on 2-D data method. The main issues to which they are mentioned in this chapter are the modeling of the available log information including as the log display, synthetic seismic display, seismic trace, stacking and check shot correction, wavelet extraction, amplitude correction, log correction and picks display. Other material of this chapter are as AVO analysis on 2-D data including as intercept and gradient analysis, Poisson's ratio analysis, and creating the cross plot and cross section of the data slices.

5.2 Well Log Display

After opening "GEOVIEW" program, it should be assign a new database to store all the well log information in the desirable location that is necessary to AVO analysis. By importing data of the available well log information, it can be plotted the logs of P-wave, density, gamma ray, resistivity and computed impedance and so on. This process is necessary for future activity in "AVO" module.

5.3 AVO Modeling

"AVO" module which is in the main window of "GEOVIEW" program is used for AVO modeling by creating the new project to store all the AVO modeling results such as seismic data gathers by loading the seismic data. Three important logs that are considered in this project are P-wave, S-wave and density logs that make several visions such that P-wave and density logs are available from well logging, S-wave

log has been specified by Castagna's equation, Poisson's ratio log also will be created by those logs. Since Castagna's equation is suitable only for wet environments, so this model for gas sand is not real log and it have to be modeled by several different calculations. As is shown in the above plot, P-wave and density have been increased sharply under the base-line gas, moreover poison's ration decreases sharply under the gas zone, which indicate the presence of something similar to the wet trend under the base-gas zone.

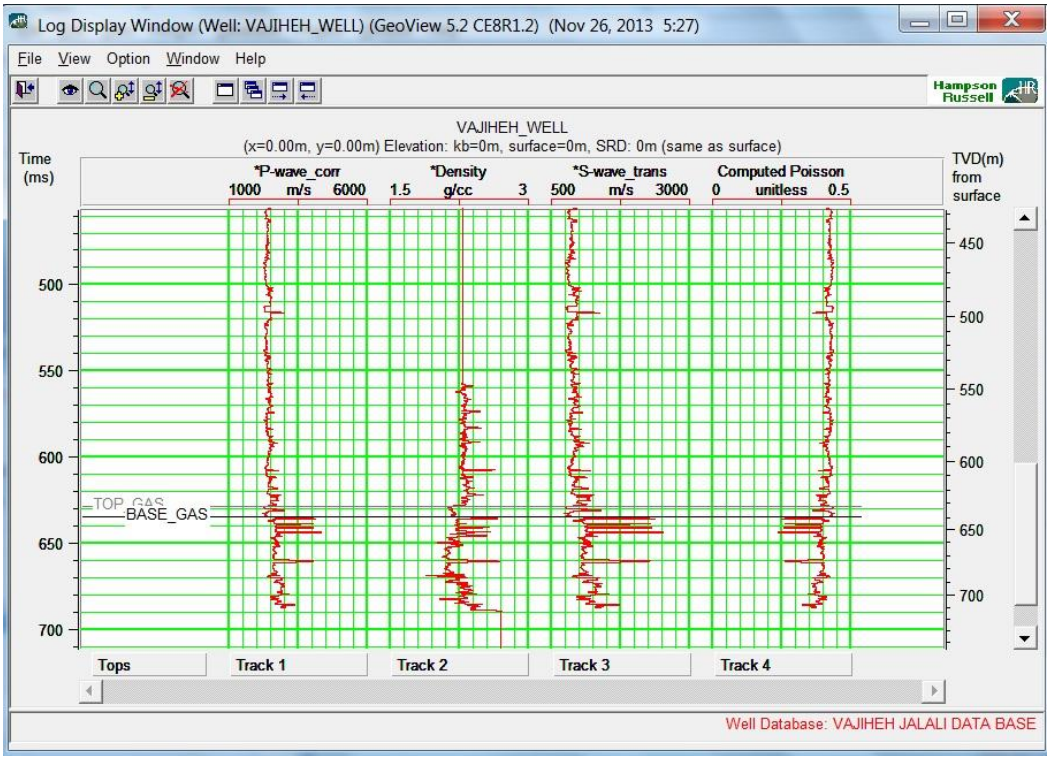

Figure 5.1: Log Display

5.4 Creating a Synthetic Seismic Display

Creating a synthetic seismic display is a process in AVO analyzing that create an offset-dependent synthetic seismic data using ray-tracing from the above logs. This model is initial and unaccepted model which is gaining on the rare data from the log and have to be modified by satisfactory wavelet, which is defined completely, later in this chapter. There are several methods, including Zoeppritz, Aki and Richard, Fatti

approximation and so on. Here it has been chosen the Zoeppritz approximation to make a synthetic seismic trace by the seismic and well log data to calculate the incidence angles and relevant amplitudes by choosing 11 offset between 0 and 600 meters to calculate reflection coefficients in various layers with depth range 600 to 700 meter to have a synthetic seismogram which is clear in the AVO modeling window as below.

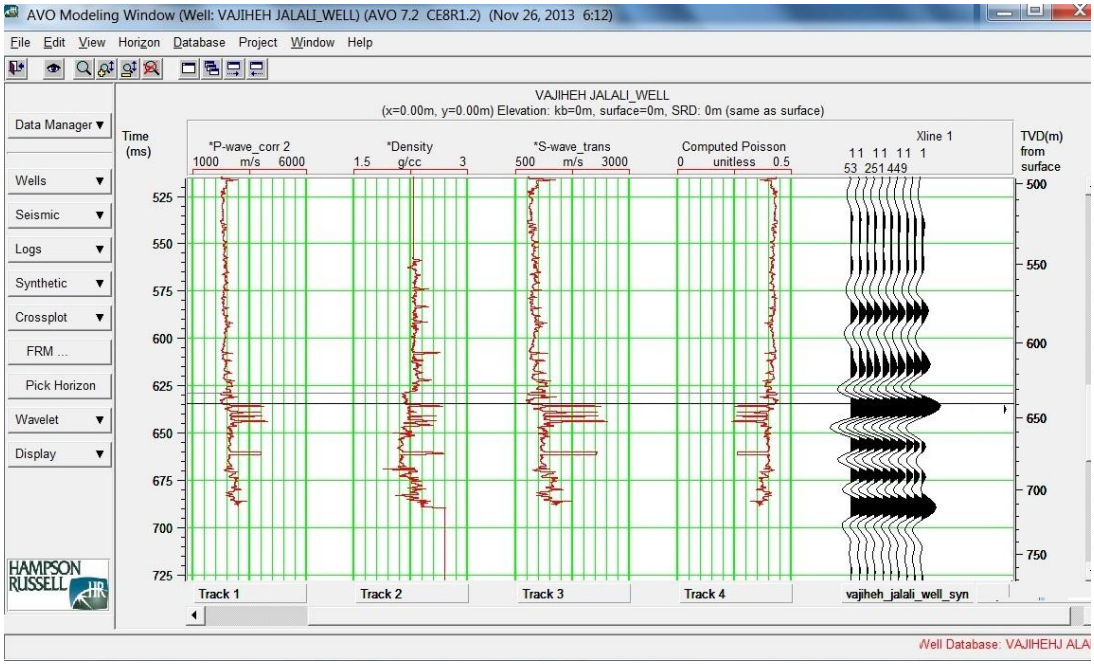

Figure 5.2: Synthetic seismic trace

5.5 Loading Seismic Data

As is shown above, we have a synthetic seismic log that has to be compared with the real seismic log which is available from real seismic data of the well logging process. To do that, we have to import gathers.sgy from SEG-Y file on “Data manager” menu on AVO modeling window. After setting and choosing the location of the CDP and offset values, and several editing, the SEGY volume named as gathers will be plotted in the main AVO window in Fig (5.3). As is shown in this figure, the P-wave log is plotted at CDP 330, which is the estimated location of the well in this case study

using the checking shot method to connect time and depth together. This log is the zero-angle trace that is the convolution of the wavelet and acoustic impedance reflectivity.

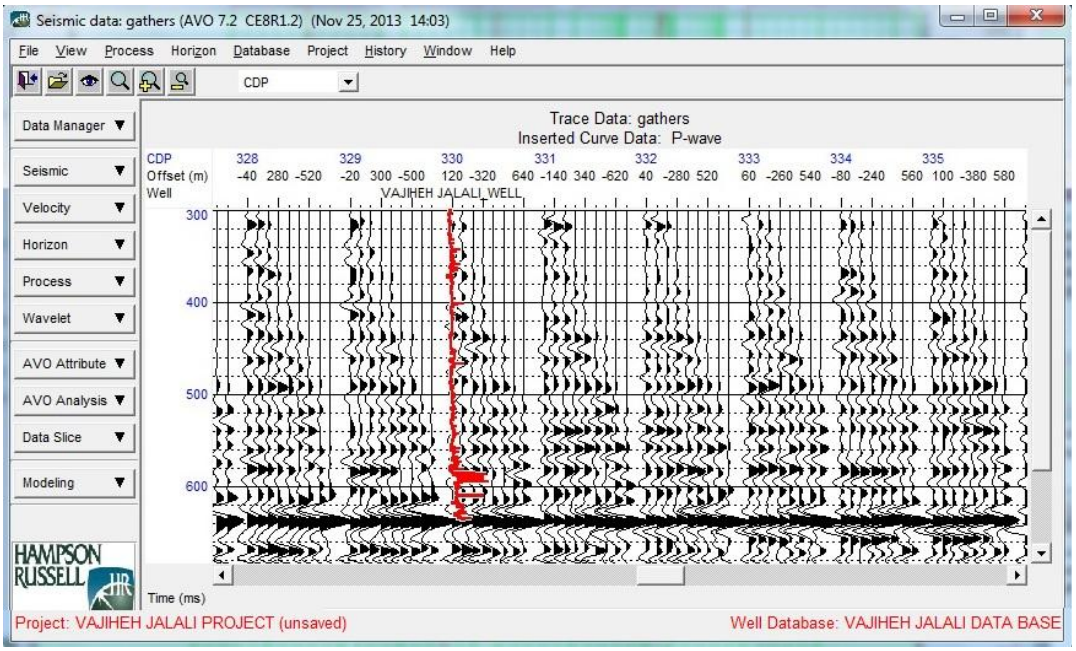

Figure 5.3: Seismic gather trace with inserted P-wave log

5.5.1 CDP Stacked Seismic Trace

Other useful process in AVO analyzing is CDP stack that average the traces of each CDP gathers by choosing “Process” menu on AVO modeling window, which is shown as below. As is shown in the highlighted portion of this snap, the seismic line, which is the average of the series of CMP gathers, shows the ”bright-spot” at 630 ms as a typical class 3 AVO anomaly, which is the location of the gas sand on the log.

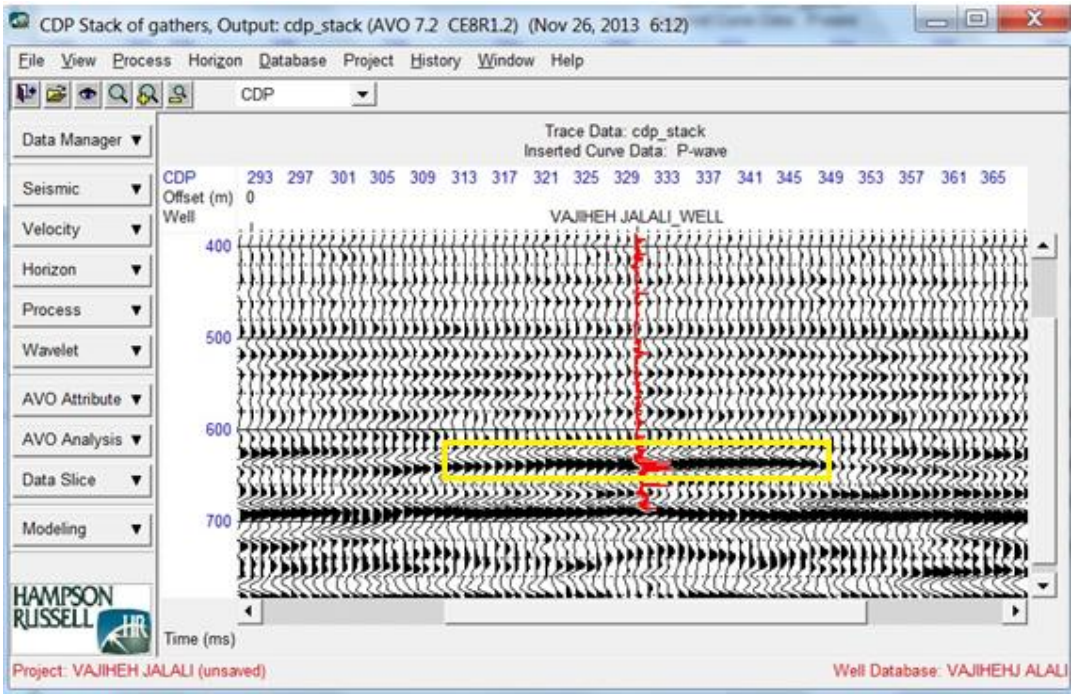

Figure 5.4: CDP stacked seismic trace with inserted P-wave log

5.5.2 Check Shot Correction

By plotting the seismic well log and the previous synthetic well log in the same window as is shown in (Fig 5.5), although it seems that sonic log (P-wave log) and seismic data are two properties that do not cover each other, it can be fixed by some correlations. Check shot correction is one important reason for the difference between synthetic and seismic well logs is that the time scale on these two logs are not the same on both of them so that the same events are not considered in specific time on both of them. This problem will be solved by the check shot correction with modification in depth- time curves, which will be done in the log correlation process.

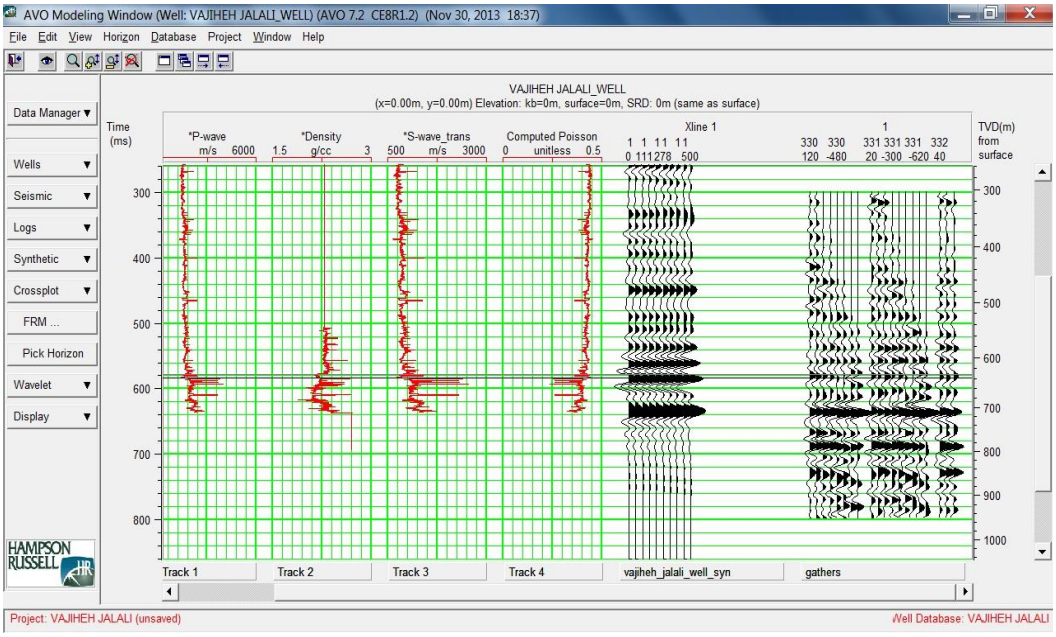

Figure 5.5: Comparison between seismic gather and synthetic trace

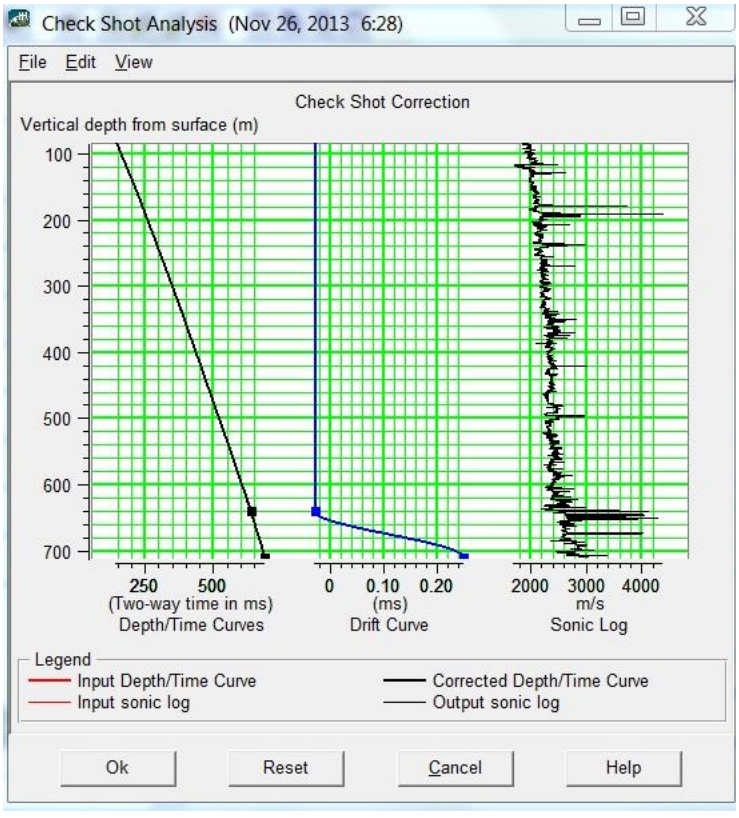

Figure 5.6: Check shot correction

5.5.3 Extracting a Wavelet

The second reason for the difference between synthetic and seismic well logs related to the wavelets that are estimated for each partial stack. Essentially, the frequency and phase variations with offset that are used in the simultaneous AVO inversion can be obtained from theses estimated wavelets that will affect the angle dependent reflectivity logs, moreover the accuracy of the inversion results is dependent to this extracted seismic wavelets. This problem can be solved by two methods of extraction to have a new wavelet. The first method uses both of the correlated well log reflectivity and seismic data to form a relation that depends on both of them. The second method which is used in this activity is related to seismic data only, to form a zero – phase wavelet with seismic-dependent amplitude spectrum which is named as Statistical Wavelet Extraction by choosing "Statistical" option from the "Extract Wavelet" menu by using the only near offset traces to avoid the NMO stretching problem on the wavelet extraction which is shown as below.

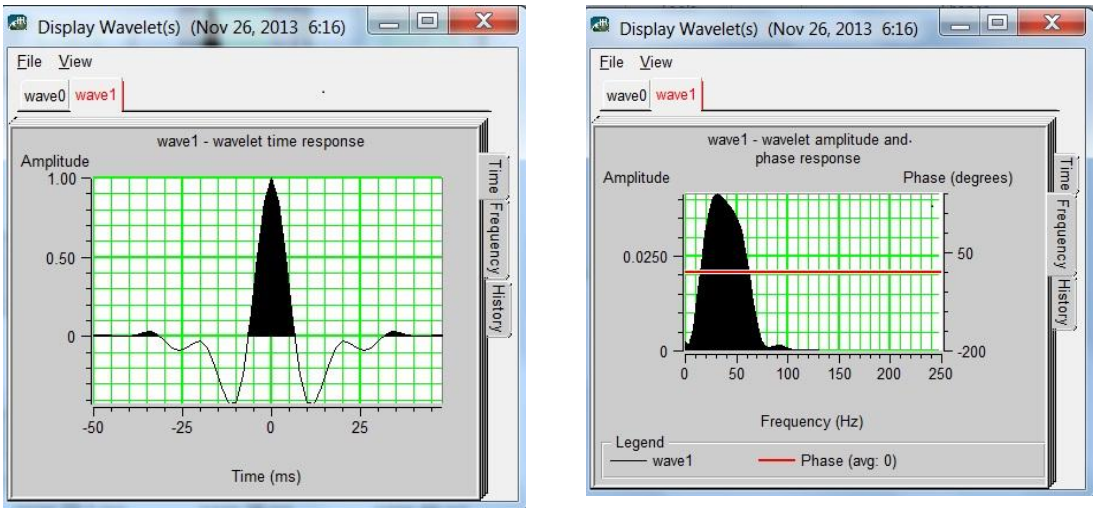

Figure 5.7: Display time and frequency wavelet

Since this statistical wavelet is zero –phase, so it is necessary to use well log wavelet extraction to correct wavelet phase, and the previous synthetic seismic data have to

be modified by this new wavelet to have a better consistent with the real data, by choosing Zoeppritz in “Synthetic” menu as before.

5.5.4 Amplitude Correction

Another difference between synthetic and seismic well log is related to their amplitudes, which is amplitude correction that is applied on synthetic seismic data by the modification of the trace excursion parameter in cases, where significant differences are observed between the synthetic and real seismic amplitudes.

5.5.5 Log Correlation

The other process which is defined here is the depth-time curve correction that is used to have a better synthetic seismic estimation by choosing the “Correlate” option from the “Log” menu which is done here for the near-offset traces to have the best match with the zero-offset synthetic. Both of the modified zero-offset synthetic and the real stacked trace at CDP 330 are shown in the AVO modeling window as below.

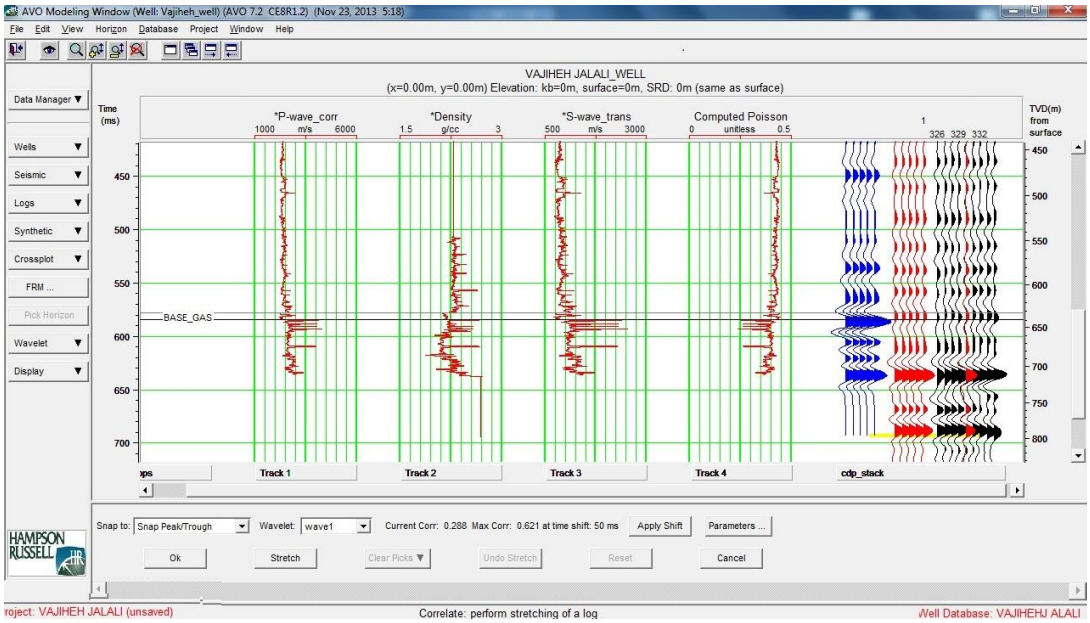

Figure 5.8: Well log and CDP stacked seismic trace

The CDP- stack (blue seismic trace) is the zero-offset synthetic, and the red trace is the average of the real seismic traces and it has to shift and stretch the synthetic trace to be matched to the real trace by clicking on the similar events that makes to connect the peaks together, which is the purpose of the log correlation. The correlation process is shown in Fig (5.9) and Fig (5.10) as below.

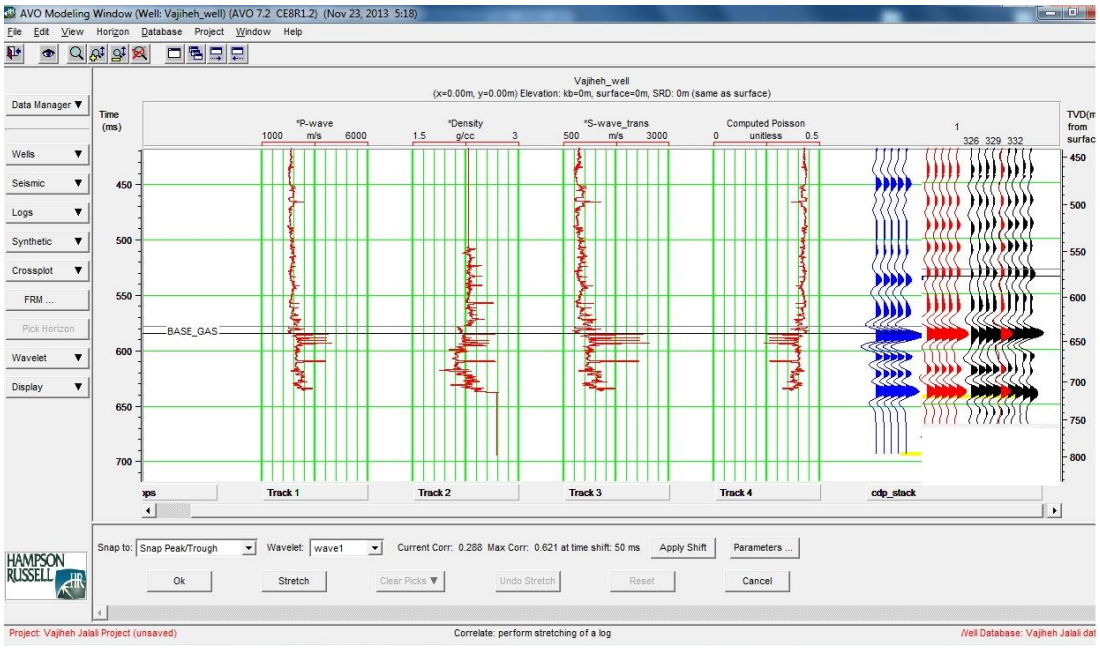

Figure 5.9: Correlated CDP stacked trace

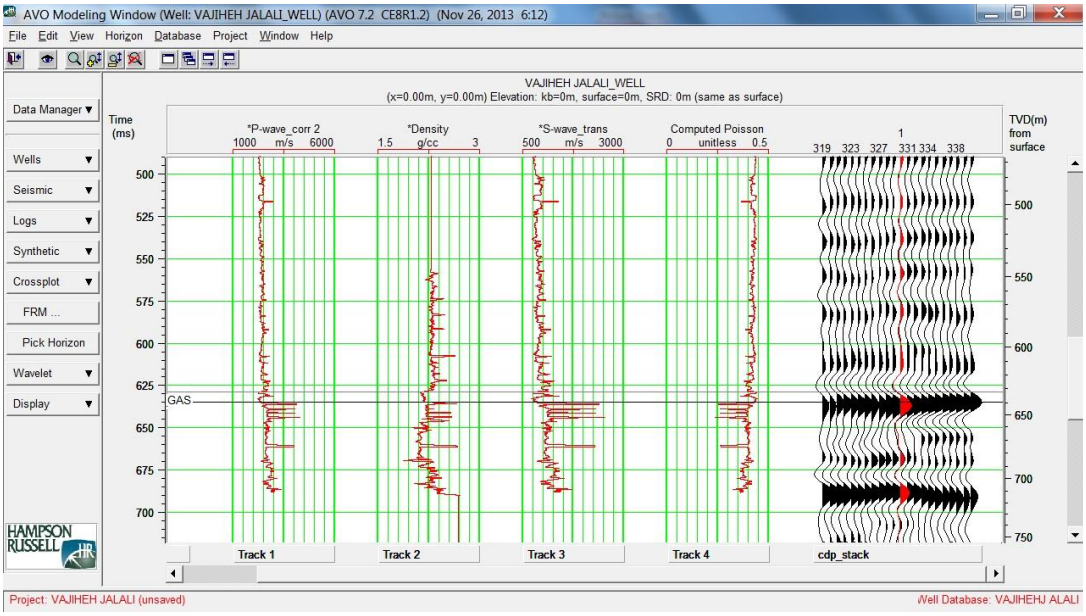

Figure 5.10: CDP stacked trace

This new sonic log or corrected P-wave is the result of those correlations is that is used to create new synthetic seismic trace, which is done by choosing “Zoeppritz” in “Synthetic” menu as before.

5.5.6 Super Gather

The next attempt to create corrected seismic trace is to improve the signal to noise ratio by stacking the data in a small range of input bins, to have the traces with better quality, which is named as super gather. This process will be done by choosing the “Super Gather” menu in “Process” tab that is shown in Fig (5.11). This sonic log shows that the sonic log (P-wave log) and seismic data tie each other, besides it shows the range of the offsets for CDP 330 is between 53 to 647 meters that is used in synthetic process. The other thing which is obtained from this log is the existence of the gas zone between 600 to 650 meters on the CDP 330 that is clear by the bright spots in this area.

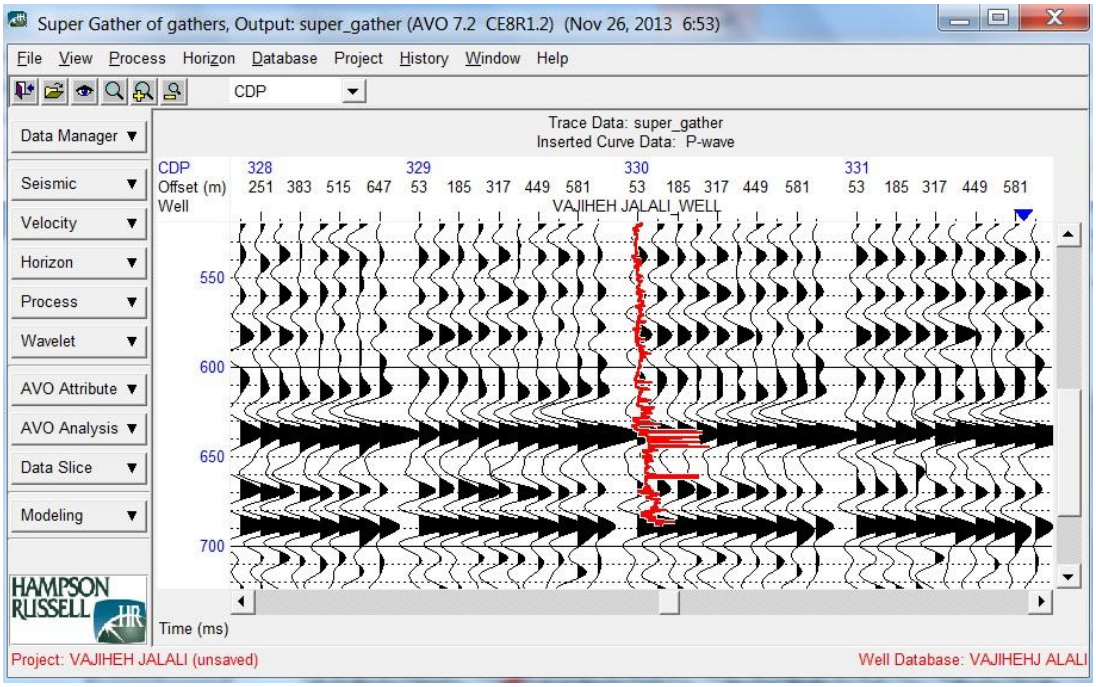

Figure 5.11: Super gather seismic trace

5.5.7 Angle Gather Trace

Since AVO theories use incident angles in their relations, the final process that has to be applied here, is the angle gather that corresponds incident angles to each relevant input sample to make parametric decisions. This process transforms the offset gather to the angle gather by P-wave log, which can be done automatically in Hampson-Russell programs by choosing the angle gathers option on “Process” menu in super gathers window.

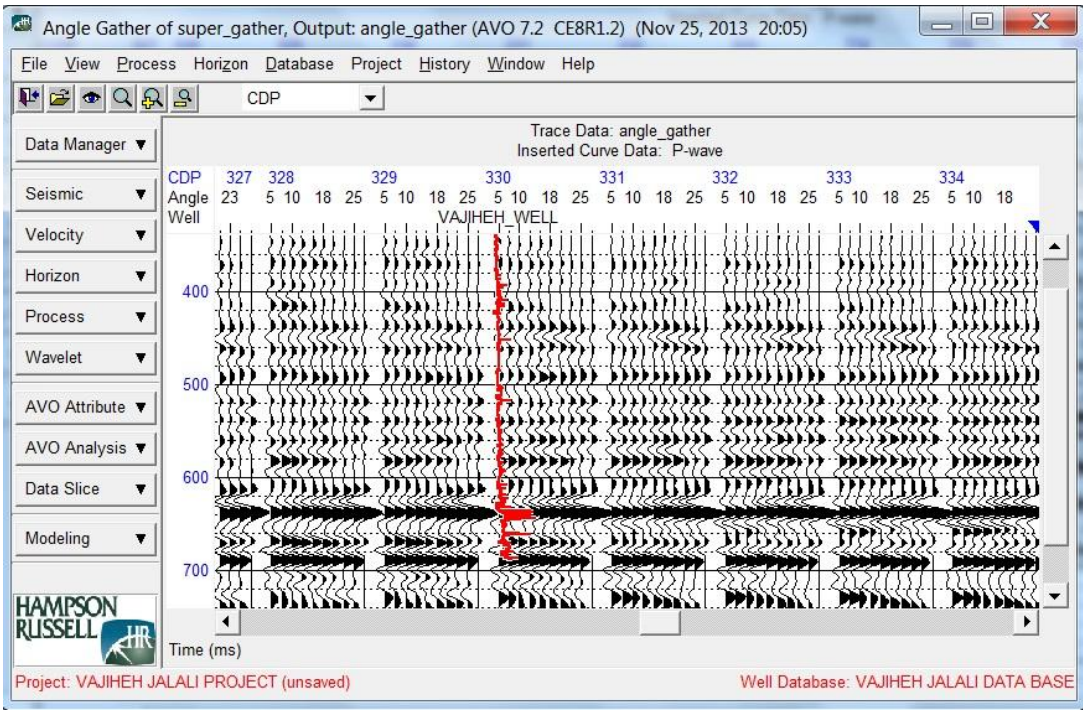

Figure 5.12: Angle gather seismic trace

5.6 Pics Display

Pics display is the process to display a plot of the amplitudes for picking horizons in any seismic window of each desired picked events from real or synthetic data including offset range, amplitude range, normalize options, normalize offset, which indicate more quantitative comparison between synthetic and real seismic traces. This process can be done by choosing Pick Horizone option on the AVO modeling window containing synthetic and super-gather Fig (5.12), and picking under and above the gas sand Fig (5.13) to have the best fit between synthetic and real seismic traces. The final snap is the synthetic and real well log traces , which is displayed be by choosing all these four sets of picks and selecting "AVO picks" option from "Display" menu as is shown in Fig (5.14). As is shown in this figure, the real picks are noisier than the synthetic picks, but they are more comparable and it shows good correlations between those events to examine the amount of gas sand.

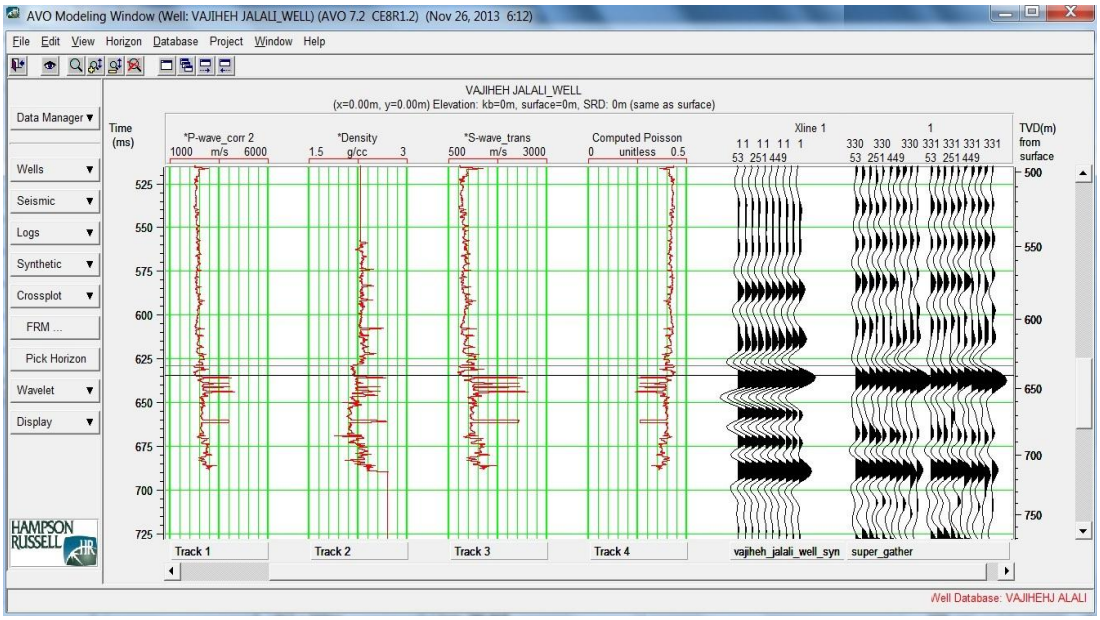

Figure 5.13: Synthetic and super gather seismic traces

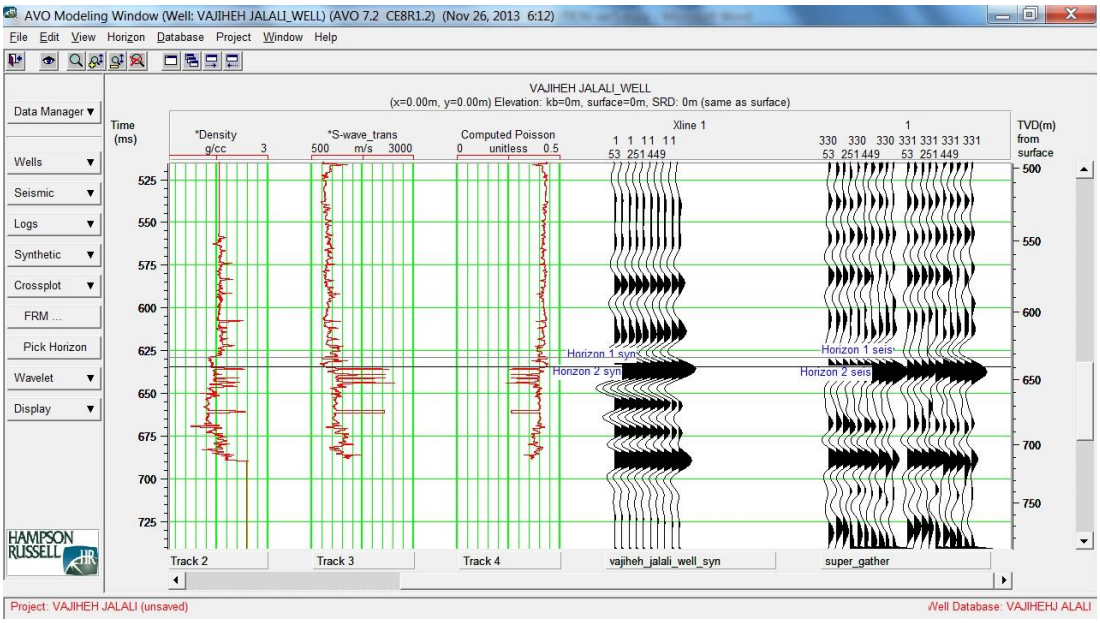

Figure 5.14: Horizon lines in synthetic and super gather seismic traces

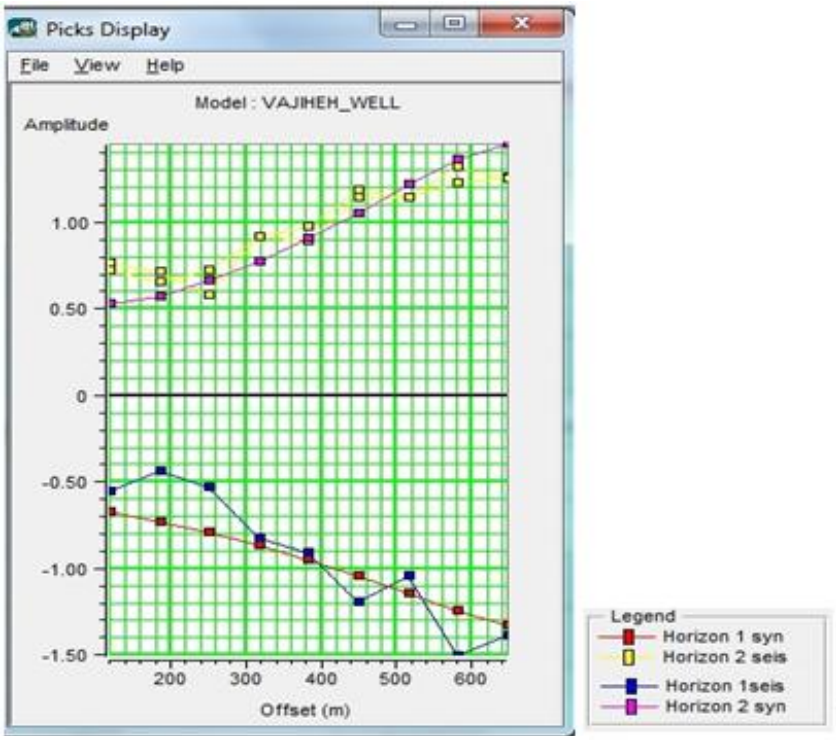

Figure 5.15: Pics Display

5.7 AVO Analysis on 2-D Data

So far we have completed the modeling of this project, and now we want to have analysis of its results. AVO Attributes analysis is the perfect process which is applied on the super-gather trace as below.

5.7.1 The Intercept (A) and Gradient (B) Attributes

The first and important attribute is the calculation of the intercept and gradient attributes by choosing the "AVO Attribute Volume" option from the "AVO Attribute" tab on the super gather window using the well log and the corrected P-wave velocity as a color plot. As is shown in Fig (5.15), the wiggle traces are intercept (A) and the color attribute is the product of intercept and gradient, (A*B), which is the perfect quantity to distinguish between gas and wet in the well.

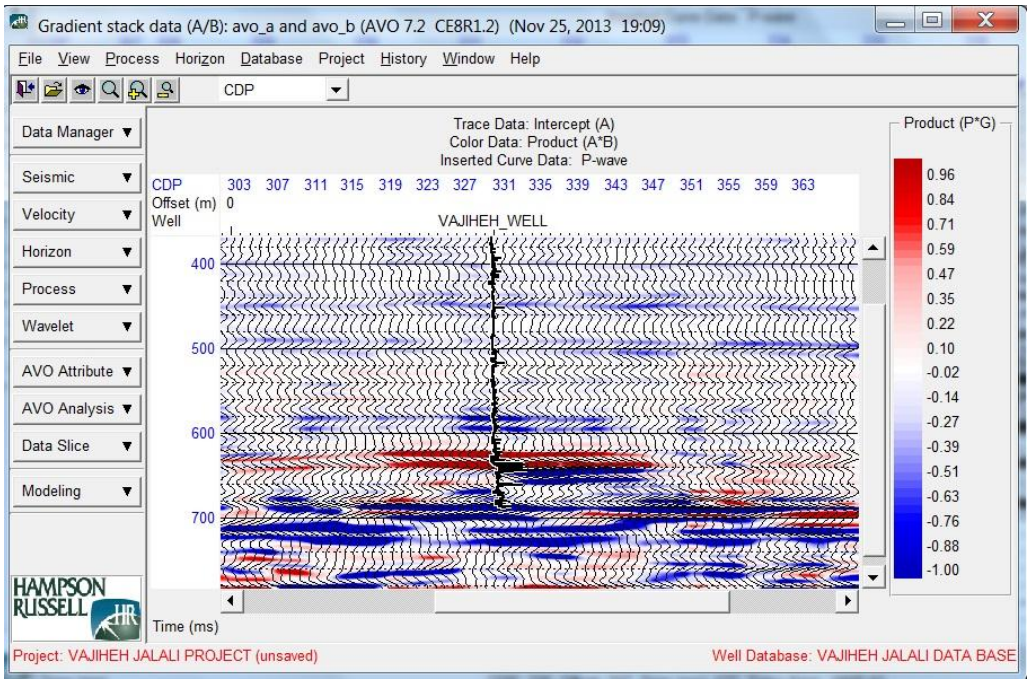

Figure 5.16: Intercept (A) and Gradient attributes plot

As is shown in this figure, the largest red area is on the top and base of the gas sand that is free of the wet, around 630 milliseconds. This process is suitable for the class 3 AVO anomaly to indicate the presence of the gas zones.

5.7.2 Scaled Poisson's Ratio Change Attribute (aA+bB)

The second applied attribute which is characterized by intercept and gradient data is the Scaled Poisson's Ratio Change that is shown with colored parts, which is a good hydrocarbon indicator. This graph is plotted by modifying the Color Data Volume menu as below.

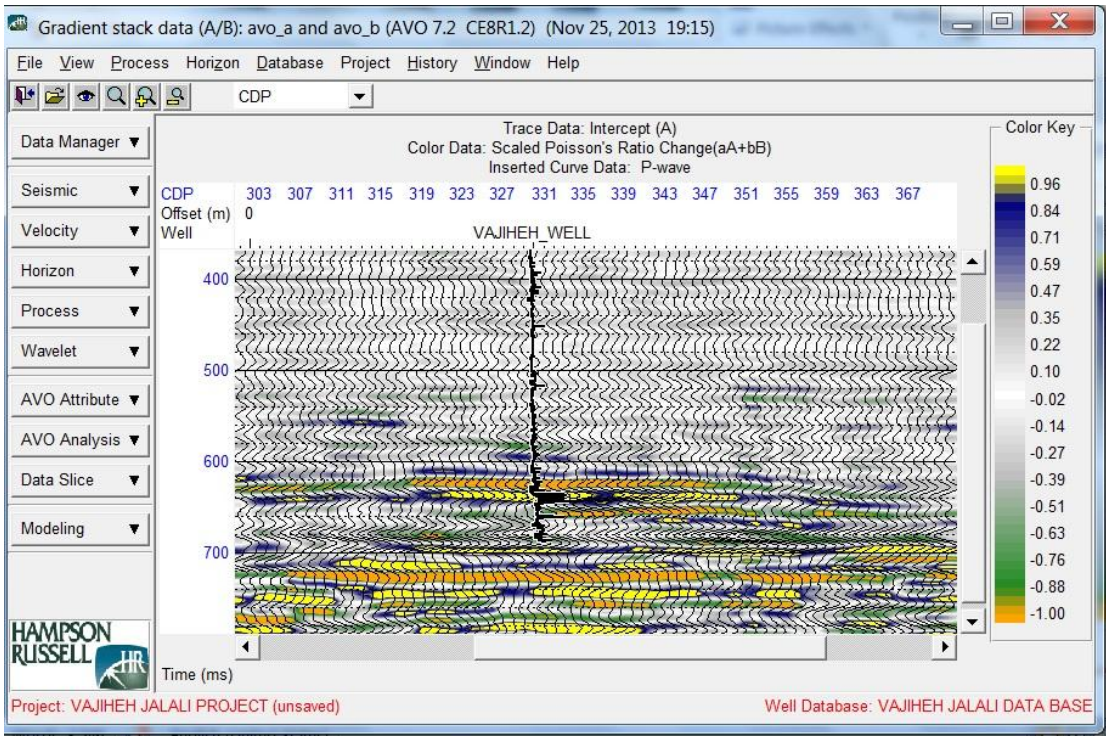

Figure 5.17: Scaled poisson's ratio change attribute plot

5.7.3 Cross Plotting of the Intercept and Gradient

The other process that is indicated here is the cross plotting of the intercept against the gradient, which is used to estimation of the porosity and matrix grain of the P-wave velocity and density logs. This plot is useful to identify the cluster or wet-trend from the gas zone of the reservoir, which is done by choosing the "Cross Plot" option from the "AVO Analysis" menu as is shown below. As is shown in this figure, there are large cluster around the origin, second and forth quadrants. Moreover several

anomalous values in the first and third quadrants indicate the Class 3 AVO anomalies.

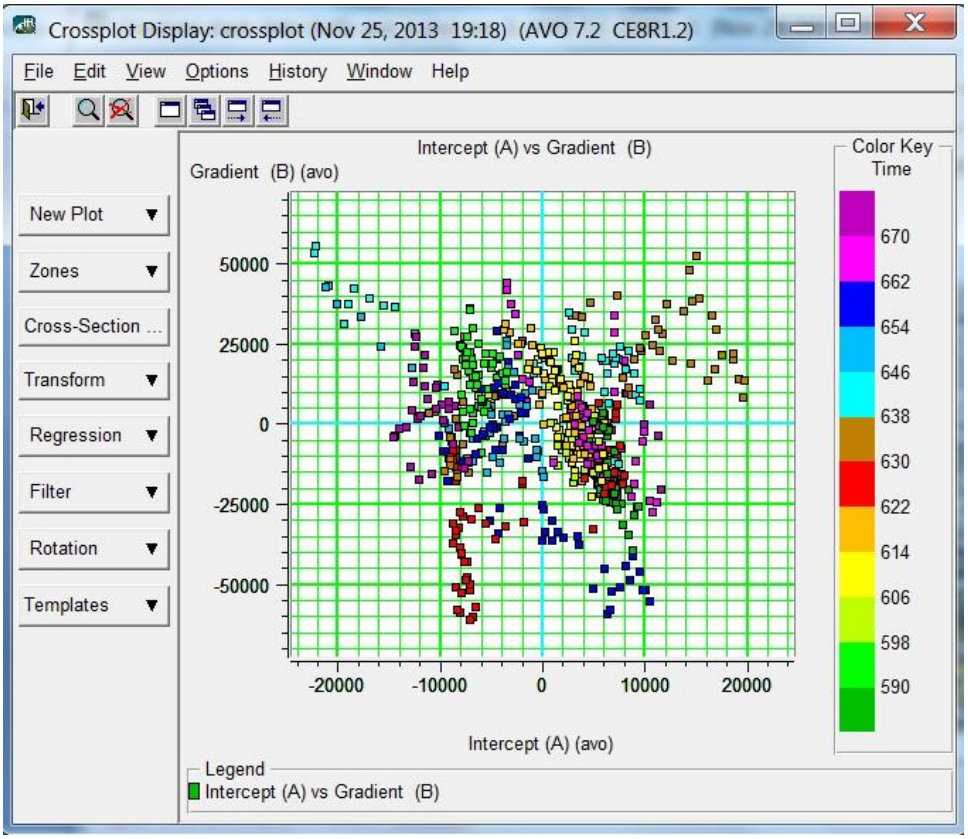

Figure 5.18: Cross plotting of intercept and gradient attribute

5.7.4 Cross Section Display

Another process that is necessary to have a better estimation of the well structure is the cross section process that need to be highlighted each of the anomalies with different colors by selecting zones. The gray ellipse area is the largest zone that covers around the areas of the origin, second and forth quadrates, which indicates cluster or wet-trend. The second zone in the first quadrant,which indicates base_gas, highlighted anomalous by blue polygon. The third zone in the second quadrant, also highlighted anomalous by green polygon, which indicates hard streak and finally the forth zone in the third quadrant indicates top_gas, which is highlighted by yellow

polygon. After selecting these four zones which is shown in Fig (5.18), the cross-section of those zones will be shown in Fig (5.19)

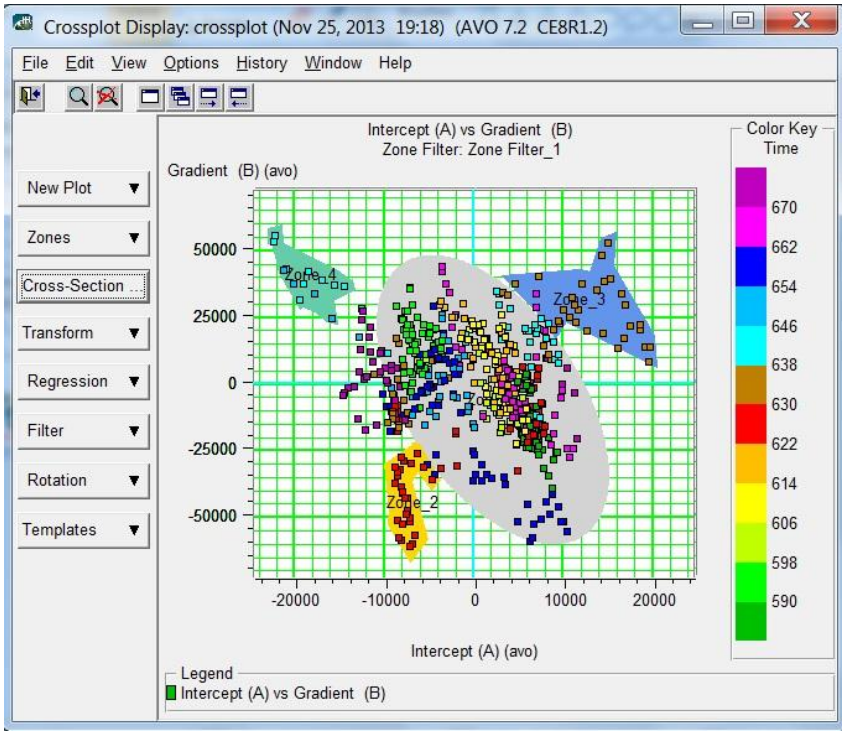

Figure 5.19: Cross plot of intercept and gradient attribute, gray is wet trend, yellow is top-gas zone, blue is base-gas zone and green is hard streak

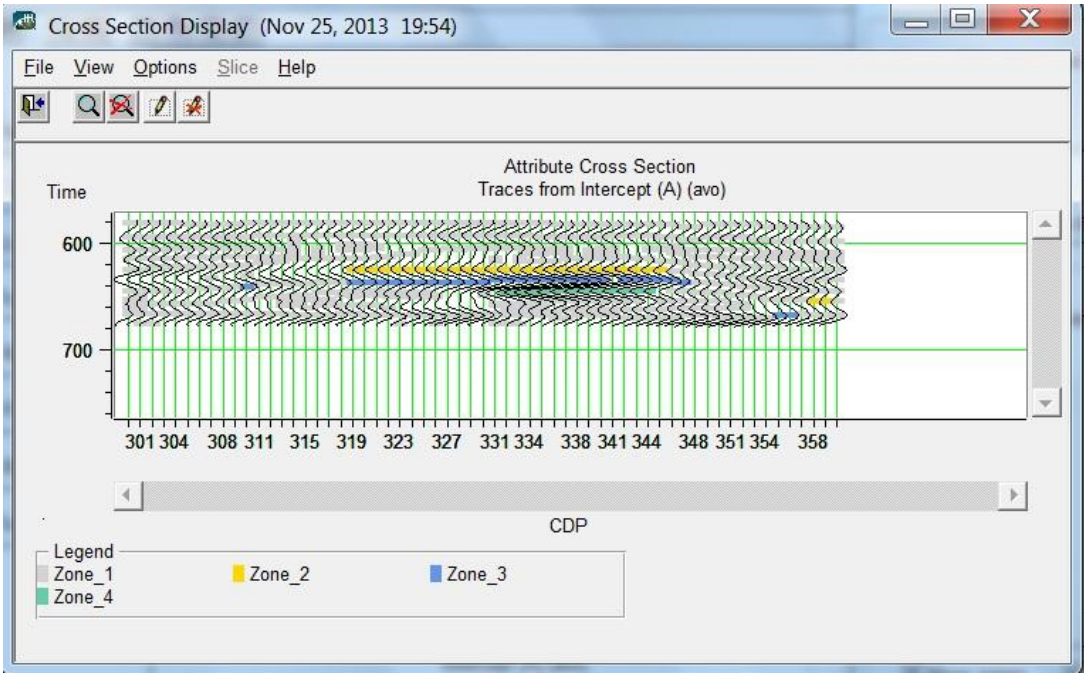

Figure 5.20: Cross section display of intercept and gradient attribute

Note that this cross section also shows the existence of gas zone around the 630 milliseconds on the CDP 330, which are shown by yellow as a top_gas sand and blue color as a base_gas sand.

5.7.5 Color Data Plot of Intercept and Gradient Attribute

Another method to display the cross plot of these zones is based on colored AVO attributes by choosing the Parameters option from the "View" tab. The first attributes that is suitable is intercept (A) as before, which display throughout the entire data set as in Fig (5.21). Here also the yellow area shows top-gas, blue area shows base-gas and blue are shows wet-trend.

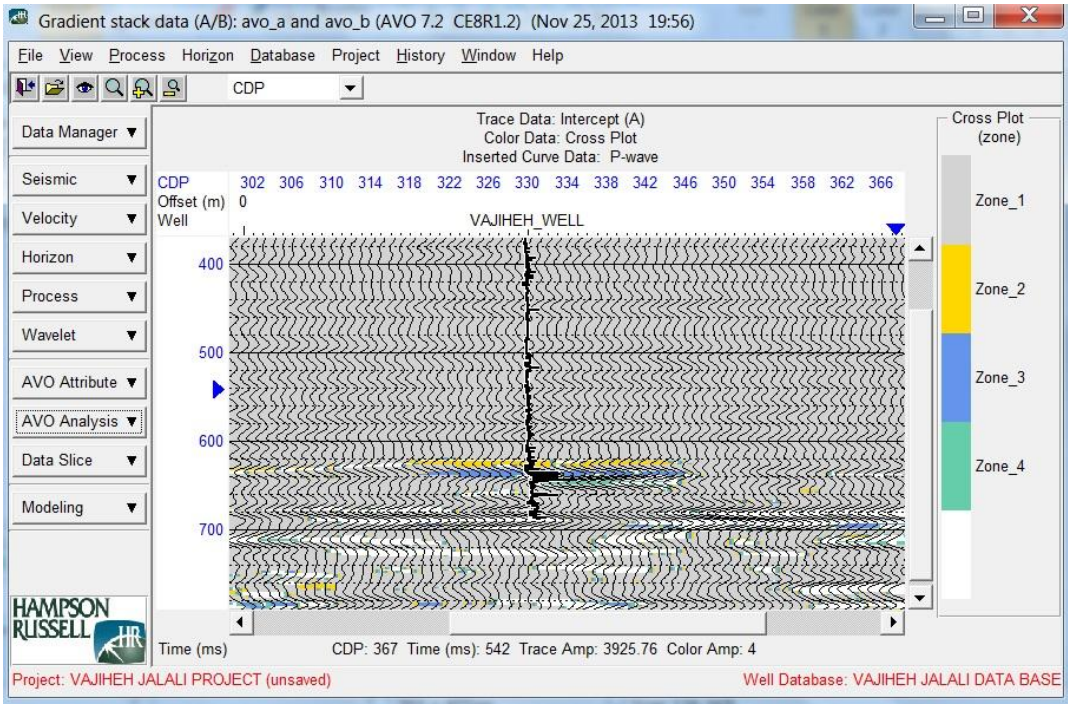

Figure 5.21: Color data plot of intercept and gradient

5.7.6 Color Data Plot of Fluid Factor

Another view of the well plot, which is done here, is to apply two term Fatti AVO attributes including reflectivity coefficients of P-wave and S-wave, Rp and Rs, from the "Super Gather" window by choosing "AVO Attribute Volume" option from the

"AVO Attribute" menu. The AVO attribute, which is displayed in this plot, is fluid factor (ΔF) that is related to the reflectivity coefficients as $\Delta F = R_p - 0.58\,R_S$ (Castagna,1985). The fluid factor reflectivity is the factor to gain the amount of the water saturated of sedimentary rocks and the gas-saturated in the carbonate and igneous rocks. The normalized changes in V_p/V_s ratios is dependent to lithology and the variation of pore fluids that is considered as V_p/V_s =2 in this study. Substituting suitable velocity information and changing the type of analysis to the special type, and accepting desired situation, the main window of fluid factor plot will be shown as in Fig (5.21). Two more plots that are informed here are related to reflectivity coefficients by changing the "Color Key" option on the "Eyeball" icon, which are shown in Fig (5.22) and (5.23).

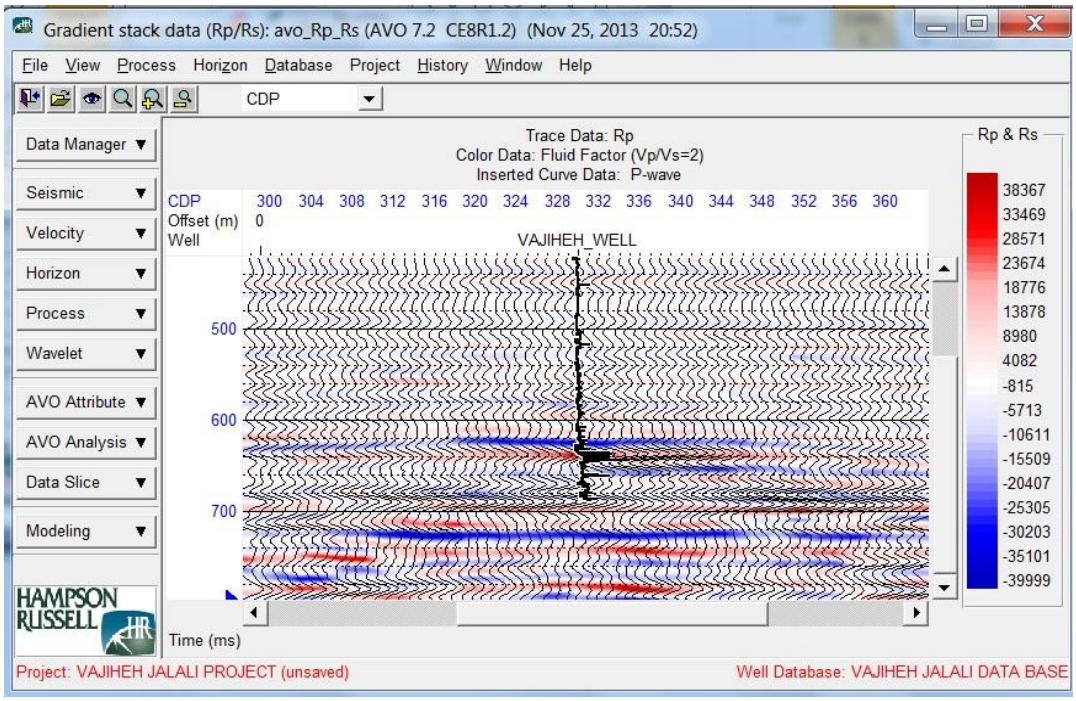

Figure 5.22: Color data plot of fluid factor

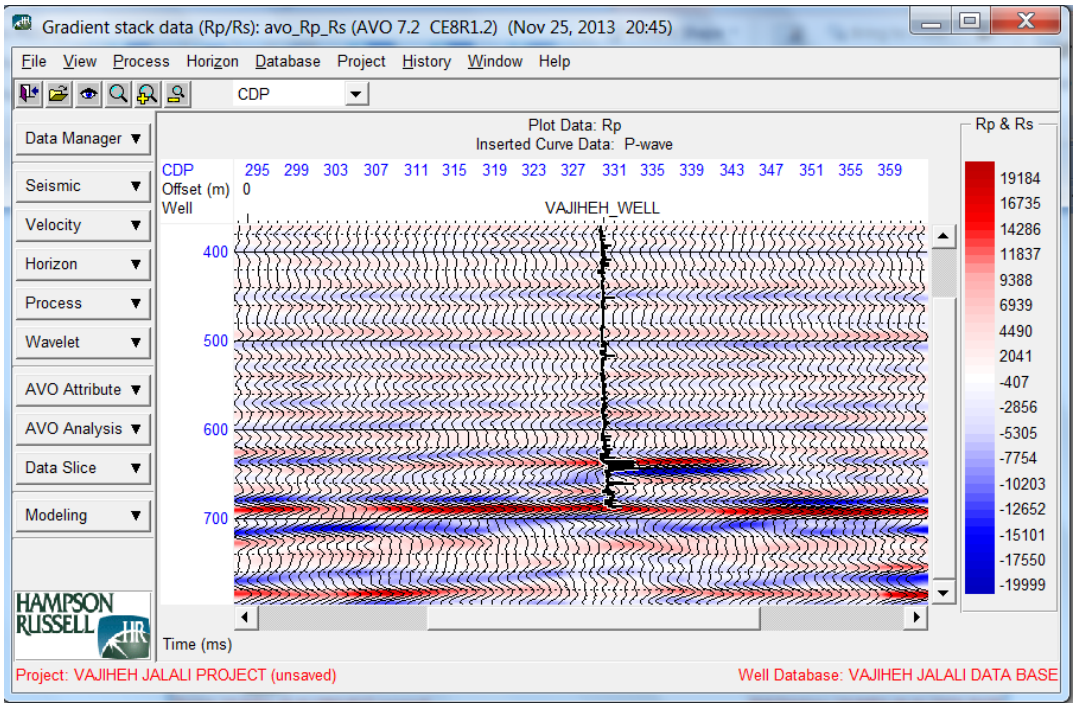

Figure 5.23: Color data plot of reflectivity coefficient

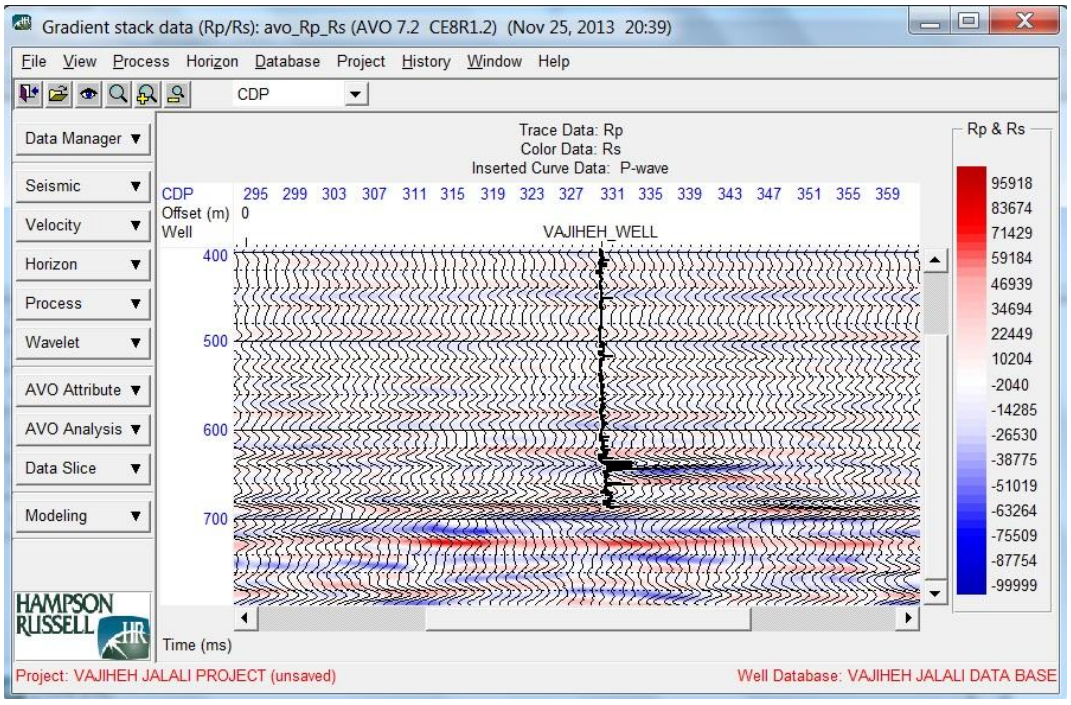

Figure 5.24: Color data plot of R_P and R_S

Chapter 6

CONCLUSION

This thesis that is based on 2-D seismic data of empirical case study using well logs and seismic data, demonstrates that AVO inversion is a suitable method in exploitation of gas zones using AVO attributes, especially the intercept and gradient, and fluid factor attribute that optimize the area of gas zones approved by well logging process. These results show the single type of Class 3 AVO anomaly, in which the wave velocity and density and finally, acoustic impedance will drop sharply in the gas zones that are enclosed by wet trends or shale in the reservoir.

AVO method stands out as a quantitative indicator and cost effective technology suited to the investigation of the subsurface layers that are the primary targets for oil or gas to reduce the exploration risk factor in reservoir prediction and avoid pitfalls in drilling investments, especially in gas sands, by combination of the seismic inversion and rock physics analysis, which had been advanced with 3-D and 4-D seismic data in recent years to maximize the accuracy probability of the interpretations.

This tutorial is a study of the reservoir properties, seismic attribute tools and the principles behind the AVO technique to interpret seismic data efficiently in applying AVO inversion which is the key subjects in the hydrocarbon industry for

Geophysicists, Reservoir Engineers, Seismic Interpreters, Exploration and Production Managers, Rock Physicists and those who are involved in interpreting seismic data in their work. Other materials that are covered by this review are the fundamentals of the reflection seismology and rock physics to introduce elasticity theory, wave propagation, energy partitioning, pre-stack seismic data, stress, strain, pore fluid saturation and several other issues in this field.

The recommendation which seems is essential for Cyprus is the development of the science in oil and gas industry that is useful for the future of this island. Most probably, Eastern Mediterranean University could play an important role in this context. Certainly, Iranian expert professors and scholars could have remarkable support to increase the science of the hydrocarbon industry in Cyprus.

REFERENCES

[1] Aki, K., & Richards, P.G., (1980), Quantitative Seismology: Theory and Methods, W.H.Freeman and Company. San Francisco. Vol. 1.

[2] Alemie, W. M., (Spring 2010). Regularization of the AVO inverse problem by means of a multivariate Cauchy probability distribution. PHD Thesis. Department of Physics. University of Alberta. Edmonton, Alberta.

[3] Avseth, P.A., (May, 2000). Combining Rock Physics and Sedimentology for Seismic Reservoir Characterization of North Sea Turbidite Systems. PHD Thesis. Department of Geophysics. Stanford University. Stanford, California.

[4] Bailey, B., & Barclay, F., & Nesbit, R., & Paxton, A., & Schlumberger, (February/March 2010). Prospect Identification Using AVO Inversion and Lithology Prediction. PESA News, 22-24.

[5] Barclay, F., & Bruun, A., & Alfaro, J. C., et al (Spring 2008). Seismic Inversion: Reading Between the Lines. Oilfield Review. 42-63.

[6] Braile, L. W., Seismic Waves and the Slinky: A Guide for Teachers. From . http://web.ics.purdue.edu/~braile/edumod/slinky/slinky.htm. February 24, 2010.

[7] Castagna, J. P., & Backus, M. M., (1993), Offset-Dependent Reflectivity; Theory and Practice of AVO Analysis. Society of Exploration Geophysicists, United States of America.

[8] Chiburis, E., & Leaney, S., & Skidmore, C., & Franck, C., & Hugo, S. M., (January 1993). Hydrocarbon Detection with AVO. SEISMICS , 42-50.

[9] Dvorkin, J., & Armbruster, M., & Baldwin, C., et al., (September 2008). The Future of Rock Physics: Computational Methods vs. Lab Testing. First break, 23, 63-68.

[10] Evans, B., (2009), A Handbook for Seismic Data; Acquisition in Exploratopn. Society of Exploration Geophysicists. United States of America. Seventh edition.

[11] Feng, H., & Bancroft, J. C., (2006). AVO Principles, Processing and Inversion. CREWES Research Report, 18, 1-19.

[12] Gregor, A. M., (January 2007). A Brief Review of AVO Anomaly Classification. GEOHORIZONS, 34-37.

[13] Hampson, D. & Russell, B., (January 2007), AVO Guide. Lecture note. Rock Physics Laboratory, Stanford University.

[14] Hampson, D. & Russell, B., (September 2004), AVO Theory. Lecture note. Rock Physics Laboratory, Stanford University.

[15] Hossain, Z., (May 2011). Rock-Physics Modeling of the North Sea Greensand. PHD Thesis. Department of Environmental Engineering. Technical University of Denmark.

[16] Kearey, Ph., Brooks, M., & Hill, I., (2002), an Introduction to Geophysical Exploration. Blackwell Science Ltd, Third edition.

[17] Keshavarz, F.K., N., (June 2007). CO_2 Quantification Using Seismic Attributes in Laboratory Experiments. PHD Thesis. Department of Exploration Geophysics. Curtin University of Technology. Austria.

[18] Larsen, A.J., (September, 1999). AVO Inversion by Simultaneous P-P and P-S Inversion. M.Sc. Thesis. Department of Geology and Geophysics. University of Calgary. Canada.

[19] Larsen, J. A., Margrave, G. F., Lu, H. X., Potter, C. C., (1998). Simultaneous P-P and P-S Inversion by Weighted Stacking Applied to the Blackfoot 3C-3D Survey. CREWES Research Report. 10, 1-23.

[20] Mallick, S., (October 2001). AVO and Elastic Impedance. Western Geo, Houston, Texas, U.S., 1094-1104.

[21] Mavko, G., Mukerji, T., & Dvorkin, J., (2009), The Rock physics Handbook; Tools for Seismic Analysis of Porous Media. Cambridge University Press, Second edition.

[22] Mustain, m., (17 Desember 2009). Amplitude vs. Offset (AVO) and Poisson's Ratio Analysis to Shallow Seismic Reflection Method for Identification of the Water Table. Seminar Nasional Teori dan Aplikasi Teknologi Kelautan, A143-A148.

[23] Sheriff, R. E., Geldart, L. P., (1995), Exploration Seismology. University of Cambridge, Second edition.

[24] Spikes, K.T., & Dvorkin, J.P., (2005). Reservoir and Elastic Property Prediction Away from Well Control. Stanford Rock Physics Laboratory, 1-7.

[25] Veeken, P., & Rauch-Davies, M., (February 2006). AVO Attribute Analysis and Seismic Reservoir Characterization. First break, 24, 41-52.

[26] Yilmaz, O., (2001), Seismic Data Analysis; Processing, Inversion, and Interpretation of Seismic Data. Society of Exploration Geophysicists.

[27] Yuping, Su., & Yunguang, T., & Tianqi, W., & Guangpo, C., & Jian, L., (2010). AVO Attributes Interpretation and Identification of Lithological Traps by Pre-stack Elastic Parameters Inversion; A Case Study in K Block, South Turgay Basin. SEG Denver, Annual Meeting, 439-443.

[28] Zhang, H., & Brown, R. J., (2001). A Review of AVO Analysis. CREWES Research Report, 13, 357-380.